

Advances in holmium-based neutrino mass experiments

Angelo Nucciotti

Università di Milano-Bicocca e INFN - Sezione di Milano-Bicocca



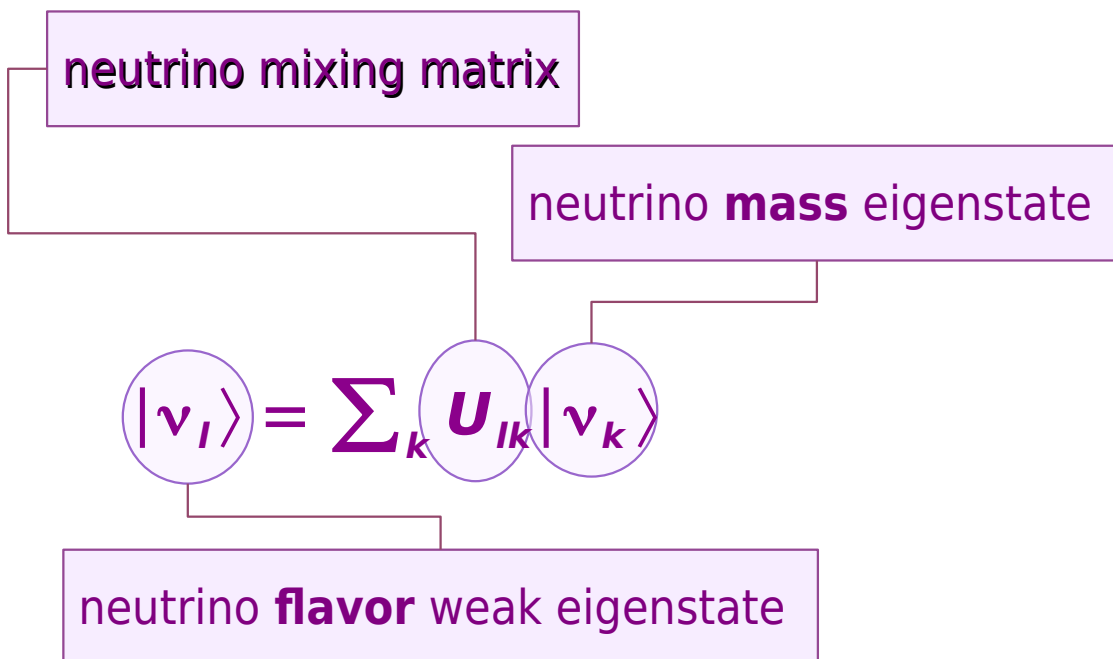
International School of Nuclear Physics - 43rd Course
Neutrinos in Cosmology, in Astro-, Particle- and Nuclear Physics
Erice, Sicily - September 16-22, 2022

Outline

- direct neutrino mass measurements
- calorimetric measurements with low temperature detectors
- low Q beta decay experiments
- ^{163}Ho EC decay calorimetric experiments
 - decay spectrum
 - statistical sensitivity
- HOLMES and ECHo experiments
 - detectors
 - isotope production and embedding
 - arrays readout, data acquisition and processing
 - present results
- future of holmium based experiments

Neutrino properties

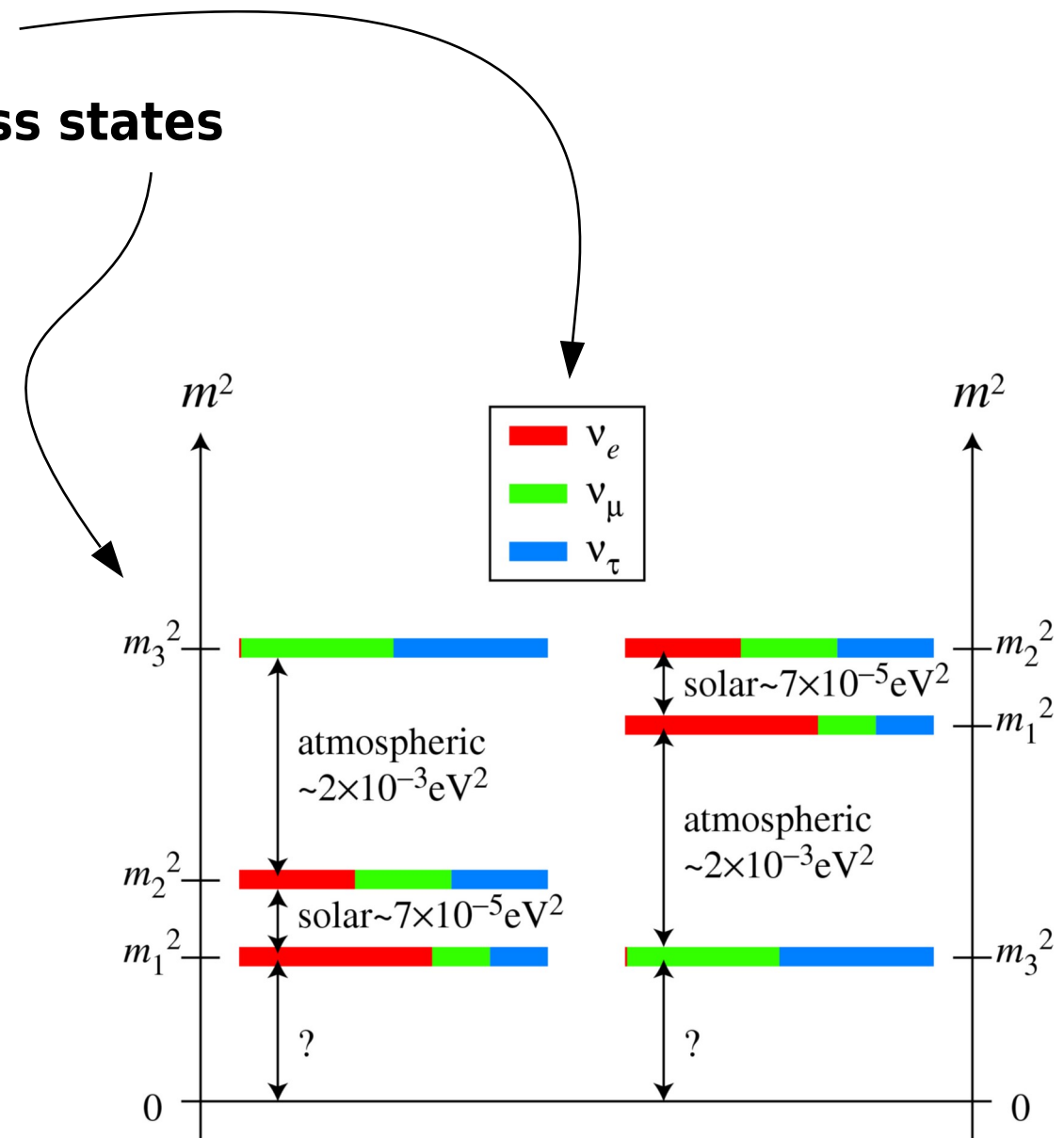
- neutrinos are massive fermions
- there are 3 active neutrino **flavors**: e, μ , τ
- neutrino flavor states are mixtures of 3 **mass states**



from neutrino oscillation experiments

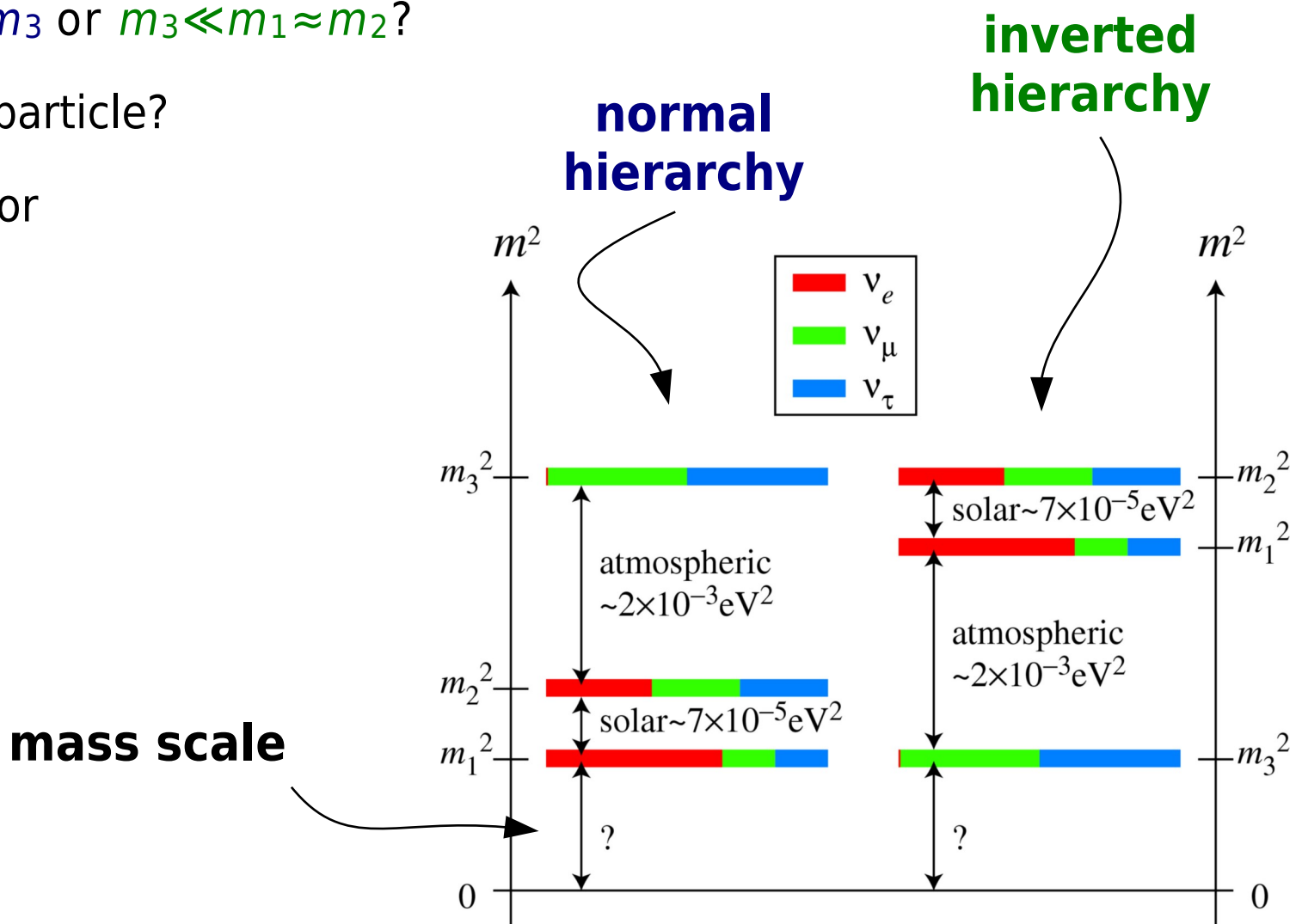
$$\Delta m_{ik}^2 = |m_i^2 - m_k^2|$$

$$\sin^2 2\theta_{ik} = f(|U_{ik}|^2)$$



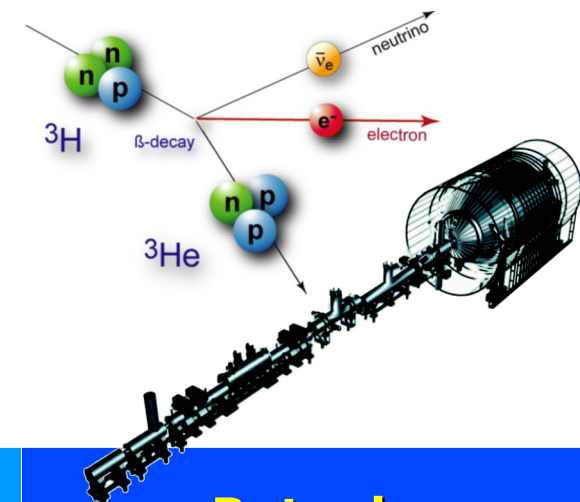
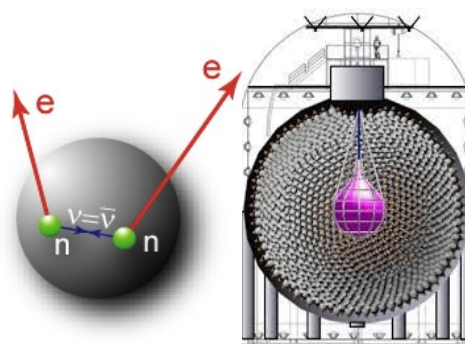
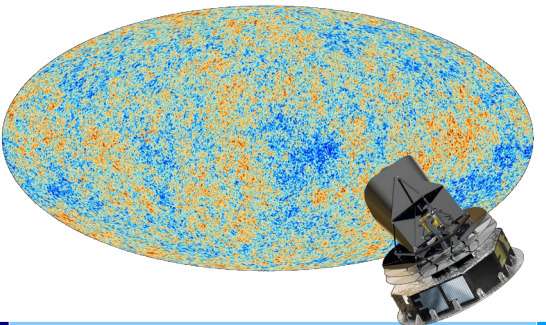
Neutrino open questions

- mass scale: i.e. mass of the lightest ν
- degenerate ($m_1 \approx m_2 \approx m_3$) or hierarchical masses
 - ▶ mass hierarchy: $m_1 < m_2 \ll m_3$ or $m_3 \ll m_1 \approx m_2$?
- $\nu = \bar{\nu}$? i.e. Dirac or Majorana particle?
- CP violation in the lepton sector



Direct v mass measurements: the status

three complementary tools available



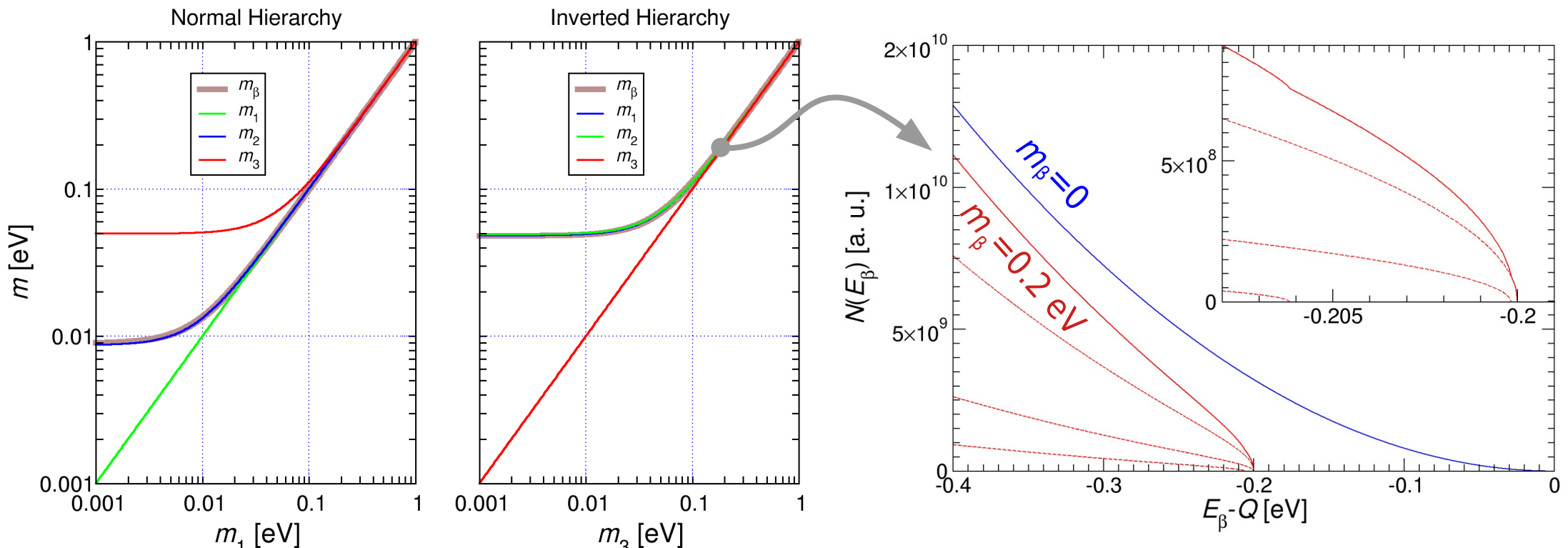
tool	Cosmology CMB+LSS+...	Neutrinoless Double Beta decay	Beta decay end-point
observable	$m_{\Sigma} = \sum_k m_{\nu_k}$	$m_{\beta\beta} = \sum_k m_{\nu_k} U_{ek}^2 $	$m_{\beta} = (\sum_k m_{\nu_k}^2 U_{ek} ^2)^{1/2}$
present sensitivity	≈ 0.1 eV	≈ 0.1 eV	≈ 1 eV
≈ 10 y future sensitivity	≈ 0.05 eV	≈ 0.01 eV	≈ 0.1 eV
model dependency	yes ☹	yes ☹	no ☺
systematics	large ☹	some ☺	large ☹

Direct neutrino mass measurements

■ kinematics of weak decays

- in beta and electron capture decays where $\bar{\nu}_e$ or ν_e are emitted $|\nu_e\rangle = \sum_k \mathbf{U}_{ek} |\nu_k\rangle$
- non zero neutrino masses $\mathbf{m}_{\nu k}$ modify the phase space
- for nuclear β decay $N(E) \propto p_\beta E_\beta (Q - E_\beta) \sum_k |\mathbf{U}_{ek}|^2 \sqrt{(Q - E_\beta)^2 - \mathbf{m}_{\nu k}^2} F(Z, E_\beta) S(E_\beta)$
- for degenerate masses ($m_{\nu 1} \approx m_{\nu 2} \approx m_{\nu 3}$)

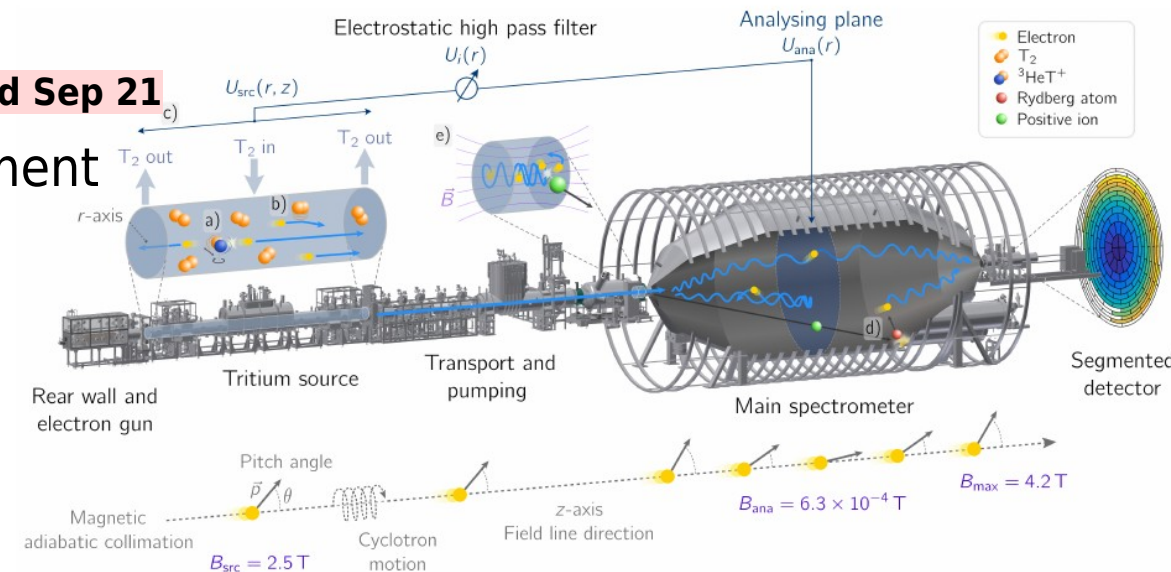
$$N(E) \approx p_\beta E_\beta (Q - E_\beta) \sqrt{(Q - E_\beta)^2 - \mathbf{m}_\beta^2} F(Z, E_\beta) S(E_\beta) \quad \text{with} \quad \mathbf{m}_\beta = \sqrt{\sum_k \mathbf{m}_{\nu k}^2 |\mathbf{U}_{ek}|^2}$$



Tritium experiments

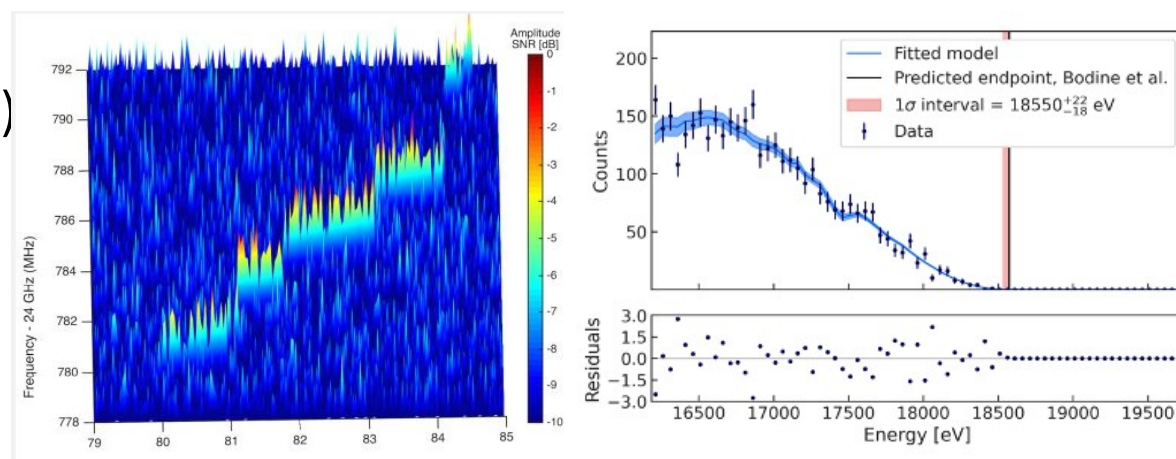
KATRIN *Nat. Phys.* 18, 160–166 (2022) **Lokhov + Schwemmer on Wed Sep 21**

- MAC-E filter: ultimate integral spectrometer experiment
- sensitivity goal: 0.2 eV 90% CL
- energy resolution <3 eV @18 keV.
- first high-purity tritium campaign in 2019
→ **$m_\nu < 0.8 \text{ eV}$ 90% CL**



Project8 *arXiv:2203.07349*

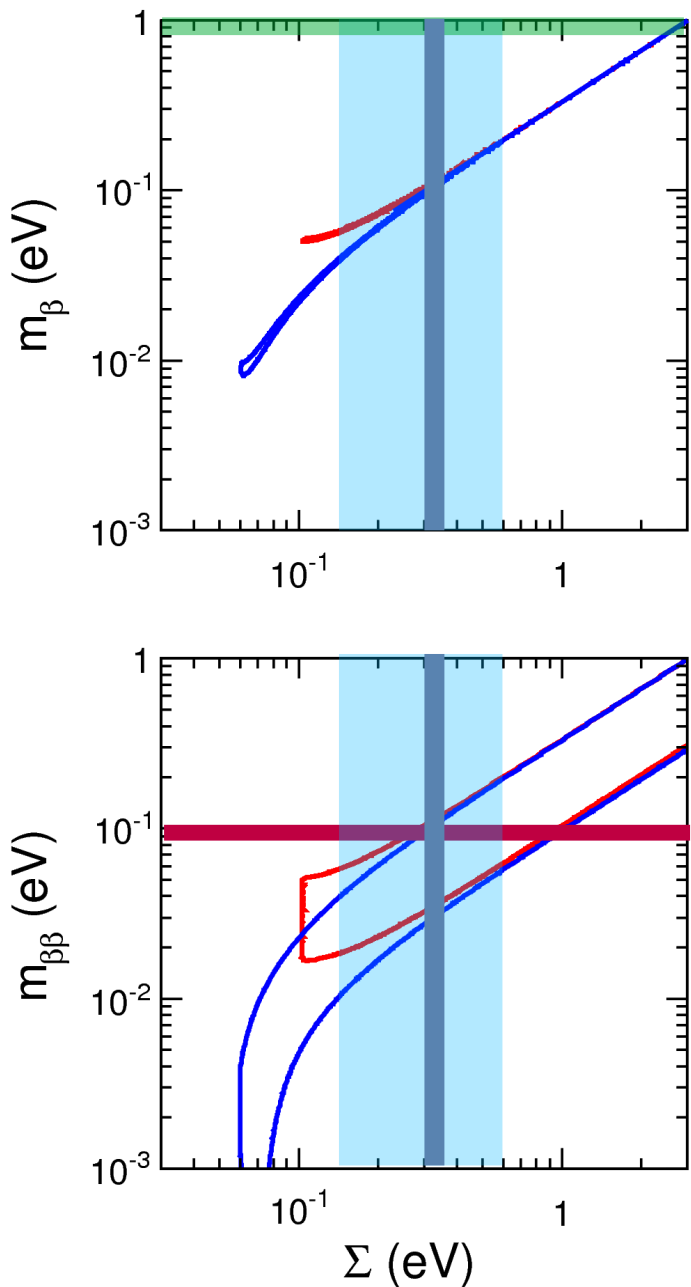
- Cyclotron Resonance Electron Spectrometry (CRES)
- sensitivity goal: 40 meV 90% CL
- 4 different experimental phases: phase III ongoing
- energy resolution $\approx 2 \text{ eV}$ @18 keV



PTOLEMY *M.G. Betti et al., Prog. Part. Nucl. Phys.*, 106 (2019)

- project to measure the Cosmic Neutrino Background via neutrino capture on tritium
- differential spectrometer combining CRES with an EM dynamic filter and hi-res microcalorimeters
- sensitivity potential: $O(10)$ meV
- presently: small prototype R&D

Direct ν mass measurements: 2022 status



NH and **IH** 2σ bands from oscillation parameters

G.Fogli et al., Phys. Rev. D 86 (2012) 013012 (only minor updates in 2022)

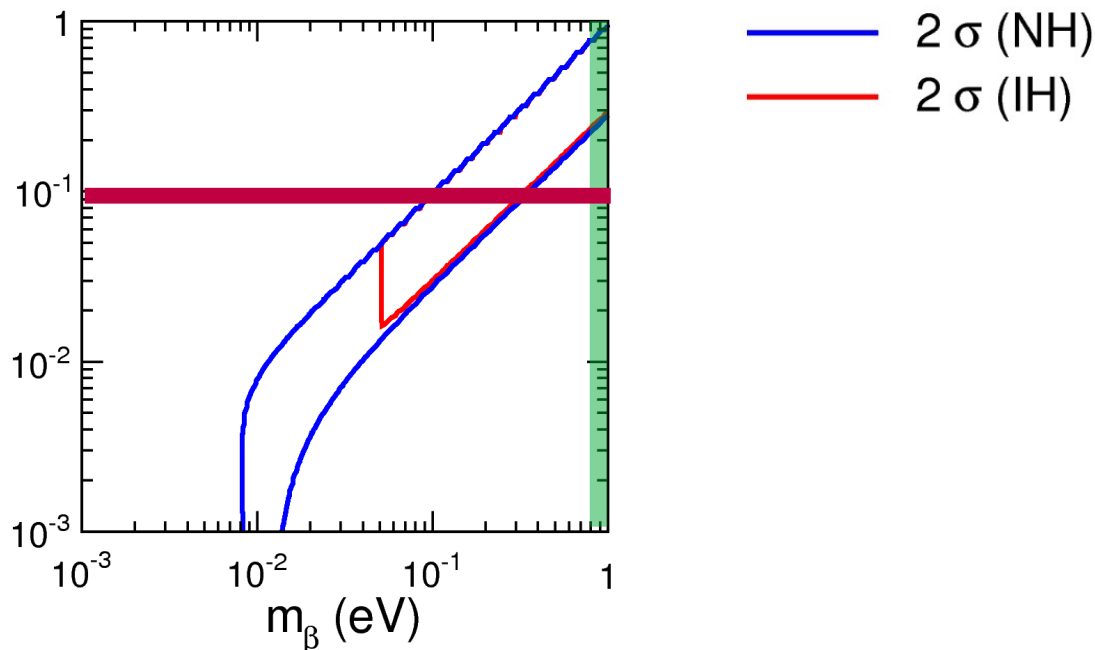
$m_{\beta\beta}$ from 0v double beta decay experiments

E. Lisi, A. Marrone, Phys.Rev.D 106 (2022) 1, 013009. arXiv:2204.09569

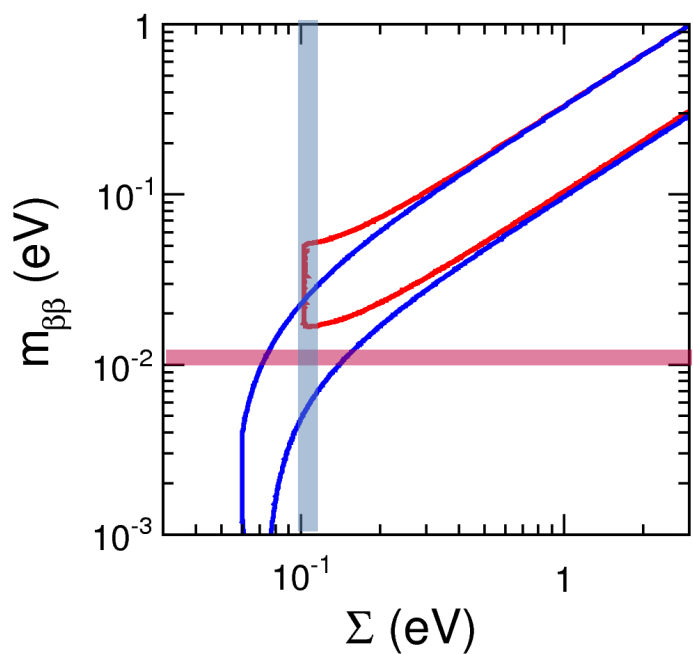
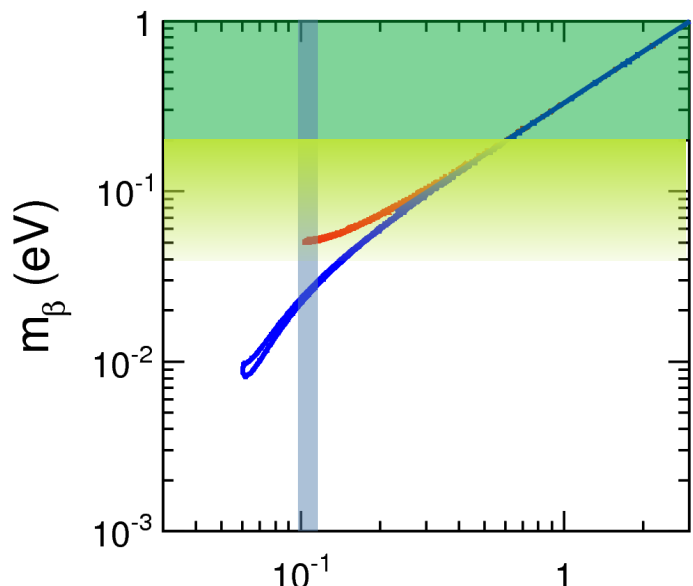
Σ from cosmic microwave background measurements

F. Capozzi, et al. Phys. Rev. D 104, 083031. arXiv:2107.00532

m_β from KATRIN *KATRIN Coll.*, Nat. Phys. 18, 160–166 (2022)



Direct ν mass measurements: role of kinematic exp.

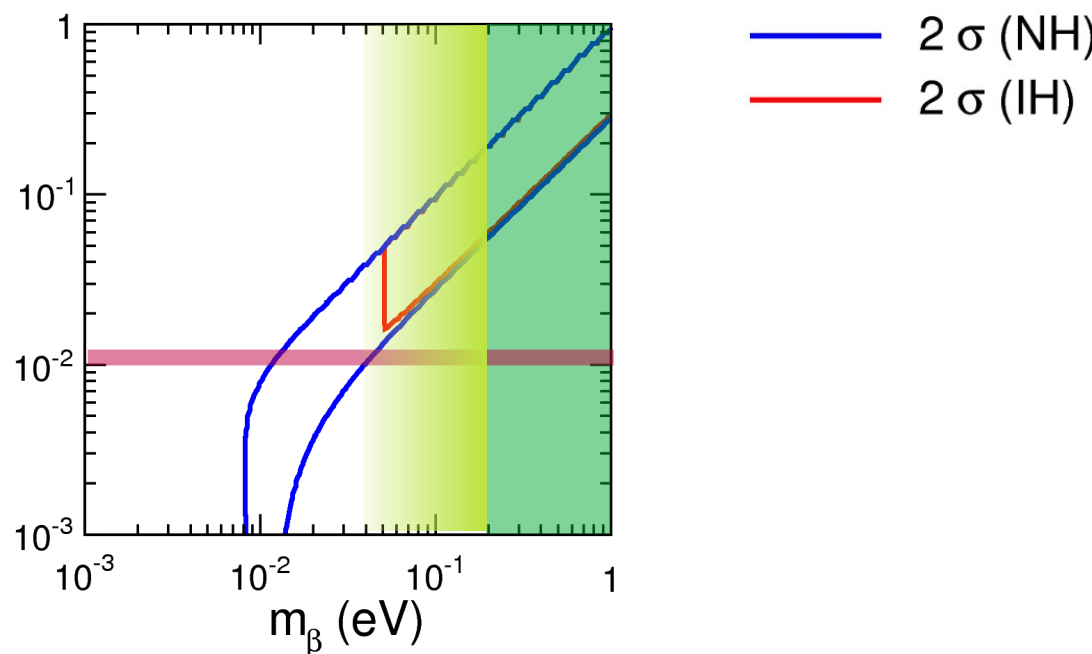


NH and **IH** 2σ bands from oscillation parameters

G.Fogli et al., Phys. Rev. D 86 (2012) 013012 (only minor updates in 2022)

m_β KATRIN goal

m_β **$m_{\beta\beta}$** **Σ** next generation experiments

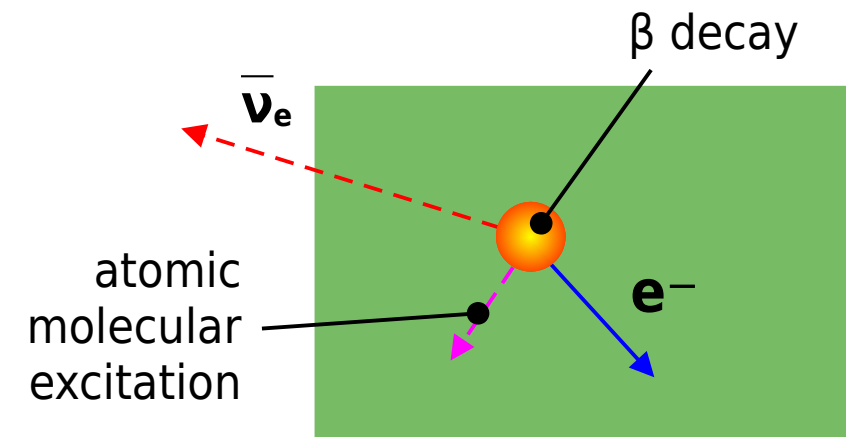


Calorimetric experiments

ideal calorimetric experiment

- radioactive source embedded in the detector(s)
 - only the neutrino energy escapes detection
- $\rightarrow E_c = Q - E_\nu$

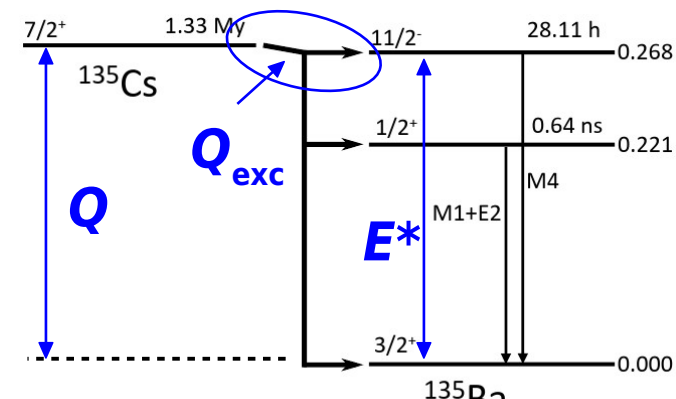
- no backscattering
- no energy losses in source
- no decay final state effects
- no solid state excitation
- low activity \rightarrow limited statistics
- pile-up background



ideal isotope has

- low Q
 - \rightarrow larger fraction of decays in ROI
 - \rightarrow easier calorimetry
- for EC: capture peak close to end-point
- short decay time

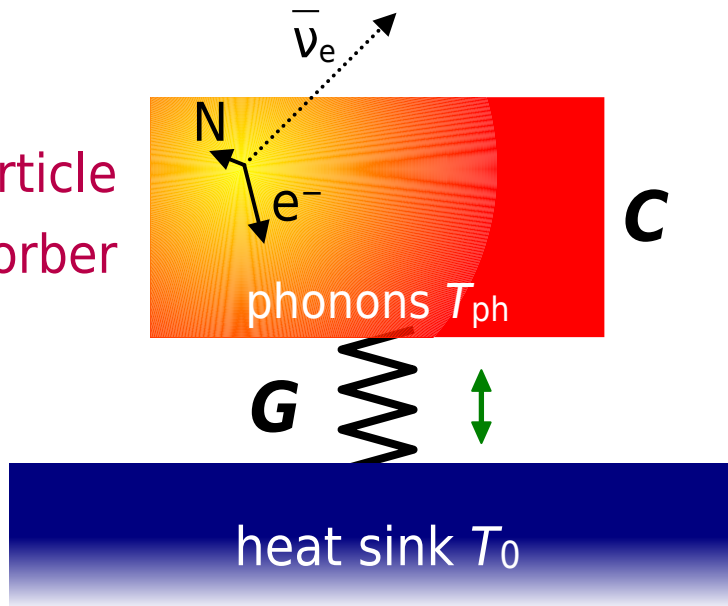
isotope	Q [eV]	$\tau_{1/2}$ [y]	decay	B.R.	experiments
^3H	18592.01(7)	12	β^-	1	Simpson's
^{187}Re	2470.9(13)	4.3×10^{10}	β^-	1	MANU, MIBETA
^{163}Ho	2833(30)	4570	EC	1	Holmes, ECHO
^{135}Cs	440	8.0×10^{11}	β^-	1.6×10^{-6}	-
^{115}In	155	4.3×10^{20}	β^-	1.1×10^{-6}	-



A. de Roubin et al. PRL. 124, 222503 (2020)

Low temperature detector principles

particle absorber



$$E \rightarrow \Delta T \approx \Delta E/C \rightarrow \Delta X(T)$$

e.g: $R=R(T)$, $M=M(T)$

$$C(T_{ph}) \frac{dT_{ph}}{dt} + G(T_{ph}, T_0) = P(t)$$

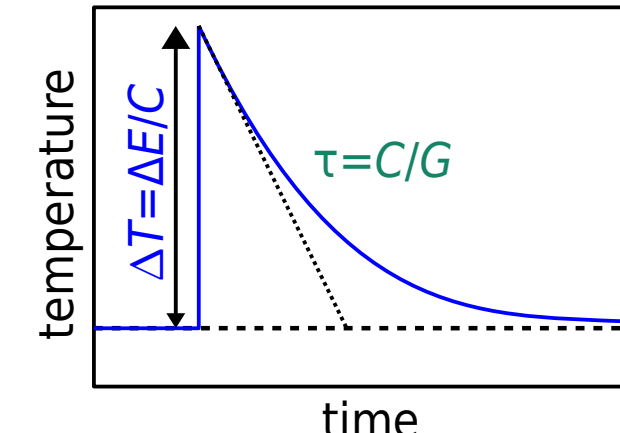
$$P(t) = \Delta E \delta(t) \rightarrow T_{ph}(t) = T_0 + \frac{\Delta E}{C} e^{-t/\tau}$$

for $t > 0$ and with $\tau = C/G$

energy resolution limited by
thermodynamic fluctuation noise TFN

$$N_{ph} = \frac{\langle U \rangle}{\langle E_{ph} \rangle} = \frac{CT}{k_B T}$$

$$\sigma_E = \Delta U_{rms} = \sqrt{N_{ph} \langle E_{ph} \rangle} = \sqrt{k_B T^2 C}$$



- detectors used for calorimetric neutrino mass experiments are more complex
- in metallic calorimeters energy is transferred to electronic system with T_e
- thermodynamics and statistical mechanics still provide for TFN $\sigma_E = \sqrt{k_B T^2 C}$

$200 \times 200 \times 2 \mu\text{m}^3$ (1.5 μg)

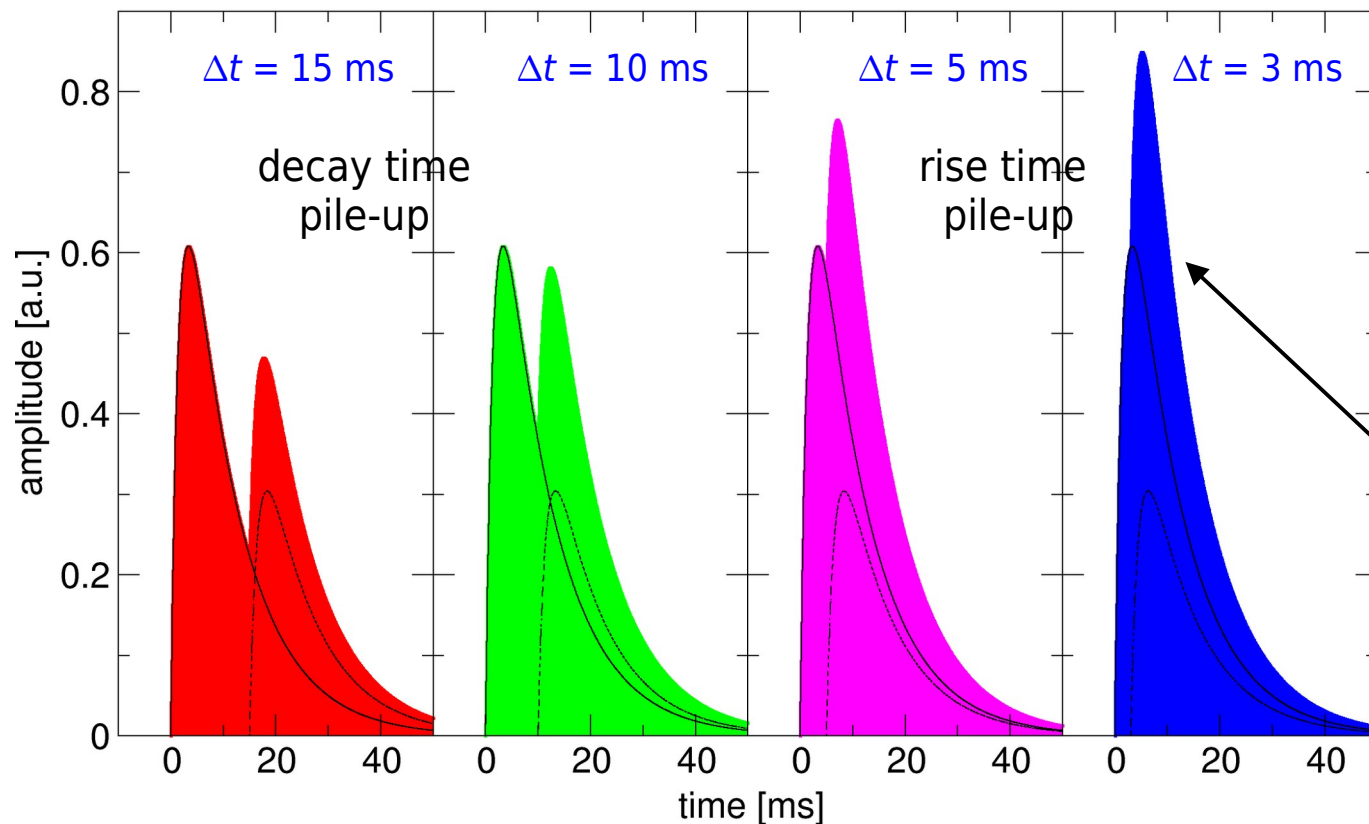


$$C \approx C_e \alpha T_e \rightarrow C \approx 5 \times 10^{-13} \text{ J/K}$$

$\sigma_E \approx 3.4 \text{ eV}$ (better estimate for TES detectors gives $\sigma_E \approx 0.4 \text{ eV}$)

Pile-up in low temperature detectors

- calorimeters detect all β source decays
- low temperature detectors are *slow* devices
- simple pulse model $A(t) = A(e^{-t/\tau_{decay}} - e^{-t/\tau_{rise}})$
 - for microcalorimeters: $\tau_{rise} \approx 0.1\text{-}10 \mu\text{s}$ and $\tau_{decay} \approx 0.1\text{-}10 \text{ ms}$



2 pulses with:

- $\tau_{rise} = 1.5 \text{ ms}$
- $\tau_{decay} = 10 \text{ ms}$
- $A_2/A_1 = 0.5$
- time separation Δt

first approximation for rise time p-up
resolving time $\tau_R \approx$ rise time τ_{rise}

for $\Delta t < \tau_R$
→ accidental coincidence
→ $E_{meas} = E_1 + E_2$

- $\Delta t \gg \tau_{rise} \rightarrow$ pile-up on the decay time \rightarrow dead time
- $\Delta t \lesssim \tau_{rise} \rightarrow$ pile-up on the rise time \rightarrow spectral distortions and background

Calorimetry of beta decays: statistical sensitivity

rise time pile-up resolving time τ_R

ROI ΔE

source activity A_β

pile-up fraction $f_{\text{pile-up}} = \tau_R A_\beta$

measuring time T_M

number of detectors N_{det}

exposure $t_M = T_M \times N_{\text{det}}$

^{187}Re example:

$$N_\beta(E, m_\nu) \approx \frac{3}{Q^3} (Q-E)^2 \sqrt{1 - \frac{m_\nu^2}{(Q-E)^2}}$$

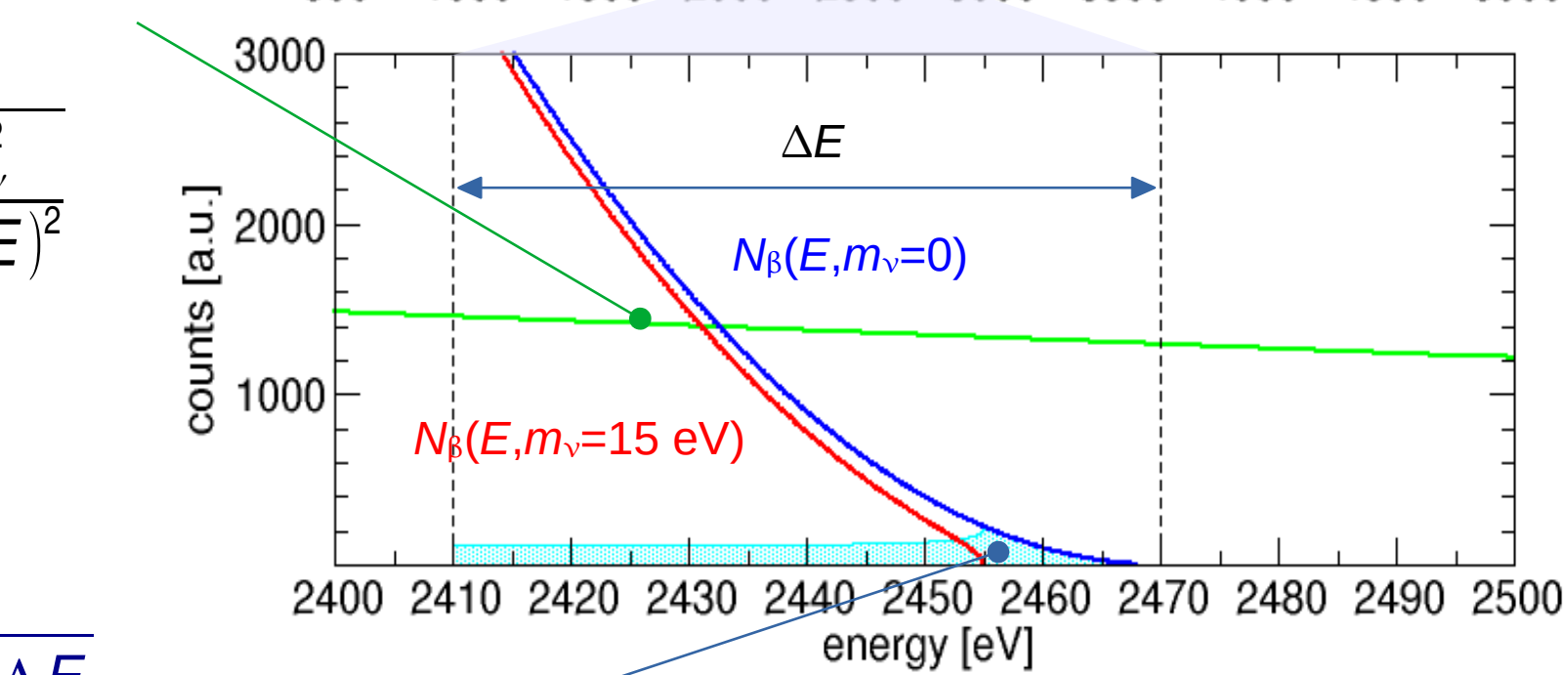
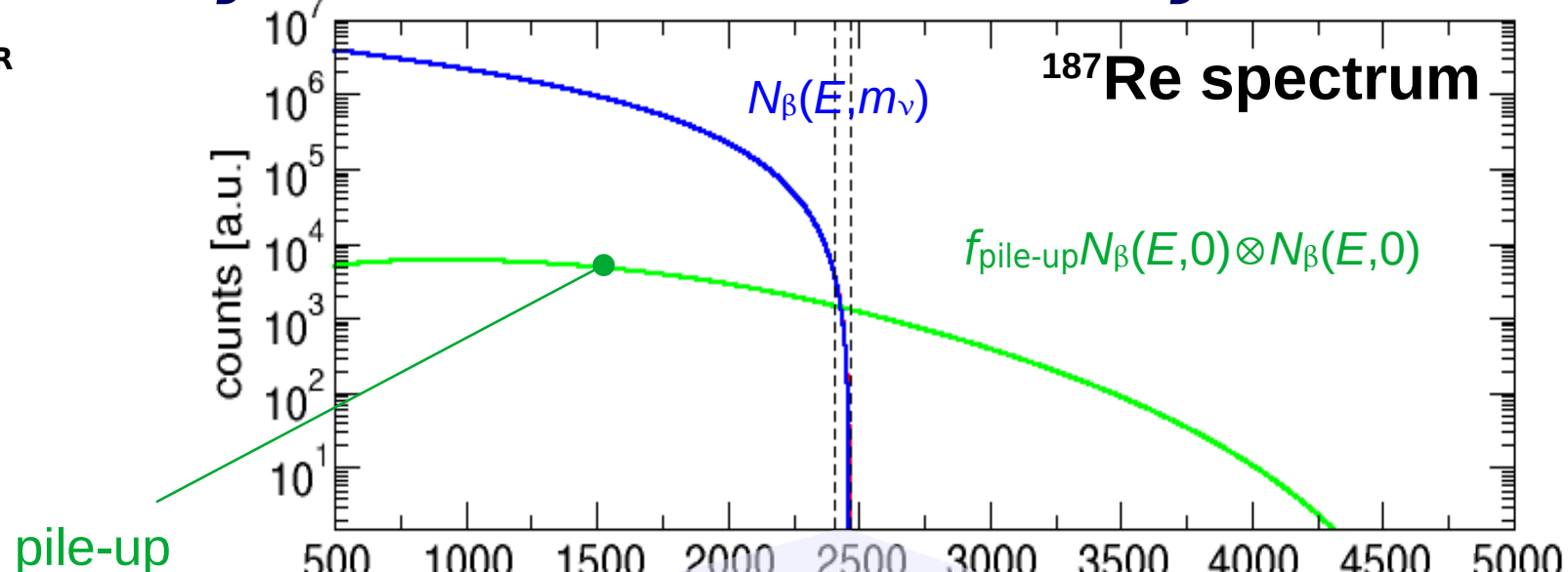
$$\Delta E \approx \Delta E_{\text{FWHM}}$$

pile-up is negligible when

$$f_{\text{pile-up}} = \tau_R A_\beta \ll \frac{\Delta E^2}{Q^2}$$

then

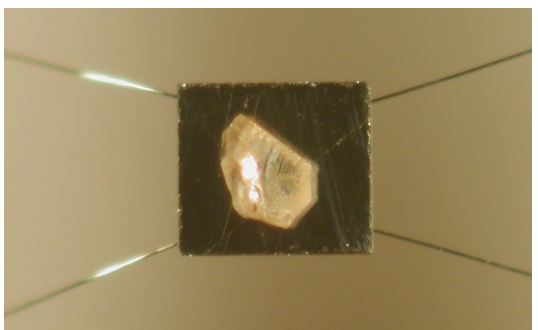
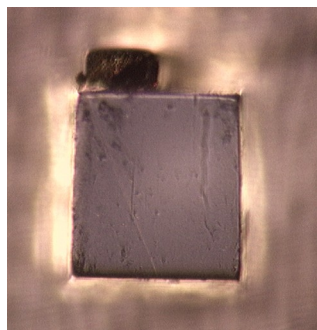
$$\sum_{90} (m_\nu) \approx \sqrt[4]{\frac{Q^3 \Delta E}{A_\beta t_M}} = \sqrt[4]{\frac{Q^3 \Delta E}{N_{\text{decays}}}}$$



$$\text{signal} = |N_\beta(E, m_\nu=0) - N_\beta(E, m_\nu=15 \text{ eV})|$$

A. Nucciotti et al., Astropart. Phys. 34, 80 (2010).

Rhenium-187 experiments



first ^{187}Re experiments: $N_{\text{ev}} \approx 10^7$ events

MIBETA @ Milano with AgReO_4

$\rightarrow m_\nu < 15$ eV 90% C.L. M.Sisti et al., NIM A 520 (2004) 125

• MANU @ Genova with metallic Re

$\rightarrow m_\nu < 26$ eV 95% C.L. F.Gatti et al., Nucl. Phys. B91 (2001) 293

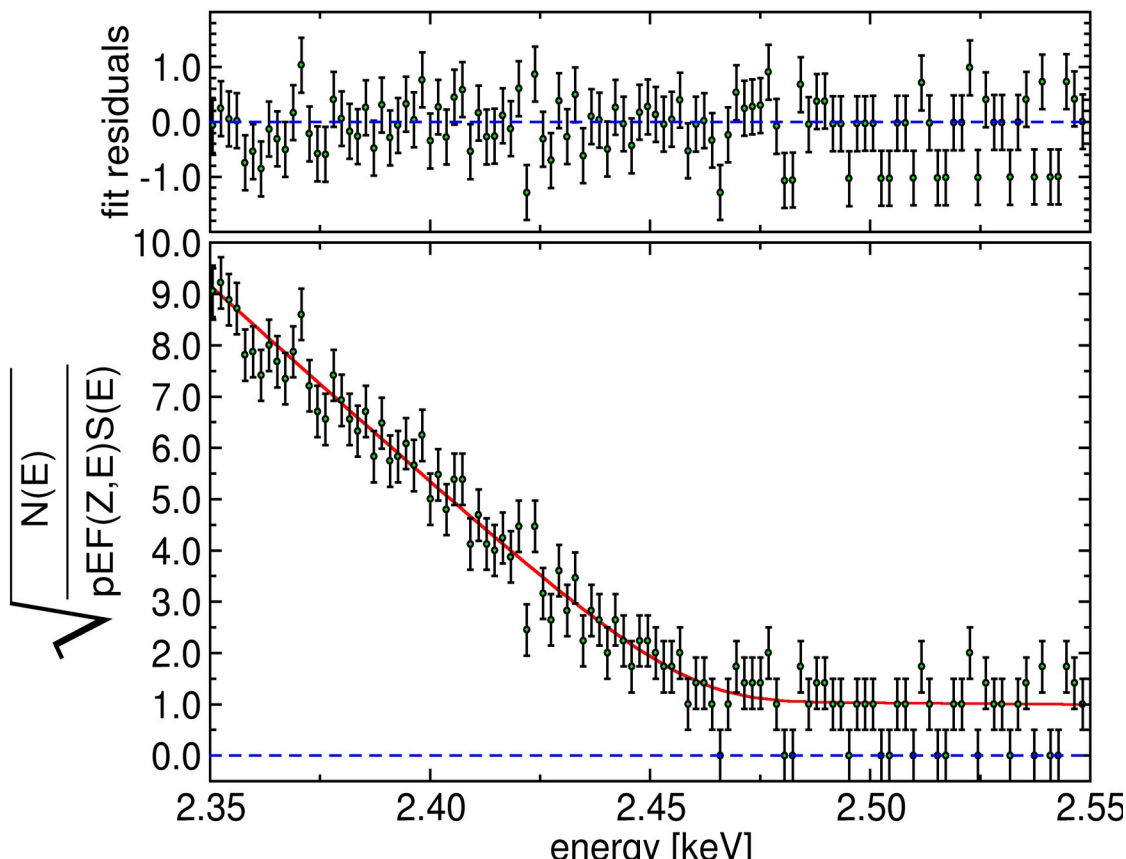
1990 → 2006 MIBETA (Milano/MilanoBicocca) + MANU (Genova)

$^{187}\text{Re} \rightarrow m_\nu < 15$ eV (+ BEFS...)

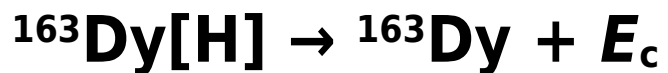
2006 MARE (Microcalorimeter Array for a Rhenium Experiment) int'l project for $m_\nu < 0.1$ eV

2007 → 2013 MARE R&D for phase 1 → Re+TES/MMC / AgReO_4 +Si-Impl

2013 MARE project with ^{187}Re abandoned due to insurmountable technical obstacles



Electron capture calorimetric experiments

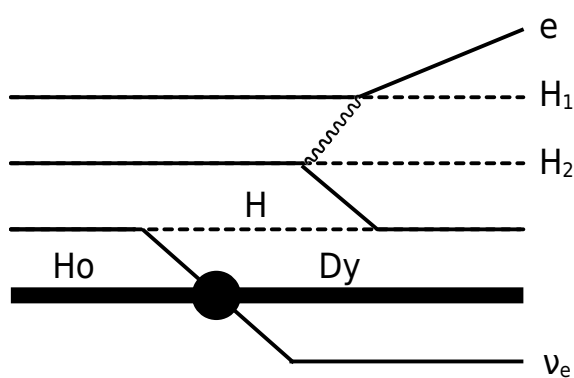


shell binding energy: $E_b(\text{M1})=2.05 \text{ keV}$

→ electron capture from shell $\geq \text{M1}$

→ H=M1, M2, N1, N2, O1, O2, P1

$$\Gamma_{\text{M1}} \approx 13 \text{ eV}$$



A. De Rújula and M. Lusignoli,
Phys. Lett. B 118 (1982) 429

- calorimetric measurement of Dy atomic de-excitations (E_c)
 - ▷ mostly Auger and Coster-Kronig ($\omega_{\text{M1,2}} \approx 10^{-3}$, $\omega_{\text{N1,2}} \approx 10^{-5}$)

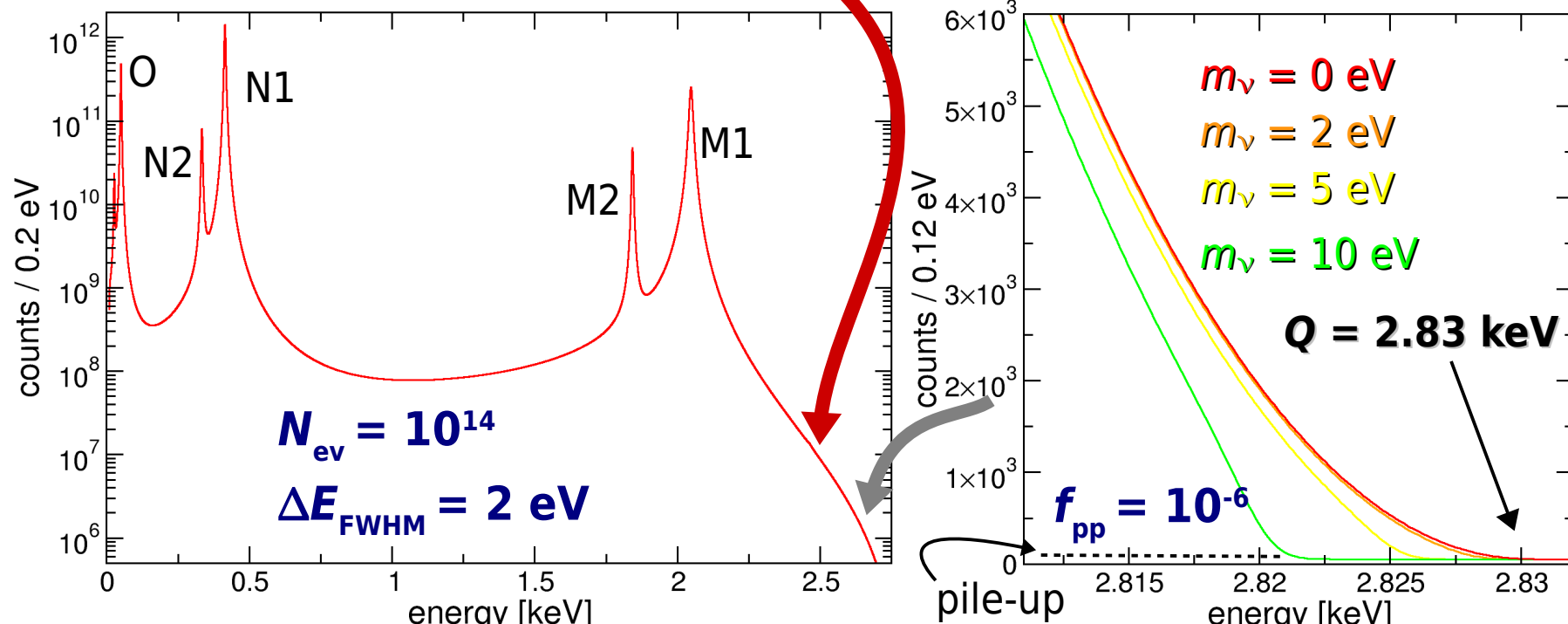
$$Q = 2.833 \pm 0.030^{\text{stat}} \pm 0.015^{\text{sys}} \text{ keV}$$

S. Eliseev et al., Phys. Rev. Lett. 115 (2015) 062501

- ▶ end-point rate and ν mass sensitivity depend on $Q - E_{\text{M1}}$

$$\tau_{1/2} \approx 4570 \text{ years} \rightarrow 2 \times 10^{11} \text{ }^{163}\text{Ho} \text{ nuclei} \leftrightarrow 1 \text{ Bq}$$

$$N(E_c) = \frac{G_\beta^2}{4\pi^2} (Q - E_c) \sqrt{(Q - E_c)^2 - \mathbf{m}_\nu^2} \times \sum_i n_i C_i \beta_i^2 B_i \frac{\Gamma_i}{2\pi} \frac{1}{(E_c - E_i)^2 + \Gamma_i^2/4}$$

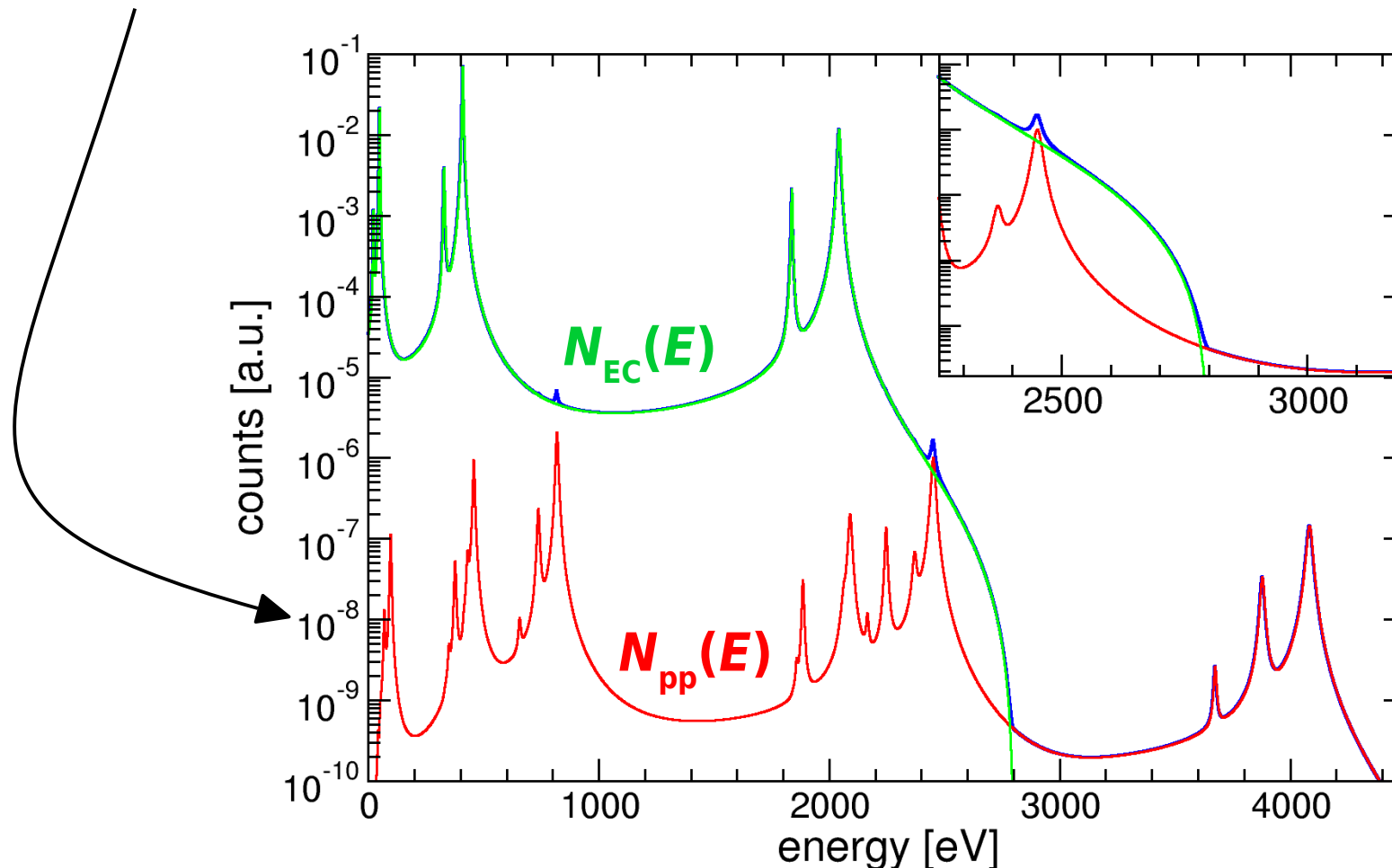


Pile-up in ^{163}Ho EC calorimetric experiments / 2

- accidental coincidences → complex pile-up spectrum
- calorimetric measurement → **detector speed is critical**

A_{EC} EC activity per detector
 τ_R time resolution (\approx rise time)

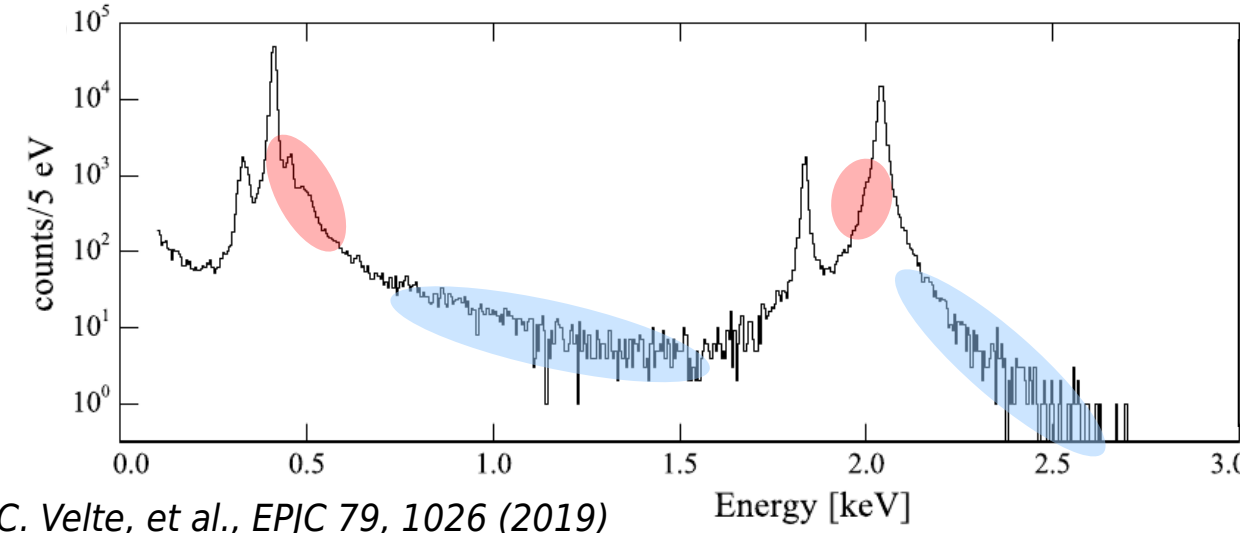
► $N_{\text{pp}}(E) = f_{\text{pp}} N_{\text{EC}}(E) \otimes N_{\text{EC}}(E)$ with $f_{\text{pp}} \approx A_{\text{EC}} \tau_R$



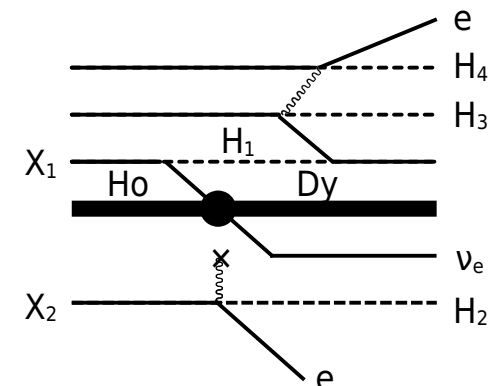
$$Q = 2800 \text{ eV}$$

$$f_{\text{pp}} = 10^{-4}$$

Double hole processes / 1



- high-statistic low background **ECHO** spectrum shows extra features
 - extra peaks close to N1 and M1
 - N/M peak asymmetries / high energy tails



Single hole: the Dy atom is left by EC with one hole in the shell (M, N, O...)

→ for H_1 in shell X_1 with binding energy $E_b(X_1)$ → resonance for $E_c = E_b(X_1)$

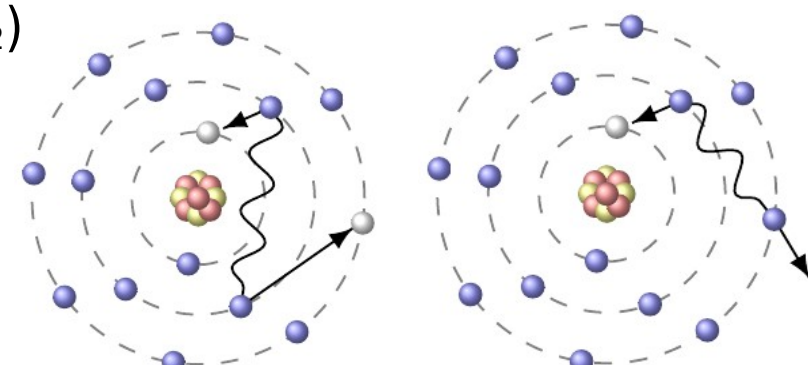
Double hole processes

the perturbation due to the nucleus charge change ($Ho \rightarrow Dy$) “shakens” one or more additional atomic electron to an upper bound state (shake-up) or to the continuum (shake-off or Auger)

→ shake up: additional hole H_2 in $X_2 \rightarrow$ resonance for $E_c = E_b(X_1) + E_b(X_2)$

→ shake off: additional hole H_2 in X_2

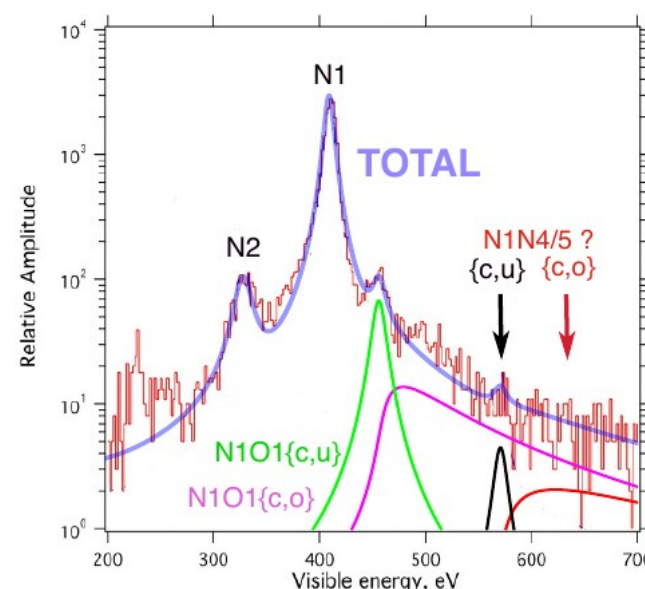
→ tail to peaks from $E_c = E_b(X_1) + E_b(X_2)$ up to $E_c = Q$



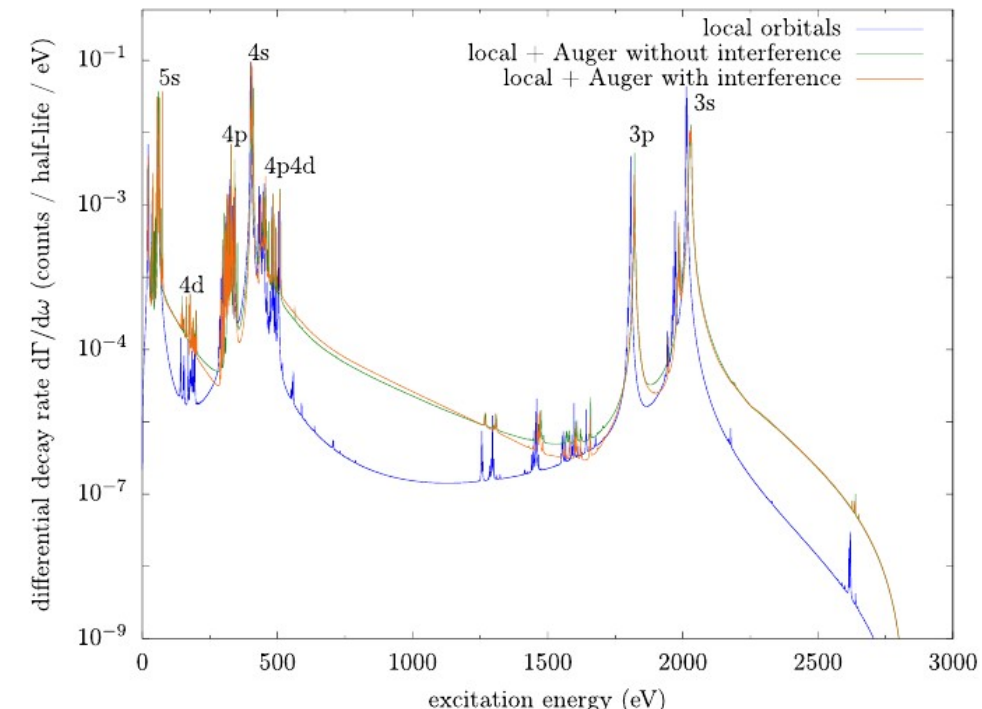
Double hole processes / 2

- several attempts to include double hole processes
H. Robertson et al., A. Faessler et al., A. De Rújula and M. Lusignoli, ...

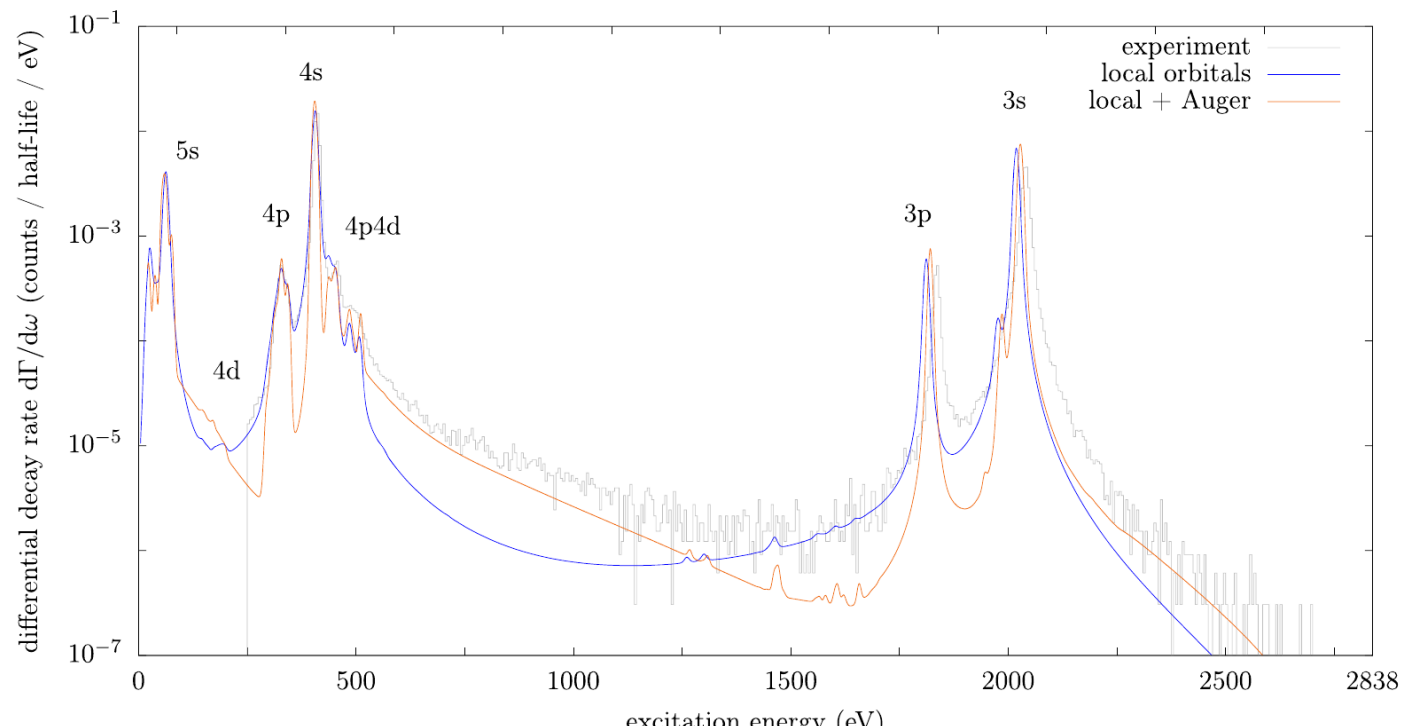
- recent work from M. Haverkort and collaborators:
ab-initio calculations including Coulomb interactions between multi core bound and unbound states (work in progress)
 - missing because of computational limits: intrinsic resonance linewidths, full shake-off contributions, radiative transitions, ...



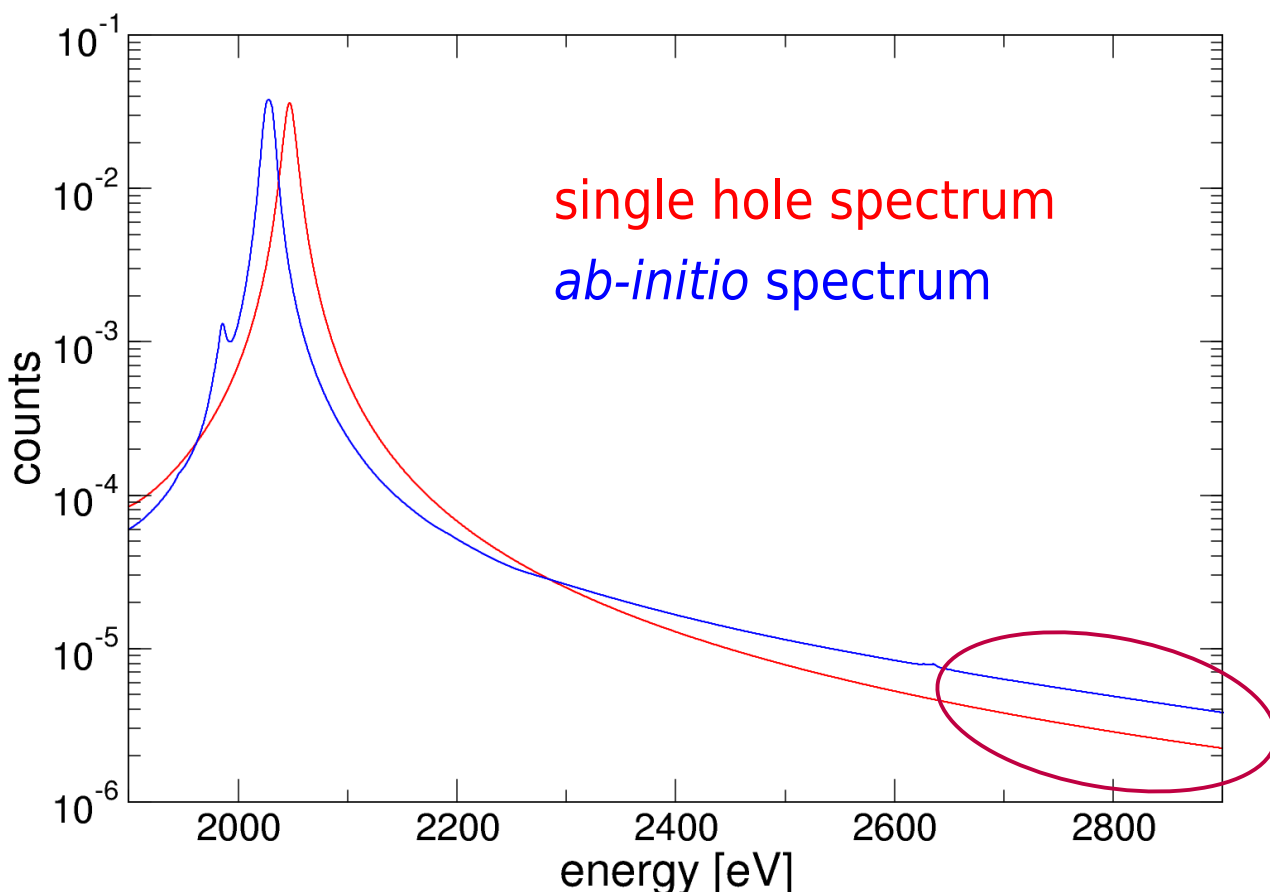
A.De Rújula & M. Lusignoli,
J. High Energ. Phys. (2016) 2016: 15



M. Brass and M. W. Haverkort, New J. Phys. 22 (2020) 093018



End-point spectral shape

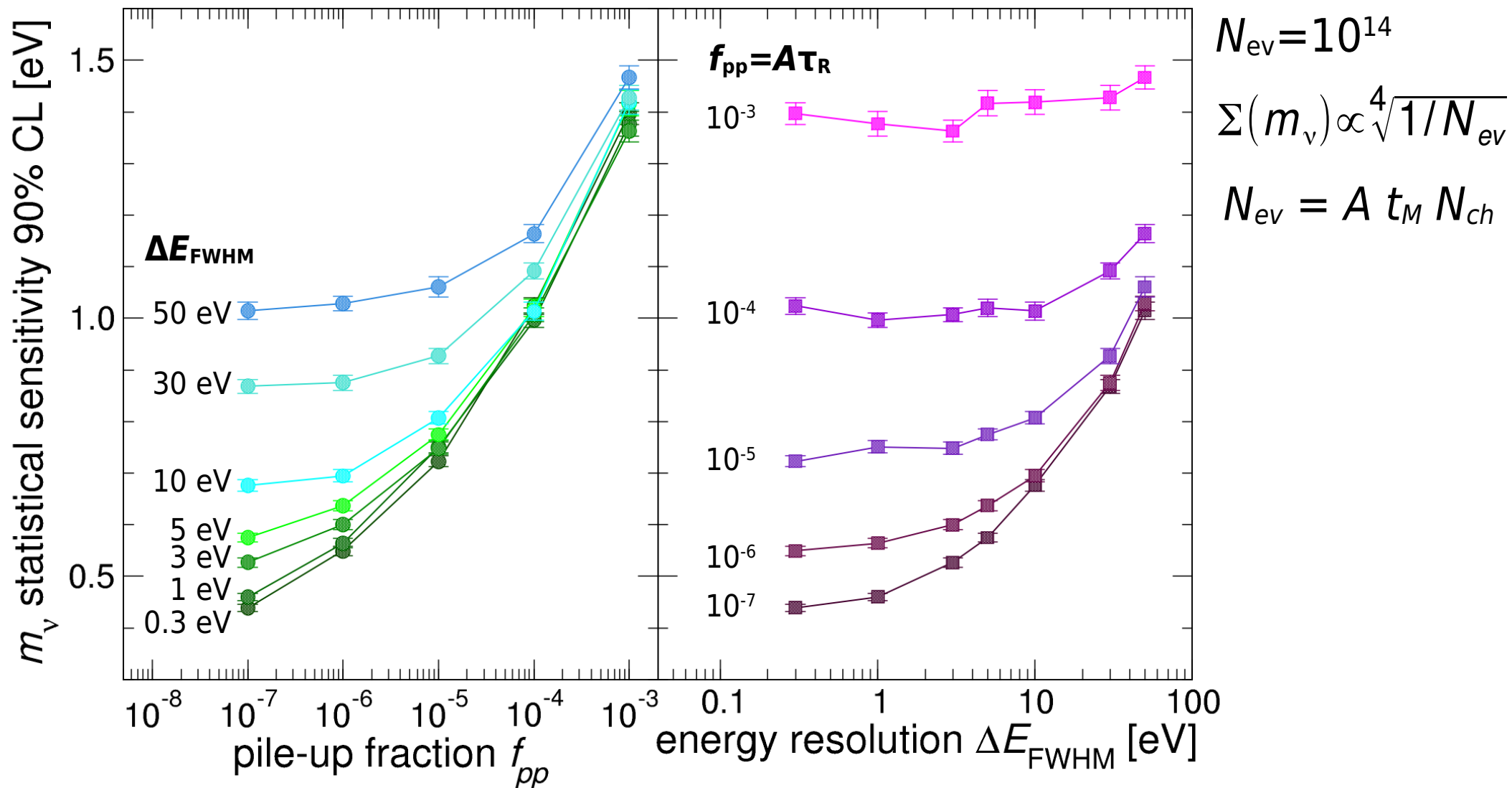


- “bare” spectra (without phase space)
- *ab-initio* with additional Lorentzian broadening
- spectra are normalized to unity
 - end-point region is smooth and featureless
 - phase space factor leaves unmistakable imprint
- possibly small systematic uncertainties
- to be proved

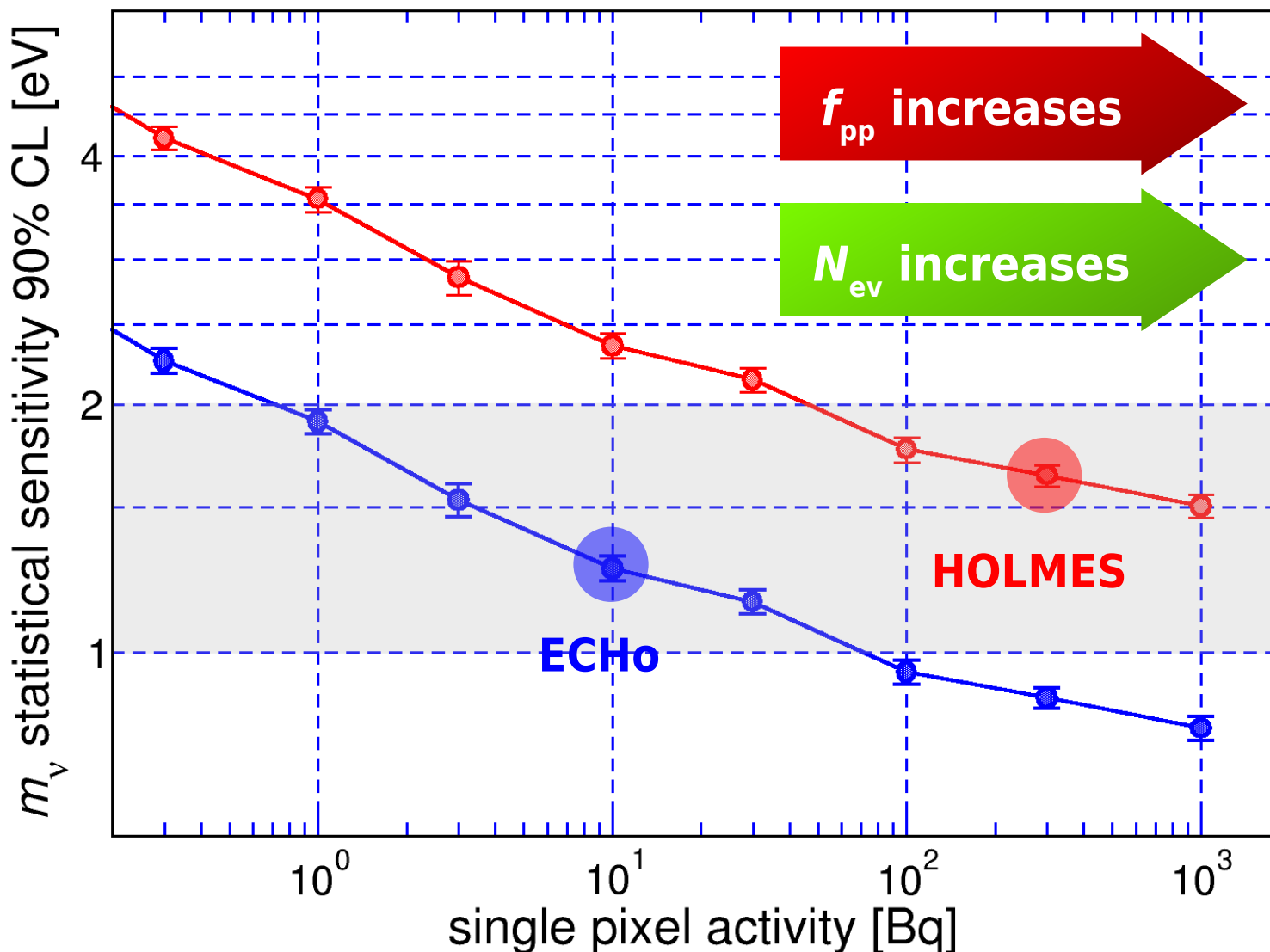
- apparently *ab-initio* spectrum has higher rate at endpoint
- also pup spectrum is higher
- small gain on statistical sensitivity

Statistical sensitivity: pile-up and energy resolution

- Montecarlo simulations for statistical sensitivity with **single-hole spectrum**
- simulations confirm that sensitivity Σ scales as $1/(N_{\text{ev}})^{0.25}$



Neutrino mass statistical sensitivity



MC simulations

A. Nucciotti, Eur. Phys. J. C 74.11 (2014)

single-hole spectrum

$\Delta E = 1$ eV

$\tau_R = 1$ μ s

$N_{det} t_M = 1000$ det \times 3 years

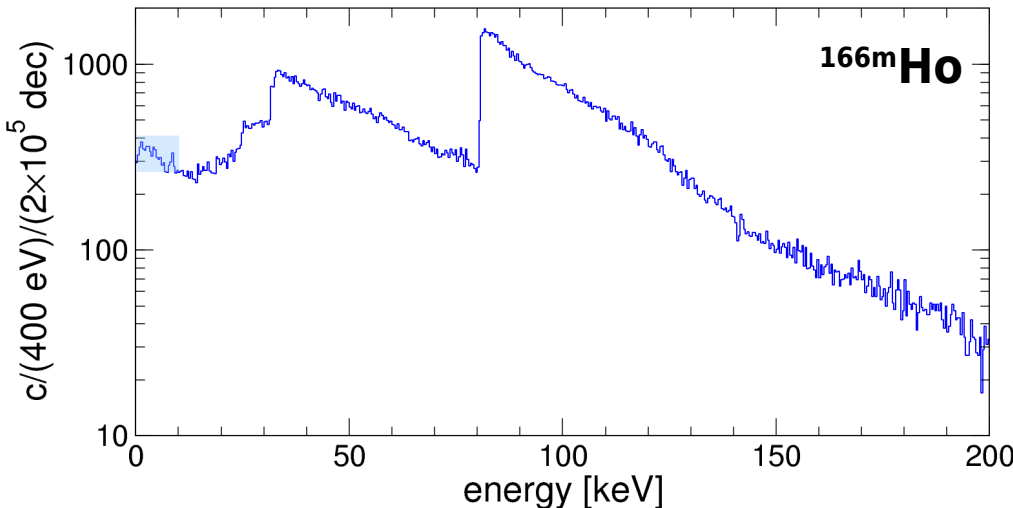
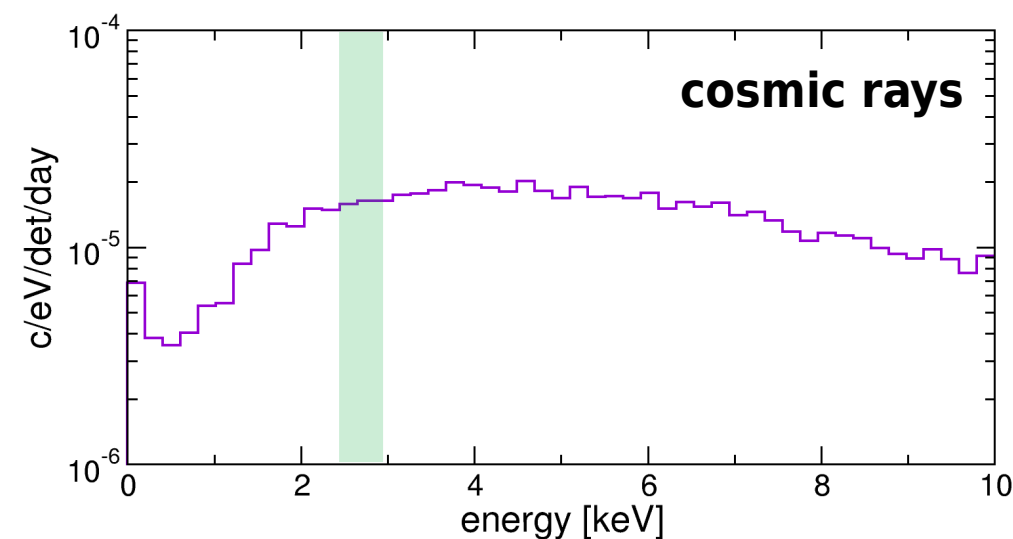
$N_{det} t_M = 12000$ det \times 3 years

high activity \rightarrow robustness against (flat) background

$A_{EC} = 300$ Bq $\rightarrow b < \approx 0.1$ counts/eV/day/det

Low energy background

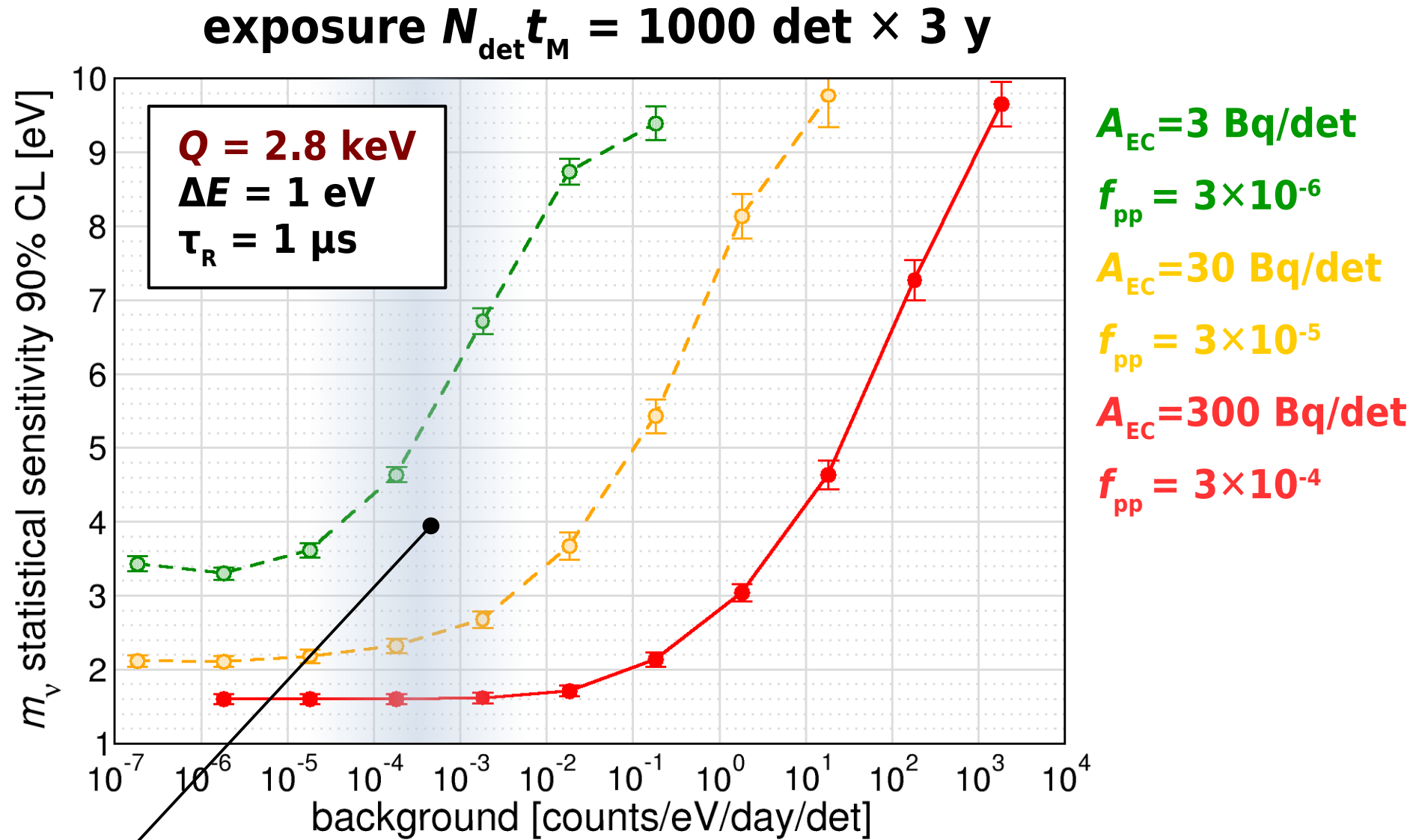
- pile-up in ROI (single-hole) $b_{\text{pp}} \approx 0.35 f_{\text{pp}} A \text{ c/eV/day}$
- environmental γ radiation
- γ , X and β from close surroundings
- cosmic rays
 - ▷ GEANT4 (HOLMES) $\rightarrow b_{\text{CR}} \approx 10^{-5} \text{ c/eV/day/det}$ (0 - 4 keV)
- internal radionuclides
 - ▷ ^{166m}Ho (β^- , $Q=1.8 \text{ MeV}$, $\tau_{1/2}=1200 \text{ y}$)
 - ▷ co-produced with ^{163}Ho : $A(^{163}\text{Ho})/A(^{166m}\text{Ho}) > 500$ (HOLMES)
 - ▷ GEANT4 (HOLMES) $\rightarrow b_{^{166m}\text{Ho}} \approx 0.3 \text{ c/eV/day/det/Bq}(^{166m}\text{Ho})$



$A(^{163}\text{Ho})$ [Bq]	f_{pp}	b_{pp} [c/eV/day]	max b^\ddagger [c/eV/day]	max $A(^{166m}\text{Ho})$	$A(^{163}\text{Ho})/A(^{166m}\text{Ho})$	$N(^{163}\text{Ho})/N(^{166m}\text{Ho})$
3	3×10^{-6}	3.2×10^{-6}	10^{-5}	3×10^{-5}	10^5	4×10^5
300	3×10^{-4}	3.2×10^{-2}	10^{-1}	0.3	1000	4000

[‡] from MC simulations

Effect of flat background on sensitivity



expected from simulations and preliminary HOLMES and ECHo measurements

The ECHo experiment

Arrays of Magnetic Metallic Calorimeters with ion-implanted ^{163}Ho

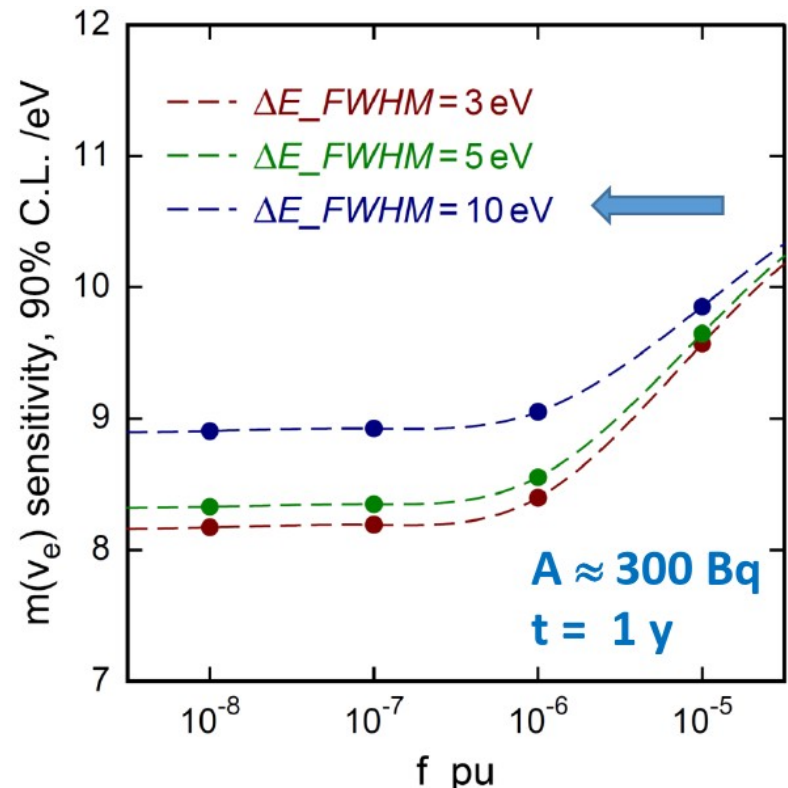
L. Gastaldo et al. Eur. Phys. J.
Special Topics 226, 1623 (2017)



ECHo-1k

- number of detectors: 60~100 pixels
- activity: 1~5 Bq/pixel
- read-out: two-stage dc-SQUID
- energy resolution: $\Delta E_{\text{FWHM}} < 10 \text{ eV}$

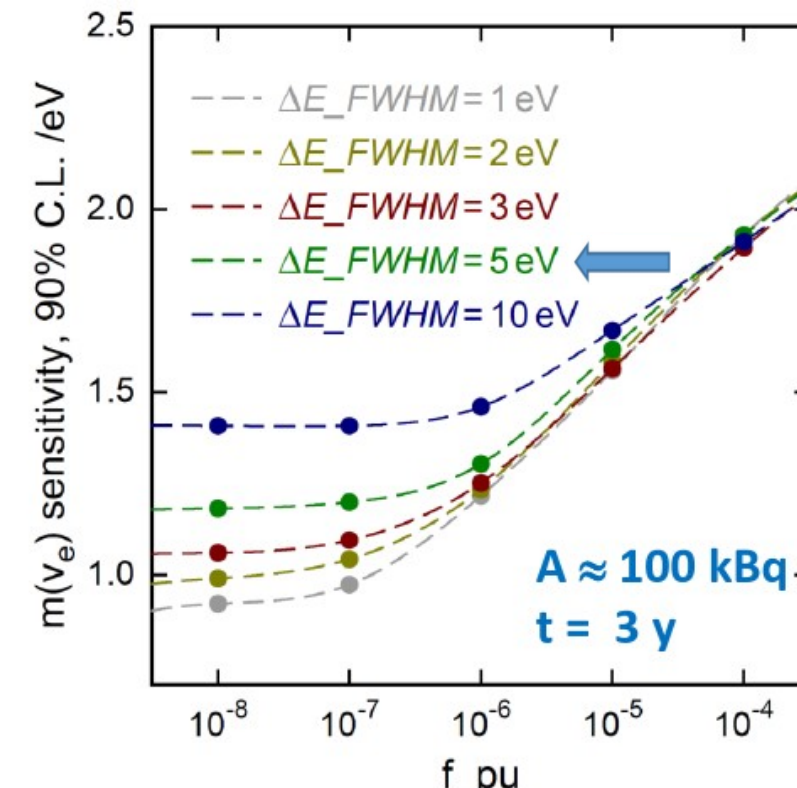
→ m_{ν} statistical sensitivity <20 eV



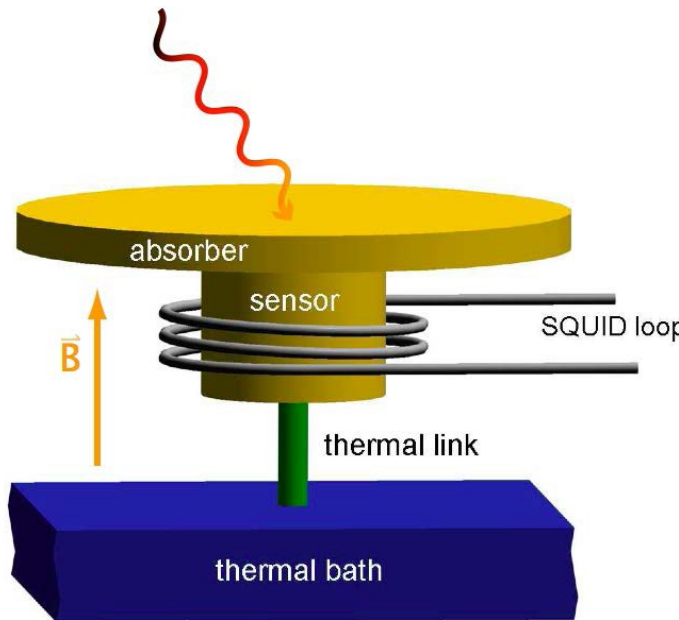
ECHo-100k

- number of detectors: 12000 pixels
- activity: 10 Bq/pixel
- read-out: microwave multiplexing
- energy resolution: $\Delta E_{\text{FWHM}} < 5 \text{ eV}$

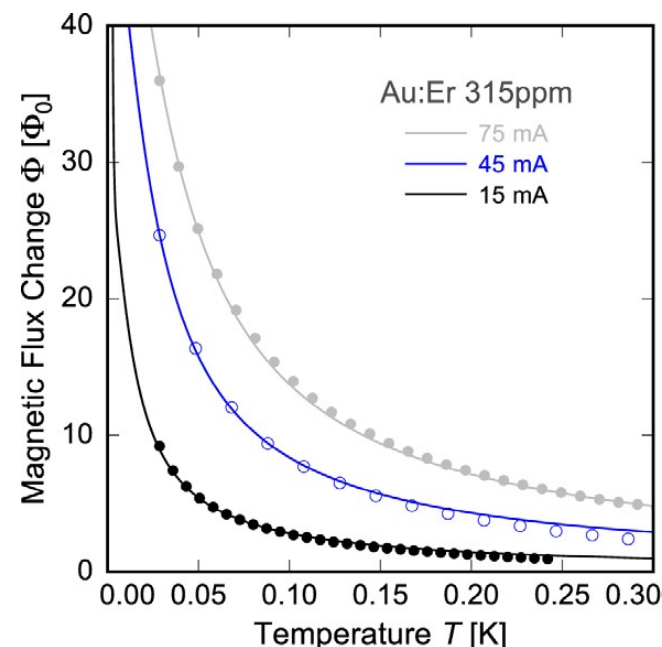
→ m_{ν} statistical sensitivity <1.5 eV



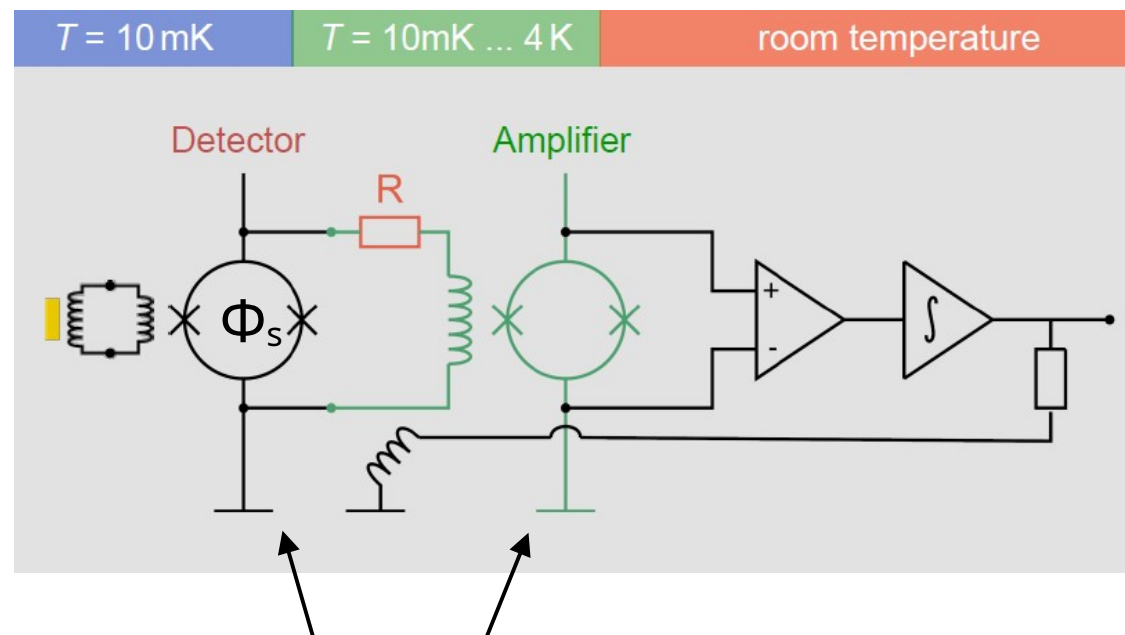
Metallic Magnetic sensors



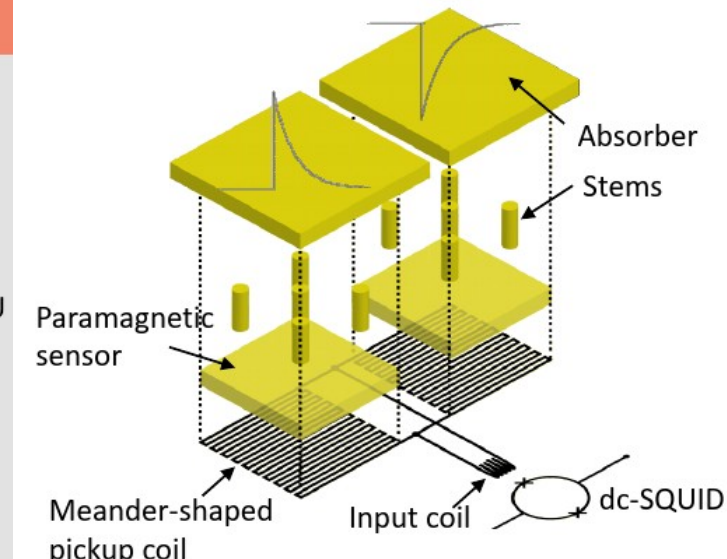
- paramagnetic temperature sensor
- Ag:Er, Au:Er ...
- no power dissipation in the sensor no Johnson noise
- SQUID read-out → multiplexing for arrays
- large operating temperature range 10 - 100 mK
 - ECHo operates at $T \approx 30$
- strong spin-electron coupling → fast rise time (≈ 100 ns)



$$\Delta T \rightarrow \Delta M \rightarrow \Delta \Phi_s$$



dc-SQUIDs



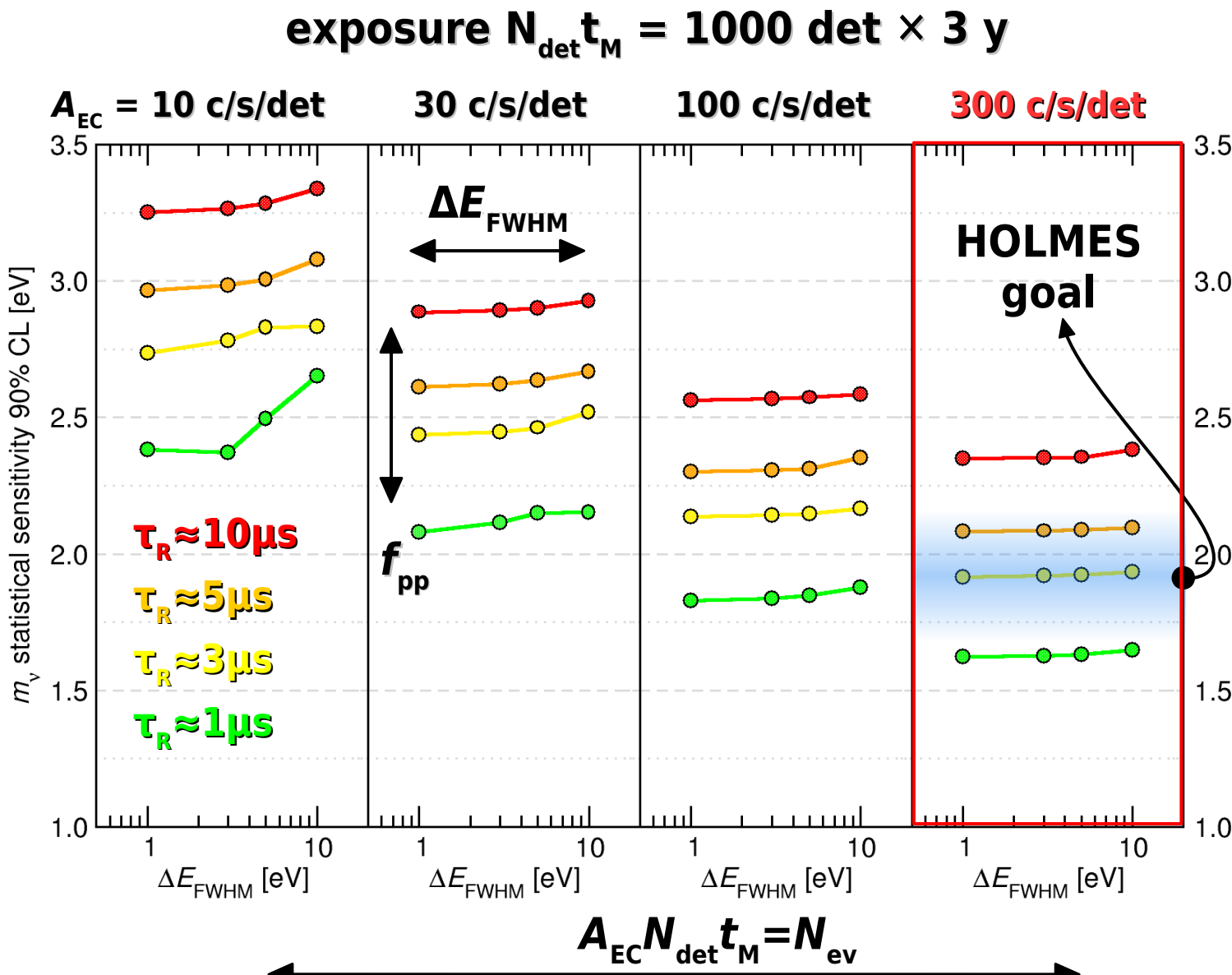
gradiometric configuration
2 MMC pixels on 1 SQUID channel

The HOLMES experiment

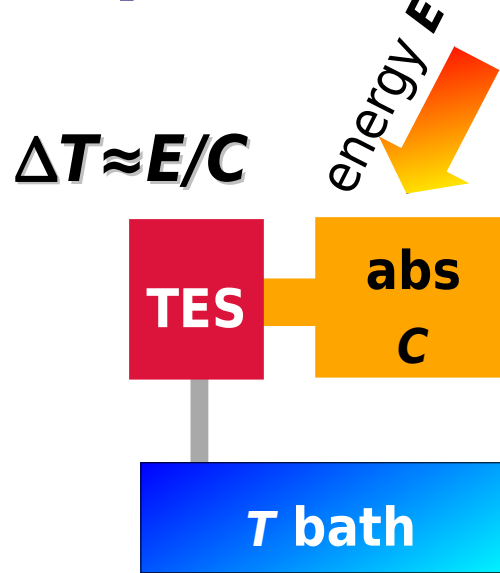
- Transition Edge Sensors (TES) microcalorimeters with ion-implanted ^{163}Ho
- 6.5×10^{13} atom/det $\rightarrow A_{\text{EC}} = 300 \text{ c/s/det}$
- $\Delta E \approx 1 \text{ eV}$ and $\tau_R \approx 1 \mu\text{s}$
- 1000 TES microcalorimeters
- 16×64 -pixel arrays with microwave multiplexed read-out
- $6.5 \times 10^{16} {}^{163}\text{Ho}$ nuclei $\rightarrow \approx 18 \mu\text{g}$
 $\rightarrow 3 \times 10^{13}$ events in 3 years
- $\rightarrow m_\nu$ statistical sensitivity $\approx 1 \text{ eV}$



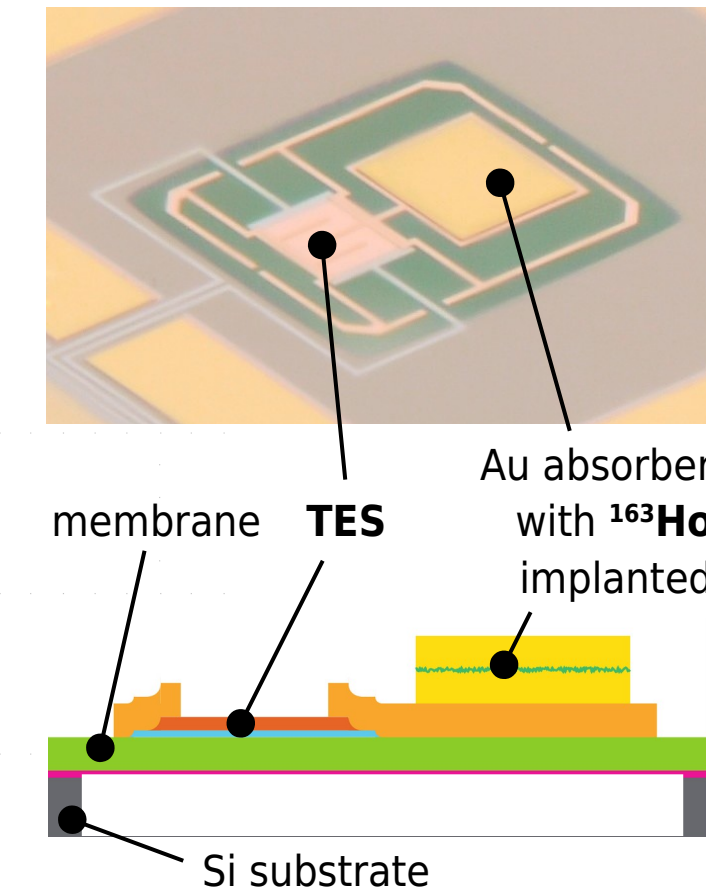
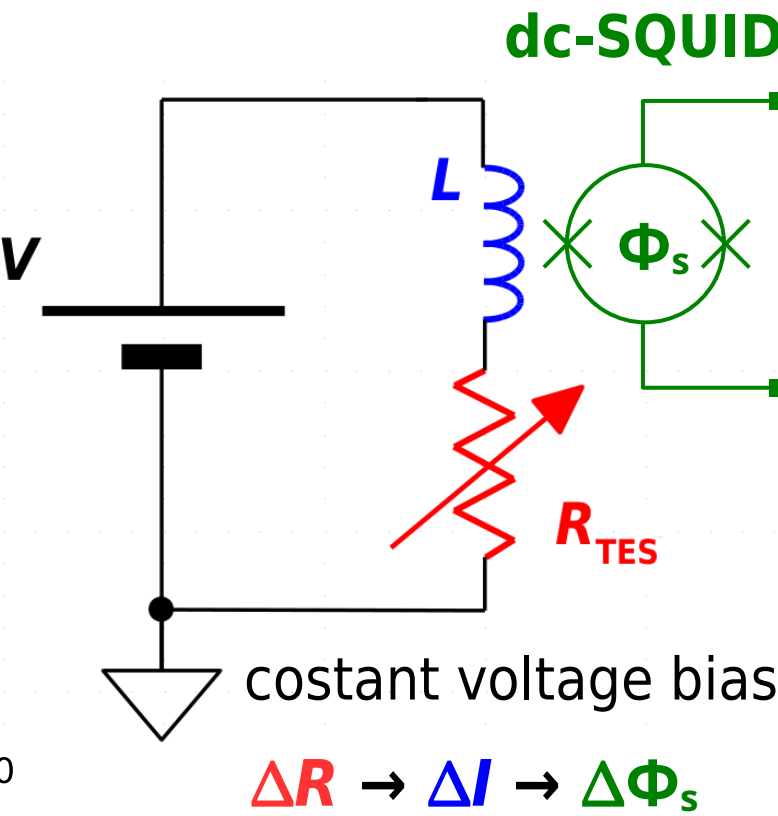
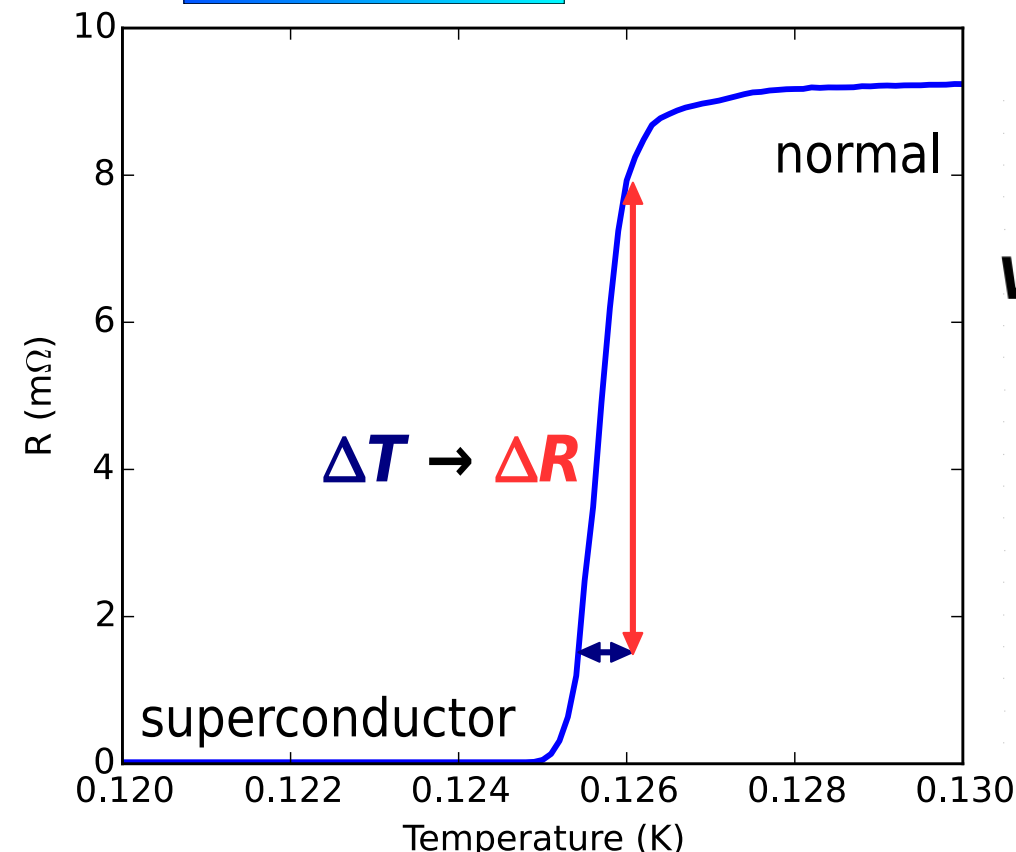
B. Alpert et al., Eur. Phys. J. C, (2015) 75:112



Superconducting transition edge sensors (TES)

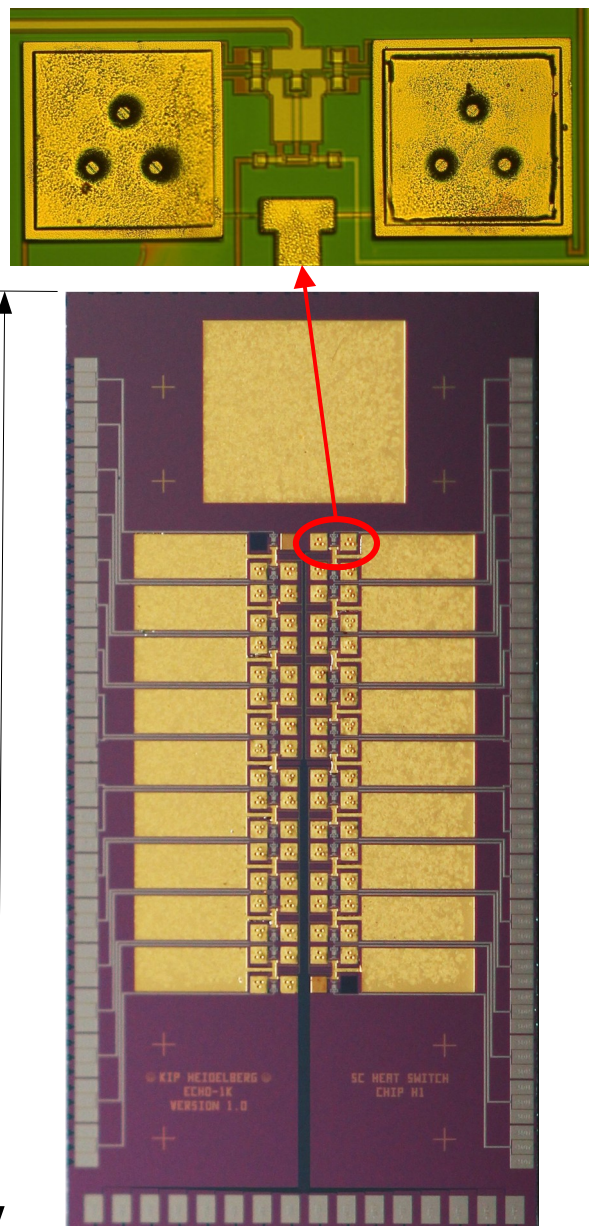


- superconducting thin films operated inside the phase transition at T_c
 - HOLMES: Mo/Cu bilayer tuned for $T_c \approx 100$ mK
- high sensitivity $TdR/(RdT) \approx 100 \rightarrow$ high energy resolution $\sigma_E^2 \approx \xi^2 k_B T^2 C$
- strong internal coupling \rightarrow high intrinsic speed
- low impedance ($m\Omega \rightarrow \Omega$) \rightarrow SQUID read-out \rightarrow multiplexing for arrays

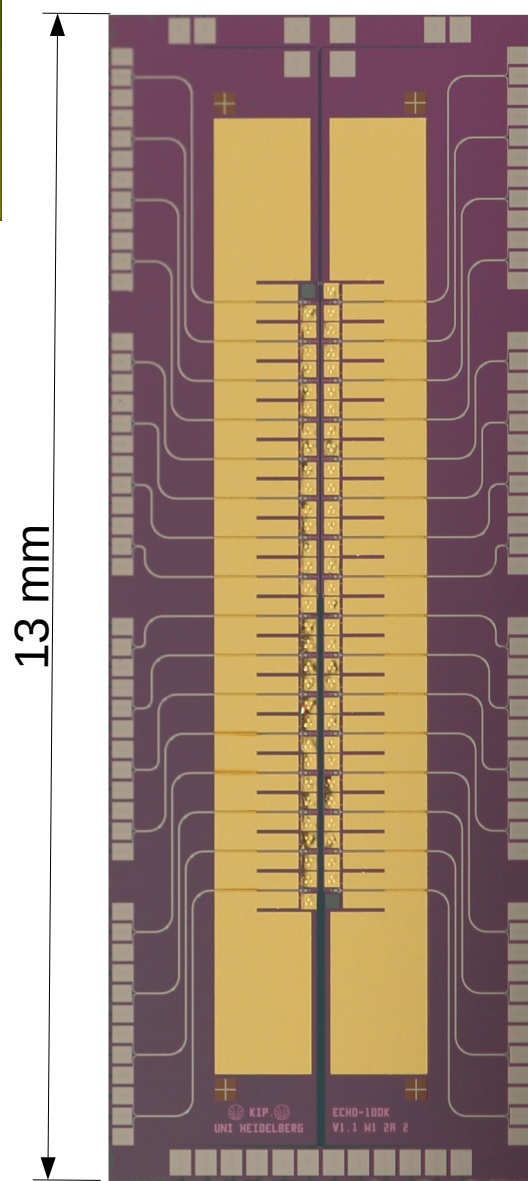


Microcalorimeters arrays

ECHo-1k



ECHo-100k

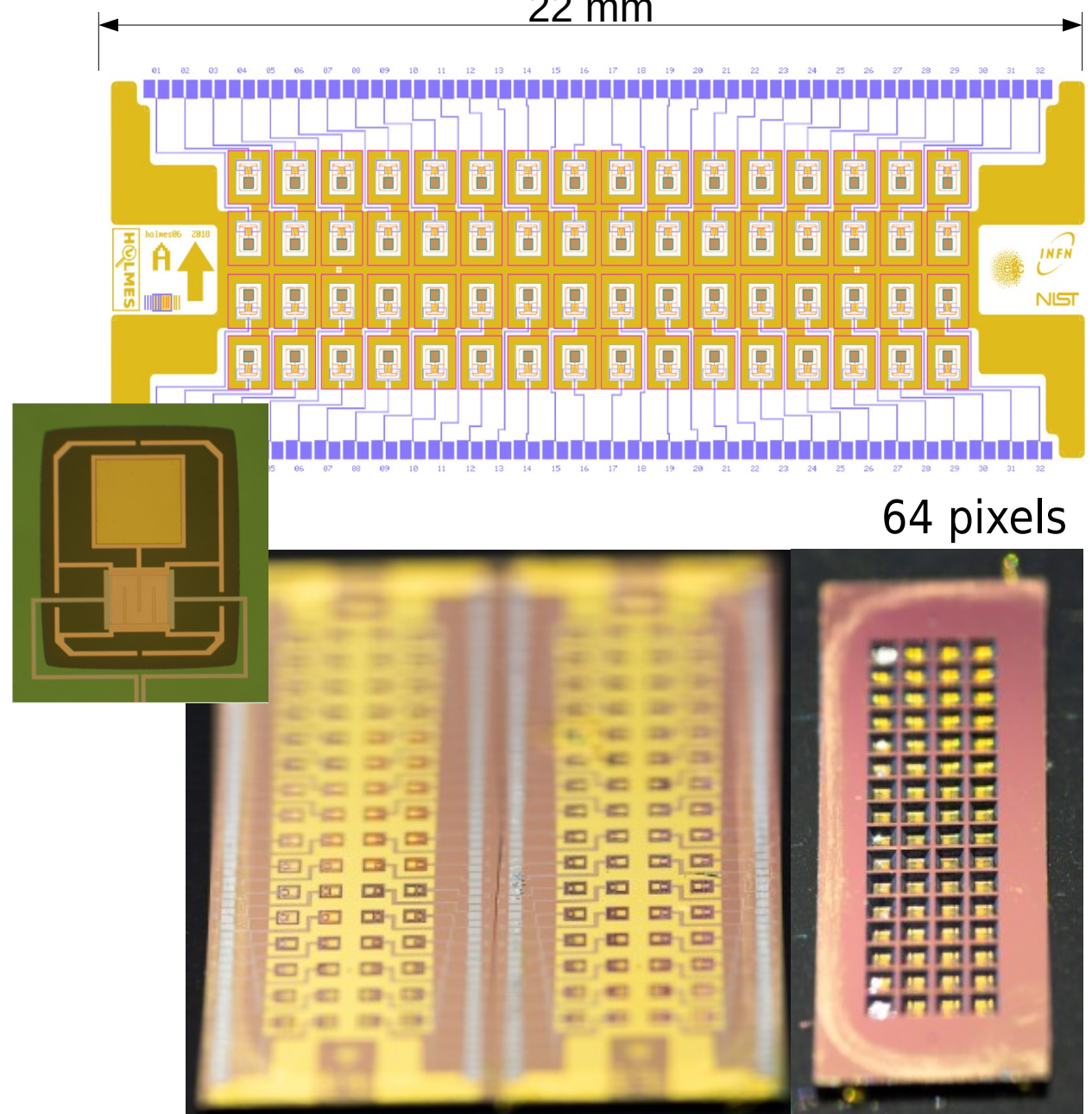


72 pixels

64 pixels

HOLMES

22 mm



KOH micromachining

Isotope production

$$^{162}\text{Er} (\text{n},\gamma) ^{163}\text{Er} \quad \sigma_{\text{thermal}} \approx 20 \text{ b}$$

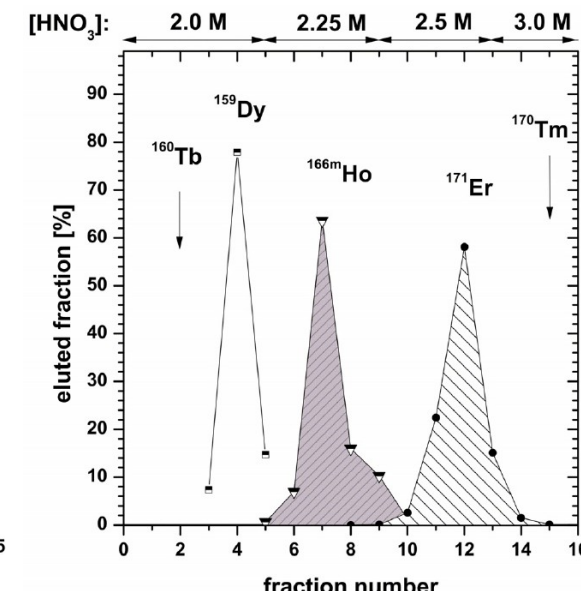
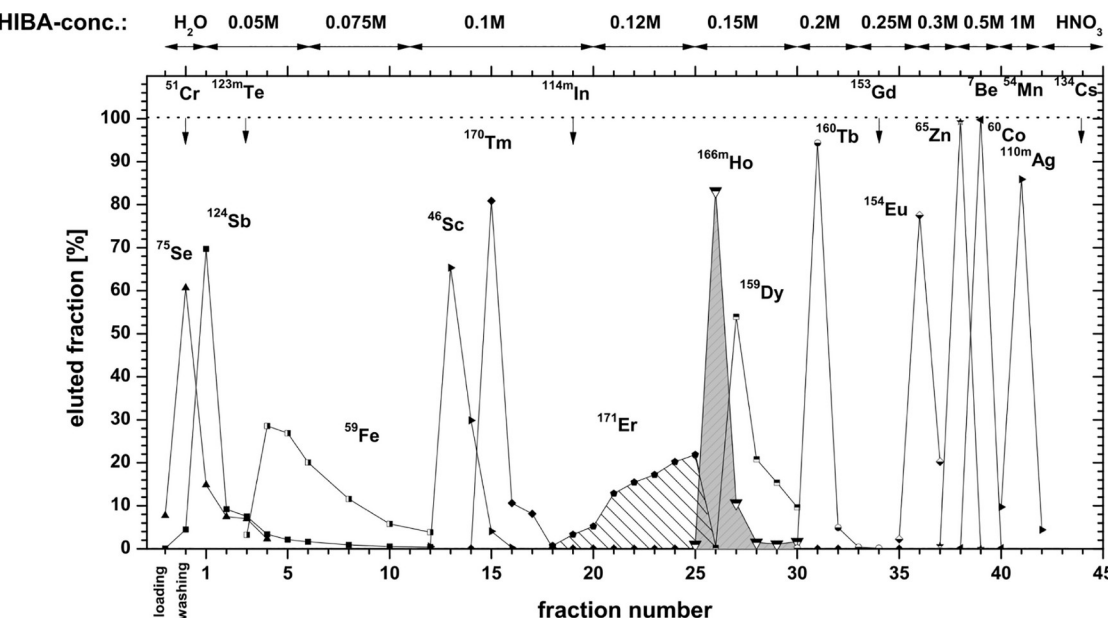
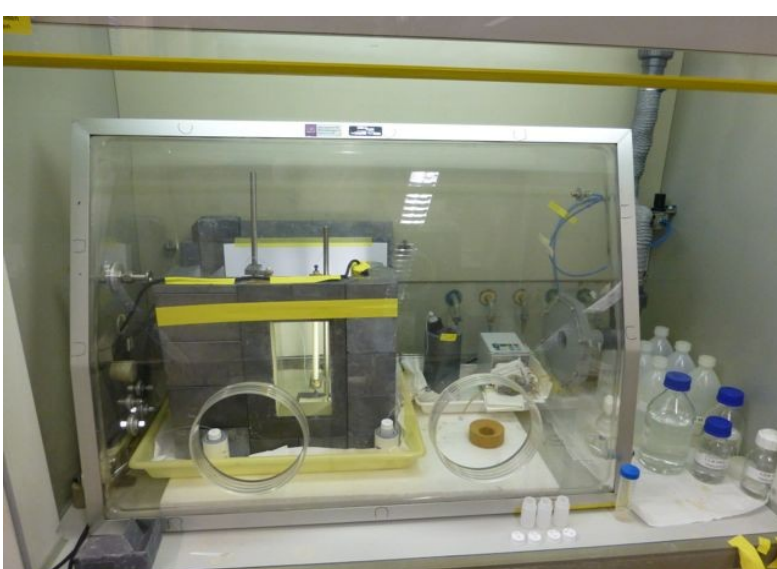
$$^{163}\text{Er} \rightarrow ^{163}\text{Ho} + \nu_e \quad \tau_{1/2}^{\text{EC}} \approx 75 \text{ min}$$

- ^{162}Er irradiation at **ILL nuclear reactor** (Grenoble, France)
 - ▶ thermal neutron flux $1.3 \times 10^{15} \text{ n/cm}^2/\text{s}$
- Ho chemical separation with ion-exchange resins in hot-cell to remove Er matrix and radioactive products
- separation efficiency >90 %
- HOLMES has collected $\approx 200 \text{ MBq}$ of ^{163}Ho (+ $\approx 400 \text{ kBq}$ of ^{166m}Ho)

Tm 163 1.81 h	Tm 164 5.1 m	Tm 165 30.06 h	Tm 166 7.70 h	Tm 167 9.25 d	Tm 168 93.1 d
ϵ β^+ ... γ 104; 69; 241; 1434; 1397...	ϵ β^+ 2.9... γ 91; 1155; 769...	ϵ β^+ ... γ 243; 47; 297; 807...	ϵ β^+ 1.9... γ 779; 2052; 184; 1274...	ϵ γ 532...	ϵ β^+ ... γ 198; 816; 447...
Er 162 0.139	Er 163 75 m	Er 164 1.601	Er 165 10.3 h	Er 166 33.503	Er 167 2.3 s 22.869
σ_{19} $\sigma_{n,\alpha} < 0.011$	β^+ ... γ 1114...	σ_{13} $\sigma_{n,\alpha} < 0.0012$	ϵ $\text{no } \gamma$	σ_{3+14} $\sigma_{n,\alpha} < 7E-5$	γ 208 $\sigma_{n,\alpha} 3E-6$
Ho 161 6.7 s	Ho 162 68 m	Ho 163 1.1 s	Ho 164 37 m	Ho 165 100	Ho 166 1200 a 26.80 h
ϵ γ 26; 78... ϵ^- γ 211	ϵ β^+ 1.1... γ 81; 1319... ϵ^- γ 58; 38... ϵ^- γ 185; 1220; 283; 937...	ϵ $\text{no } \gamma$ 4570 a	ϵ β^- 1.0... γ 91; 73... ϵ^- γ 37;	ϵ β^- 1.0... γ 81; 712... ϵ^- $\sigma_{3.1+58}$ $\sigma_{n,\alpha} < 2E-5$	β^- 0.7... γ 184; 810; 712... ϵ^- σ_{3100}
Dy 160 2.329	Dy 161 18.889	Dy 162 25.475	Dy 163 24.896	Dy 164 28.260	Dy 165 1.3 m
σ_{60} $\sigma_{n,\alpha} < 0.0003$	σ_{600} $\sigma_{n,\alpha} < 1E-6$	σ_{170}	σ_{120} $\sigma_{n,\alpha} < 2E-5$	$\sigma_{1610+1040}$	β^- 1.3... γ 95; 515... σ_{2000} σ_{3500}

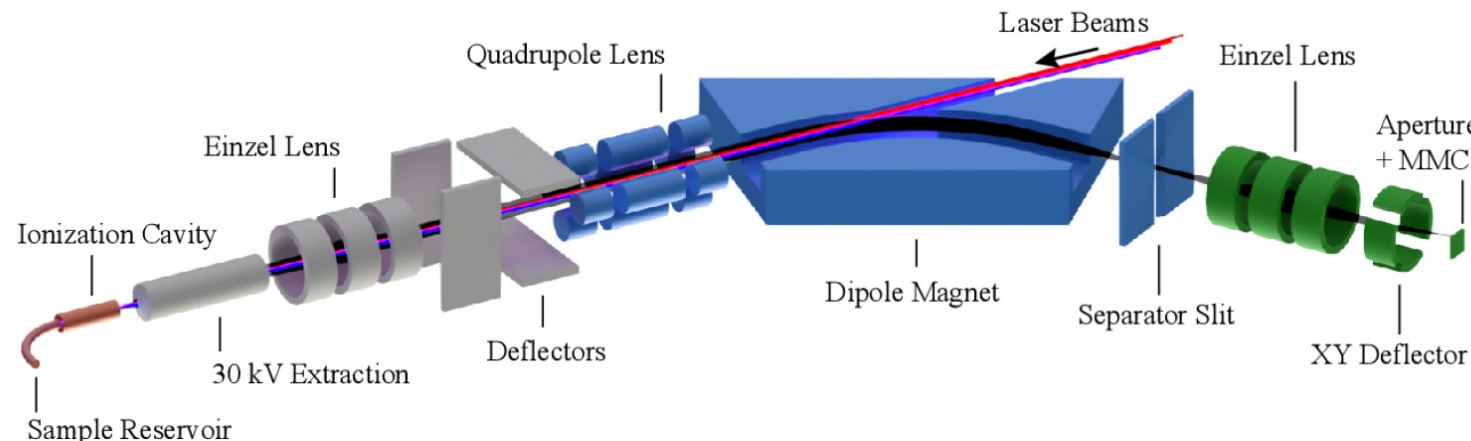
H. Dorrer et al., Radiochim. Acta, 106 (2018) 535

S. Heinitz et al., PLoS ONE 13(8): e0200910



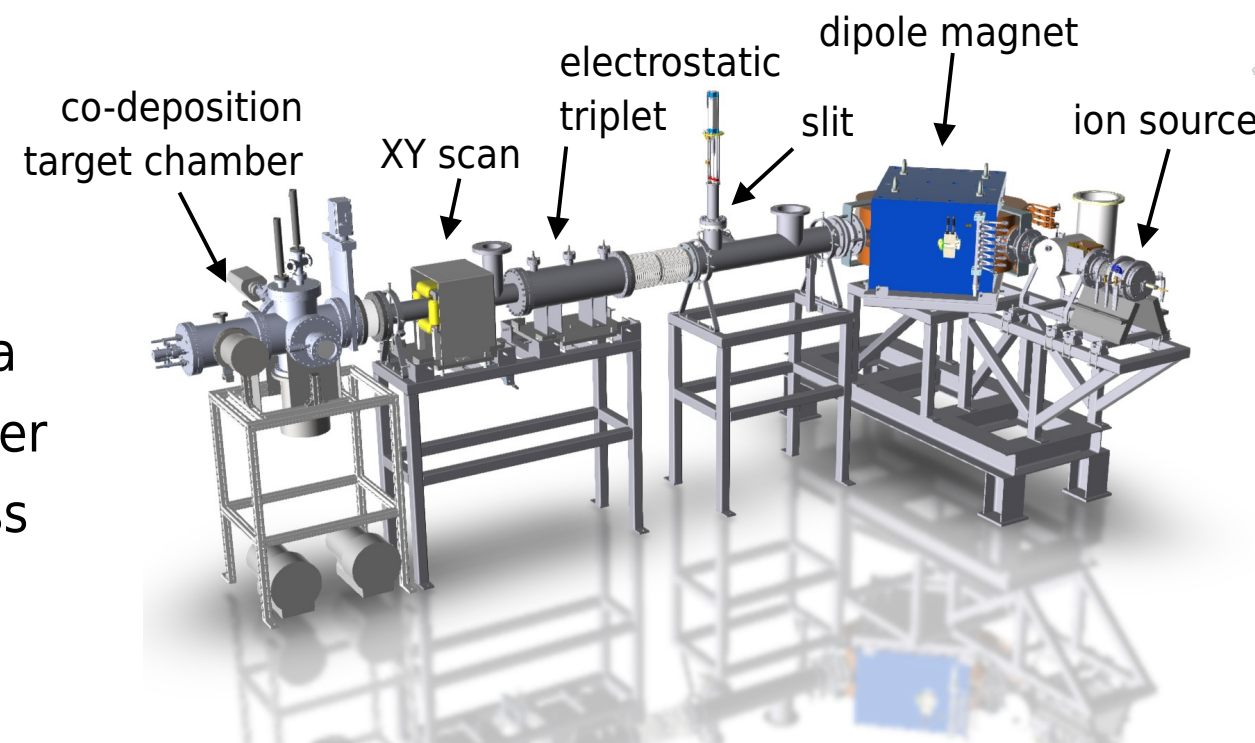
Mass separation and isotope embedding

^{166m}Ho must be separated by magnetic mass spectrometer
requires high current, high source and geometrical efficiency



HOLMES: Ar plasma sputter ion source

- all components ready for installation in Genova
- now testing without triplet/XY-scan and chamber
- high current ion source optimization in progress

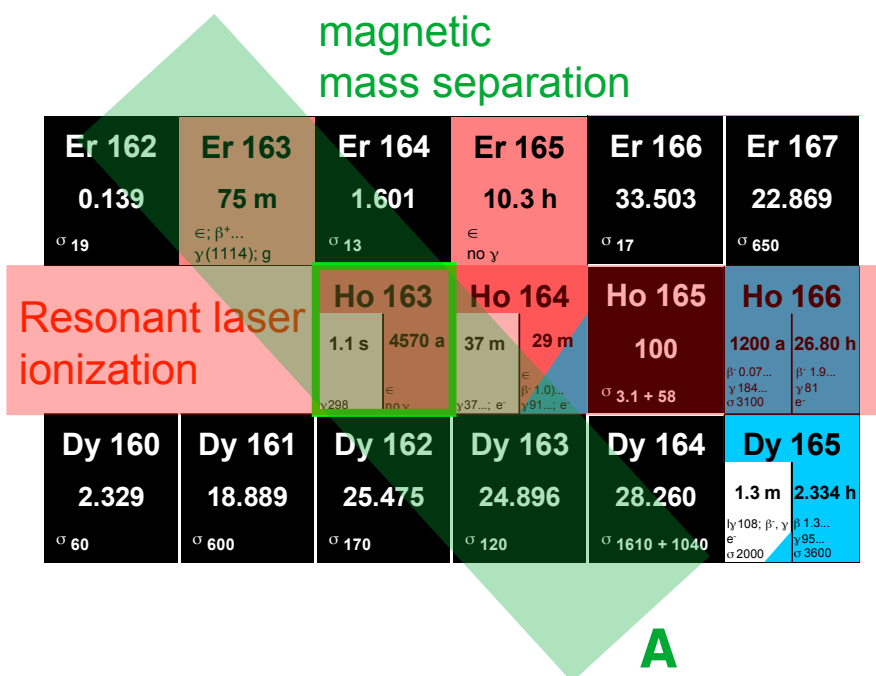


ECHO: resonant ionization laser ion source (RILIS)

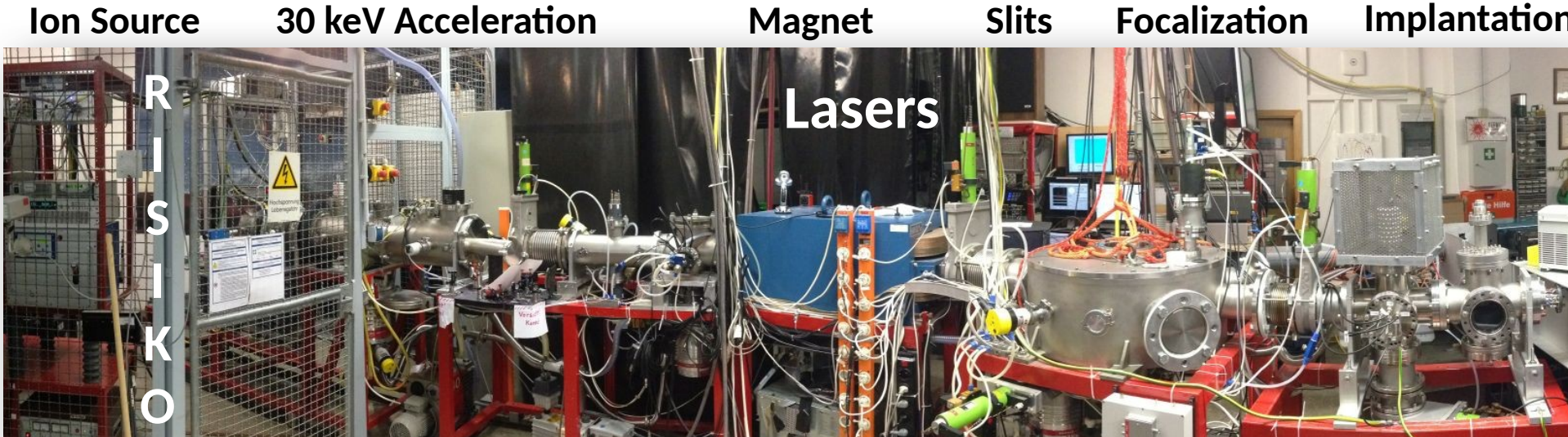
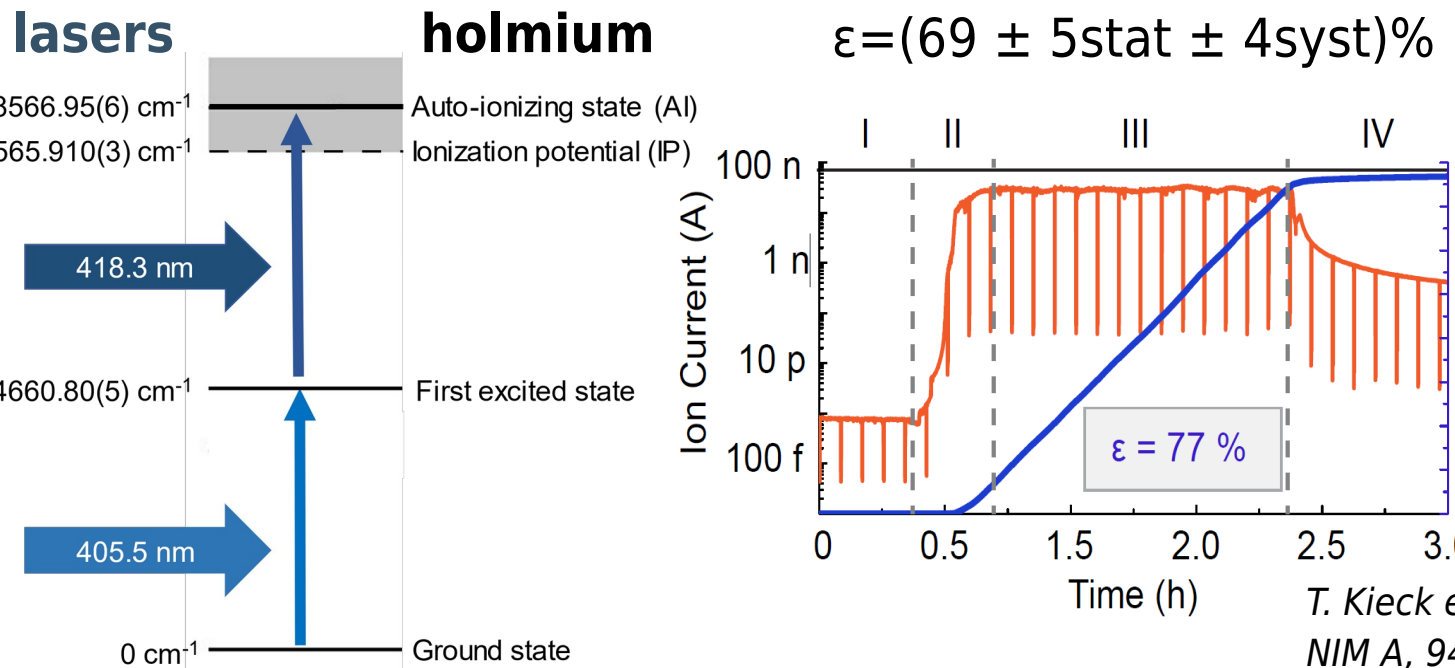
- RISIKO at Mainz University
- efficiency: $(69 \pm 5\text{stat} \pm 4\text{syst})\%$
- $^{166m}\text{Ho}/^{163}\text{Ho} < 4(2)10^{-9}$

T. Kieck et al., NIM A, 945, 2019, 162602.

RISIKO for ECHO

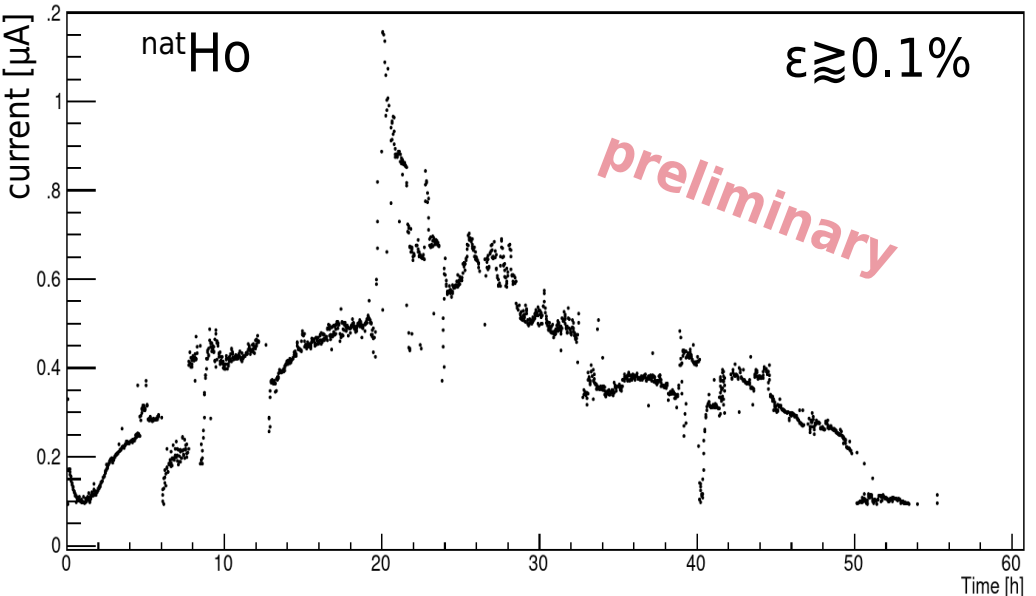
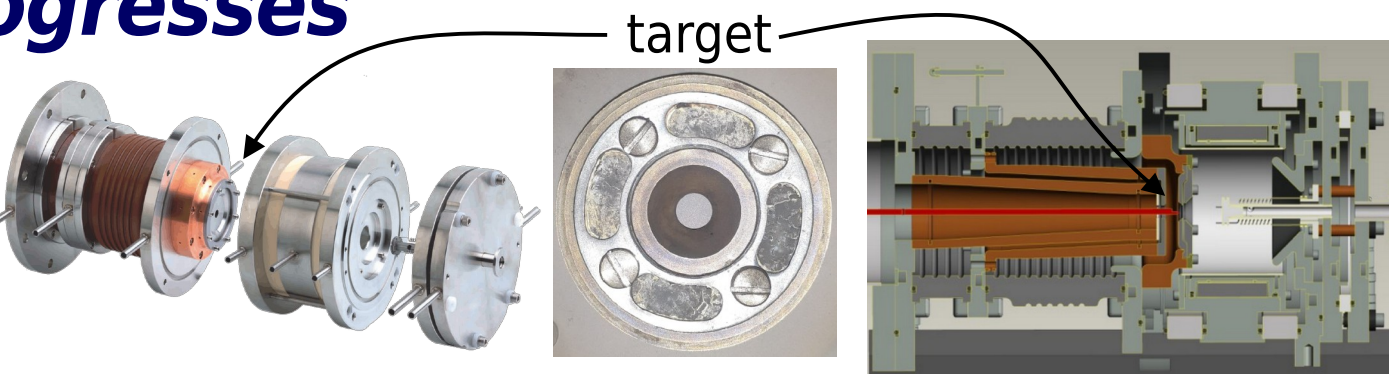


- Resonant laser ionization
 - 2 lasers tuned to selectively ionize Ho
 - high ionization efficiency ion source

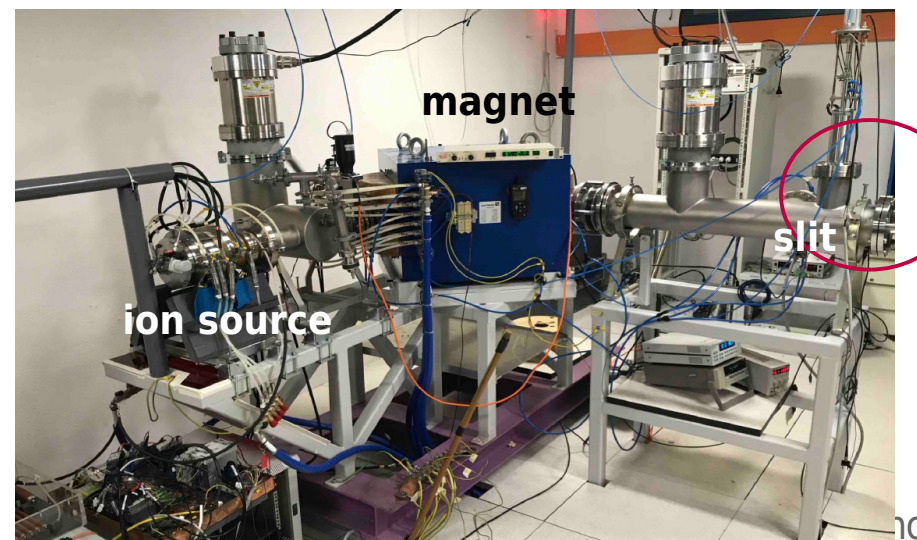
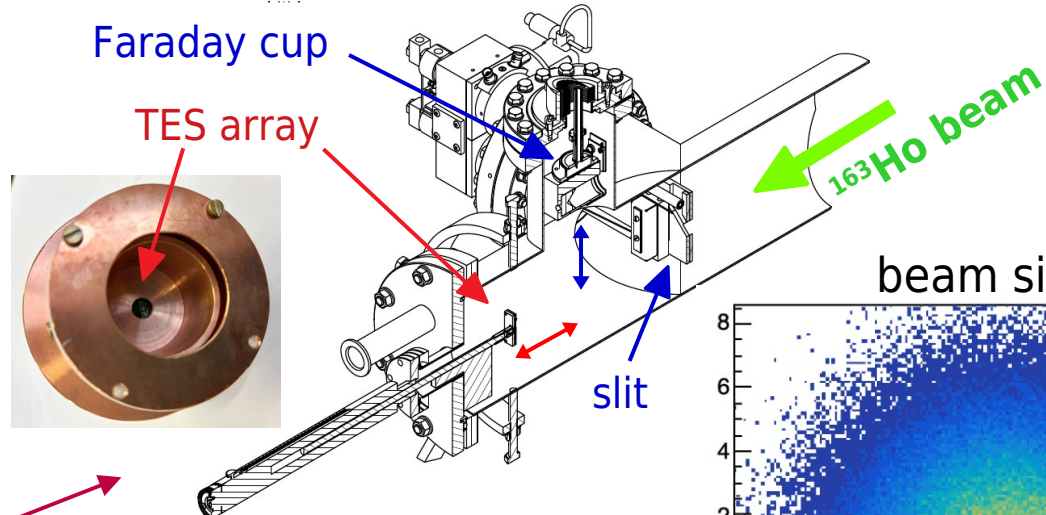


HOLMES ion implanter progresses

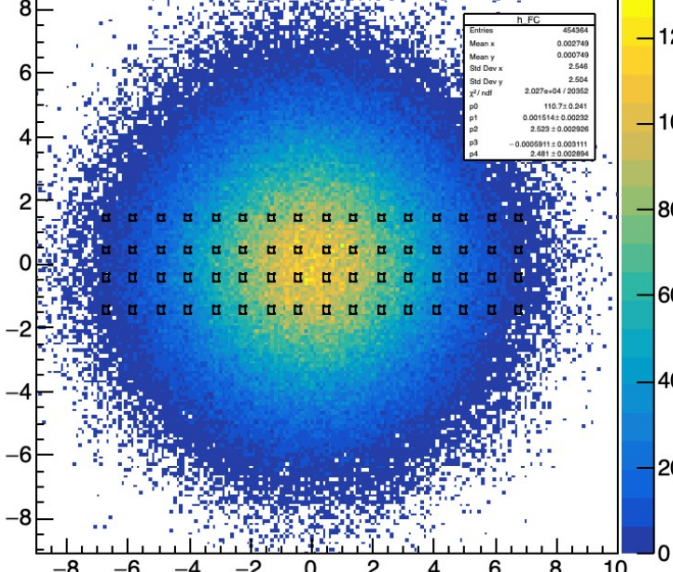
- high current sputter source
- several sputter targets tested
- sintered Zr-Y-Al-Ho(NO_3)₃
- highest efficiency, current and stability



configuration without focussing
for first low activity implants



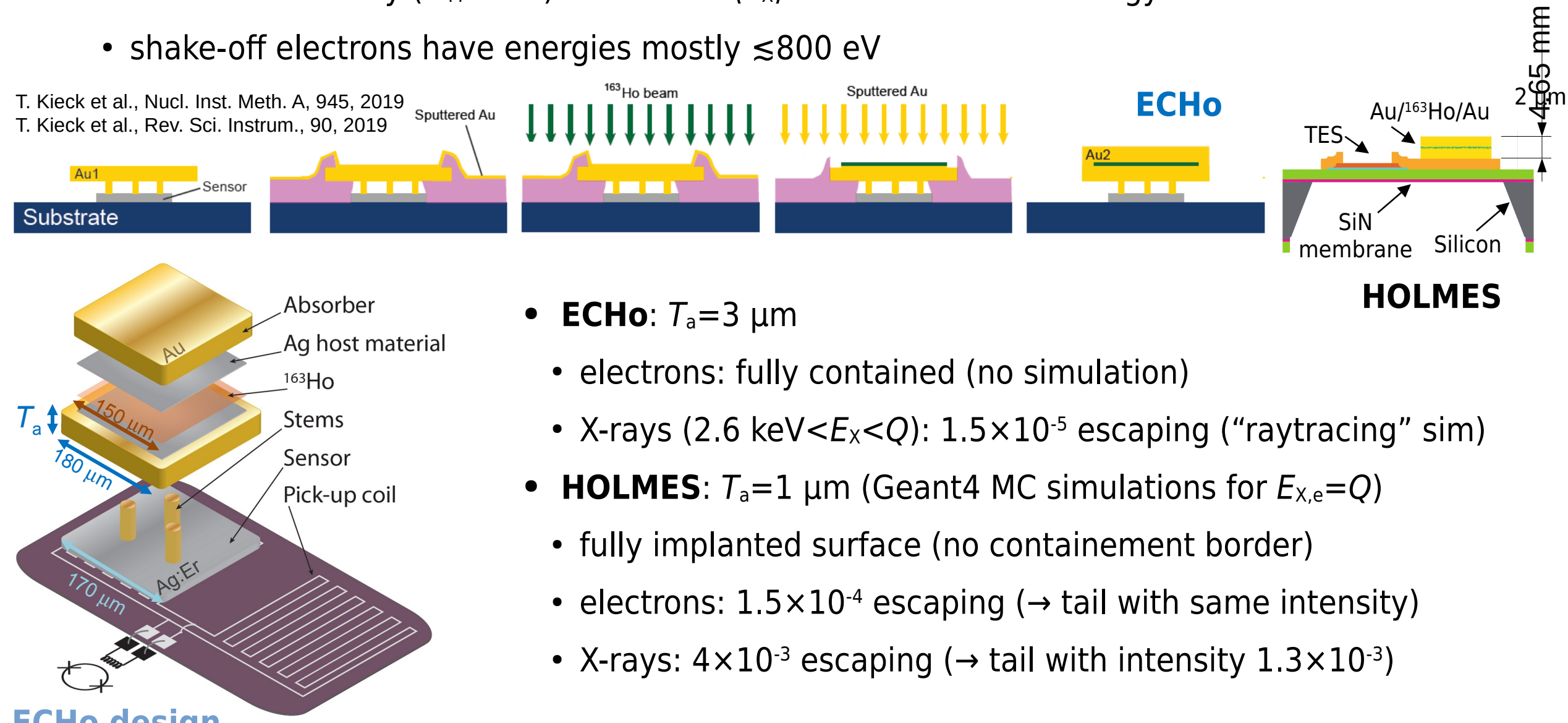
8 MBq of ${}^{163}\text{Ho}$ in ${}^{\text{nat}}\text{Ho}$ (0.35%)
 $I({}^{\text{nat}}\text{Ho}) = 0.2 \mu\text{A}$ for 24 h
 → peak pixel activity $\approx 1 \text{ Bq}$
 uniform activity with 3 shots



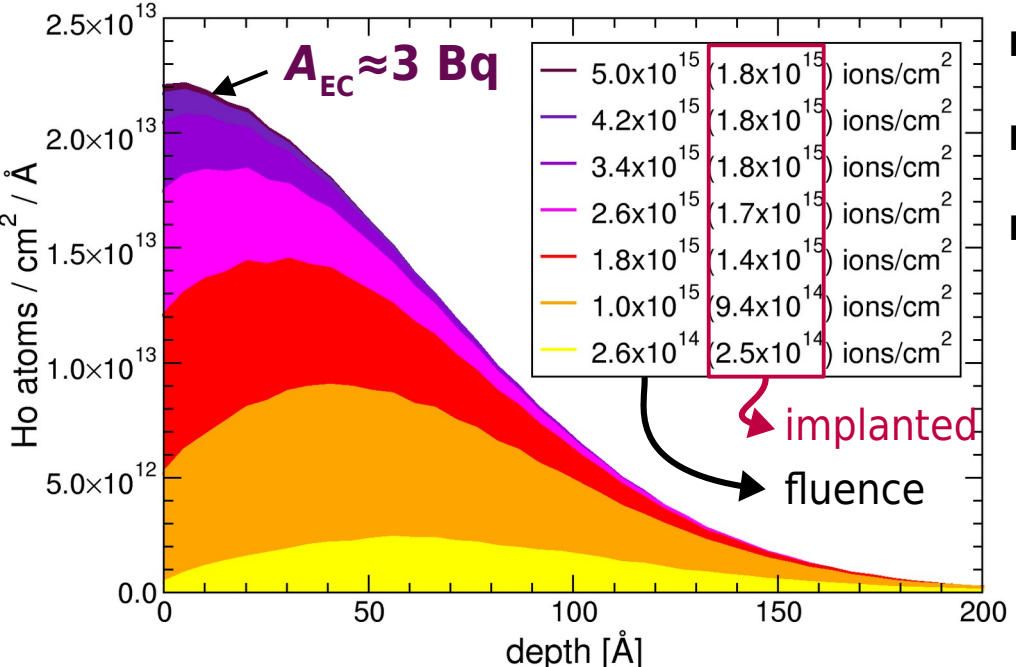
Detector absorbers for calorimetry

- Au absorber must stop all radiation from atomic de-excitations with $E_c \approx Q$
 - for H=M1 \rightarrow 3-4 Auger/C-K electrons carry most of E_c (the most energetic with $\langle E_e \rangle \approx 2$ keV)
 - for H=M1 \rightarrow rarely ($\omega_M \approx 10^{-3}$) one X with $\langle E_X \rangle \approx 2.5$ keV and low energy electrons
 - shake-off electrons have energies mostly $\lesssim 800$ eV

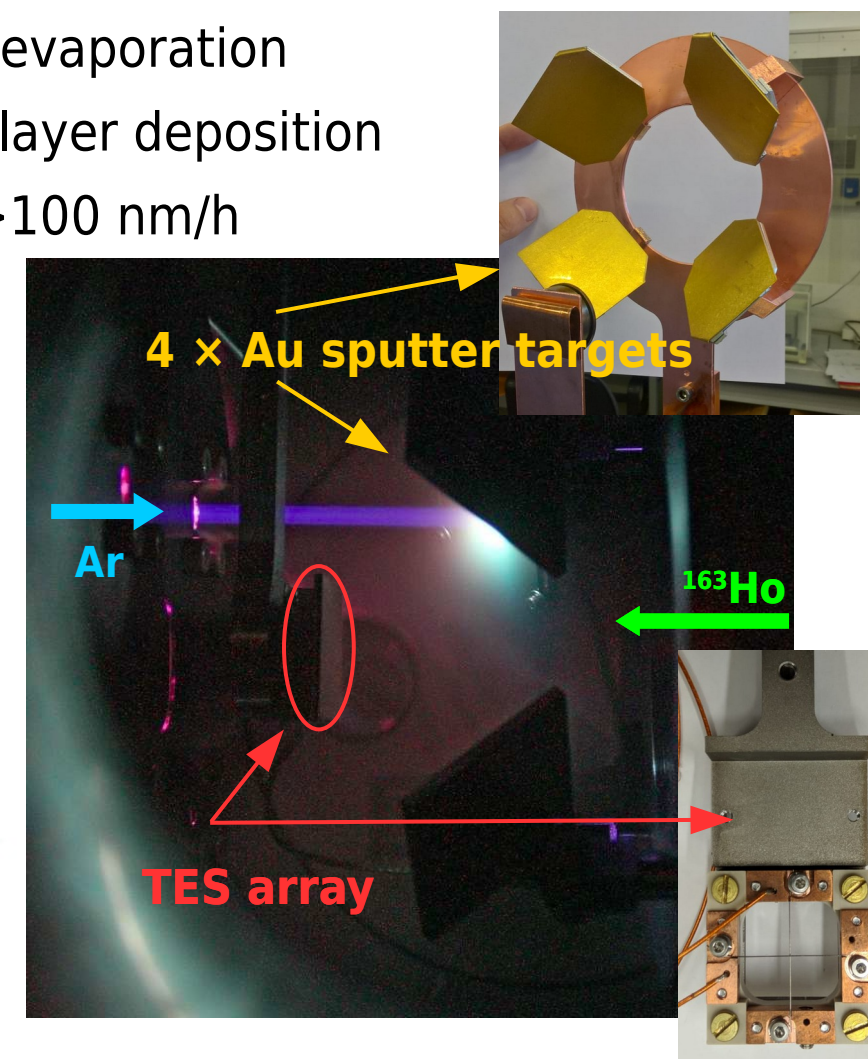
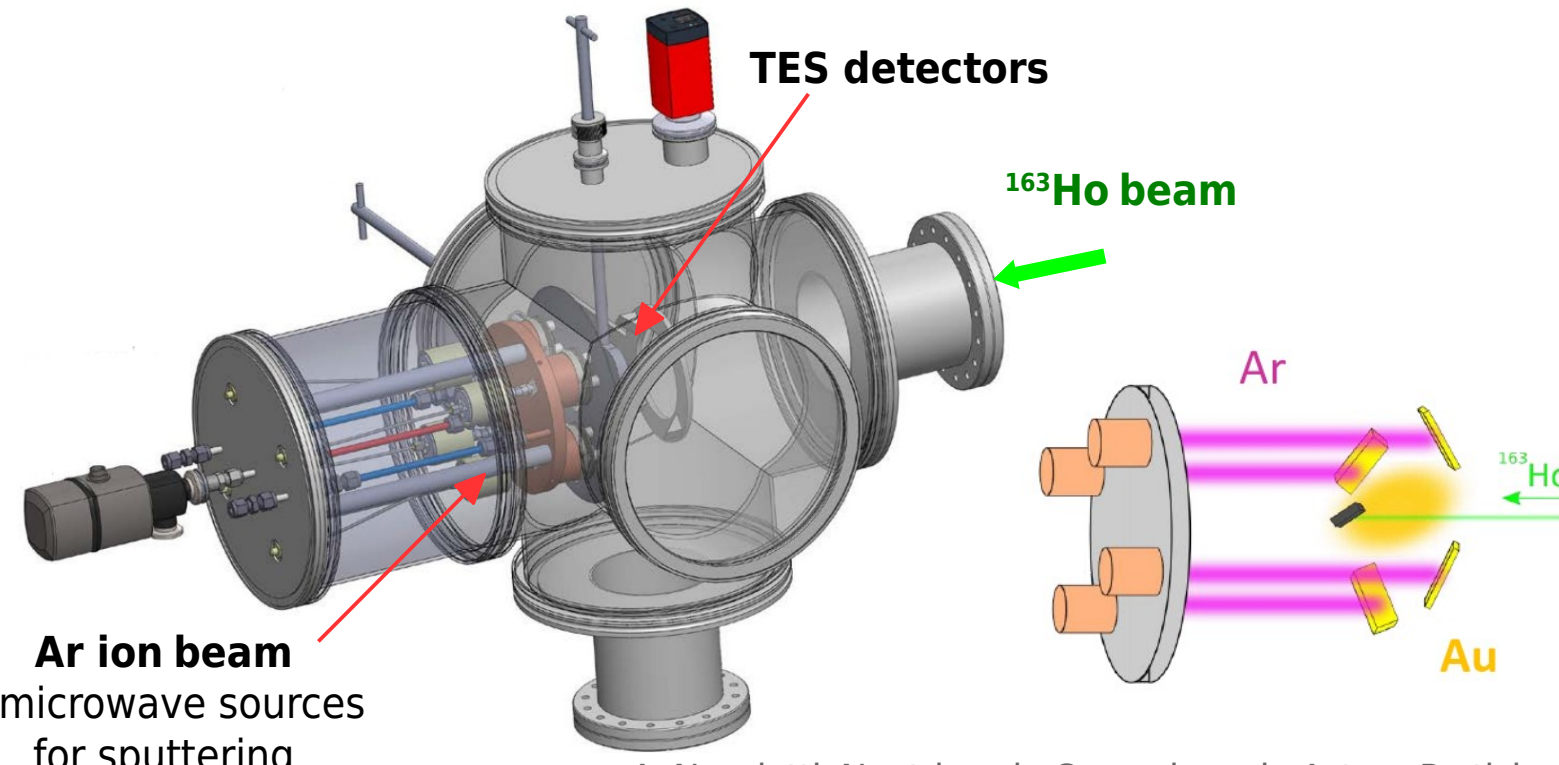
T. Kieck et al., Nucl. Inst. Meth. A, 945, 2019
T. Kieck et al., Rev. Sci. Instrum., 90, 2019



HOLMES co-deposition system



- ion implant simulation with SRIM2013
- ^{163}Ho ions on Au ($E_{ion} = 50 \text{ keV}$)
- ^{163}Ho ion beam sputters off Au from absorber ($\approx 26 \text{ Au/Ho}$)
 - implanted ^{163}Ho saturates at $A_{EC} \approx 3 \text{ Bq}$ (HOLMES design)
 - compensate by Au co-evaporation
 - in situ upper 1 μm Au layer deposition
→ with 4 ion sources >100 nm/h



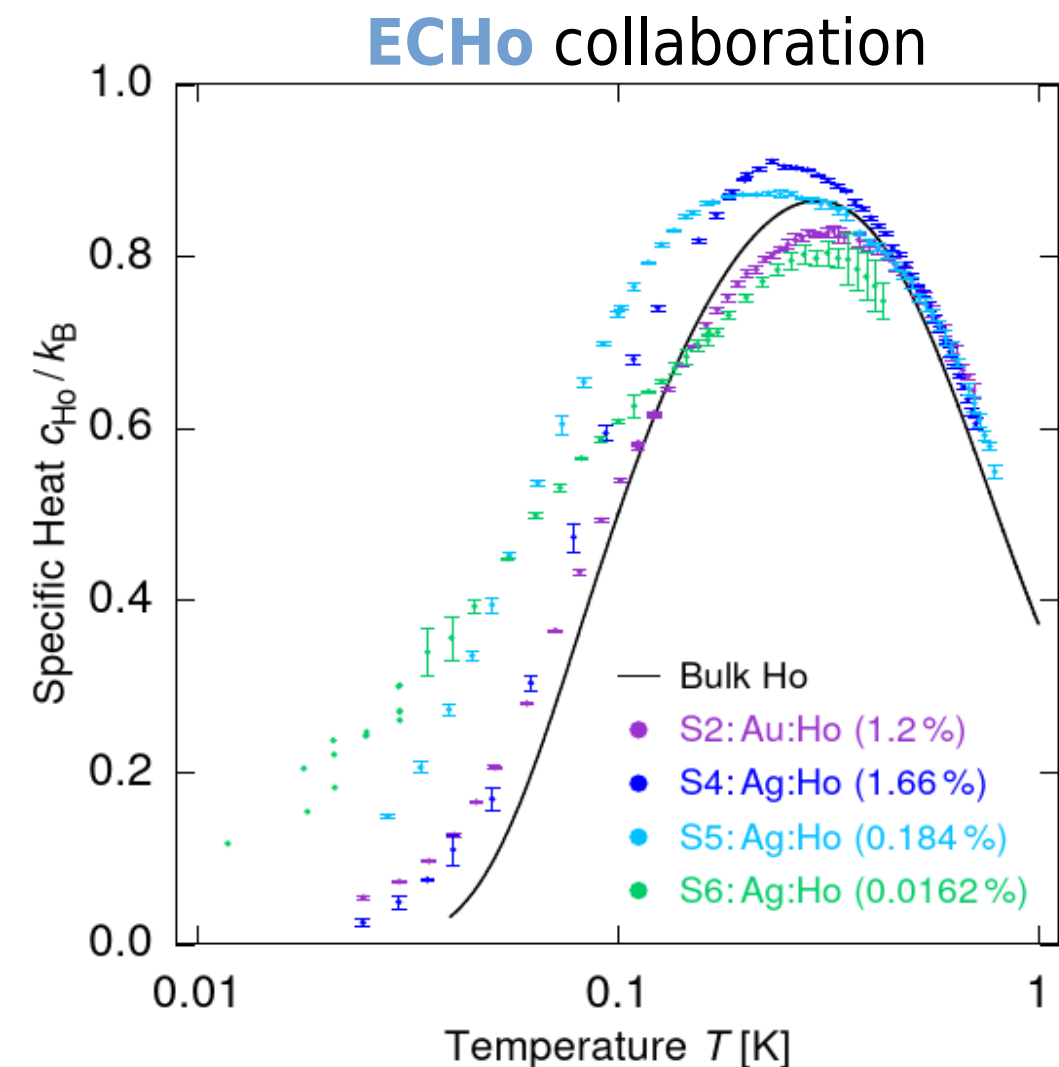
Implanted Ho heat capacity

- optimal ΔE depends on C and T

$$\Delta E \propto T\sqrt{C}$$

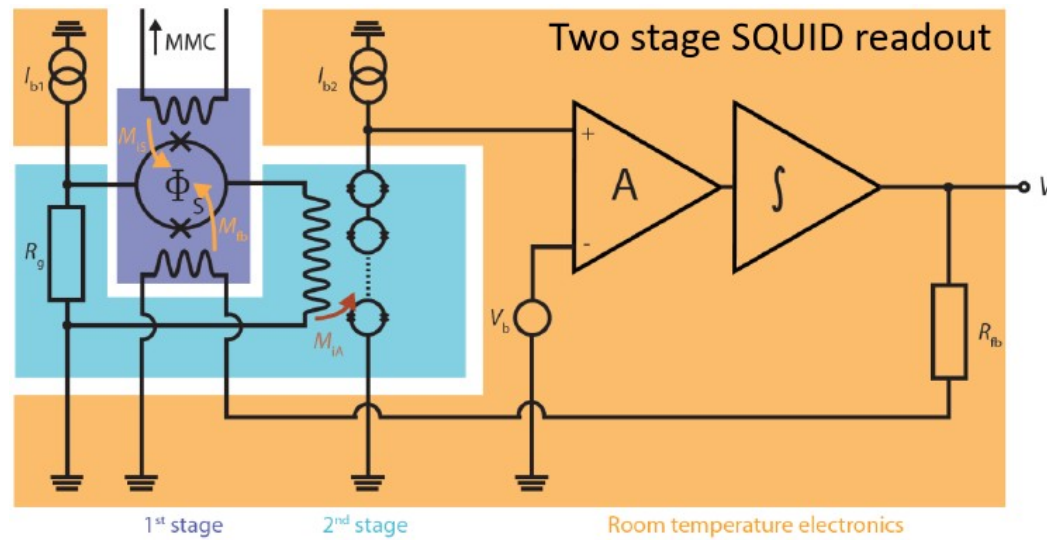
$$C = C_a + C_{\text{Ho}}$$

- Ho heat capacity C_{Ho} dominated by a Schottky anomaly at ≈ 300 mK
 - $J=8$ and $I=7/2 \rightarrow$ hyperfine and crystal field splittings
- contradictory C measurements for Ag:Ho
 - still under investigation
- high activities could be manageable
 - operating at 30 mK or below
 - $A=300$ Bq $\rightarrow x_{\text{Ho}} > 10\%$ \rightarrow closer to bulk C
 - to be explored by HOLMES

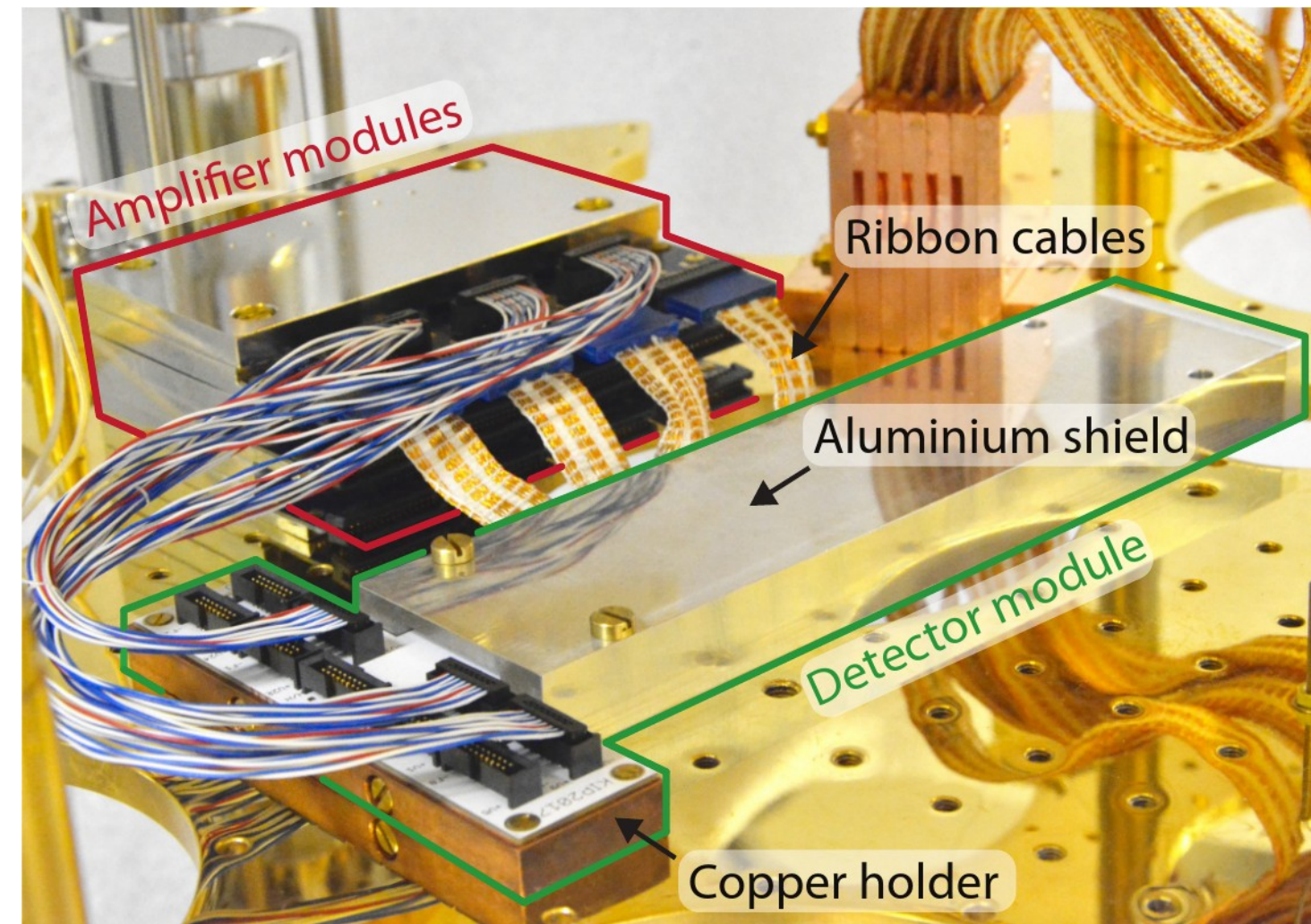


Herbst, M. et al., J Low Temp Phys 202, 106-120 (2021)

ECHO-1k read-out



parallel SQUID read-out
1 SQUID channel for 2 pixels



72 read-out channels for ECHO-1k

10 wires/channel to room temperature

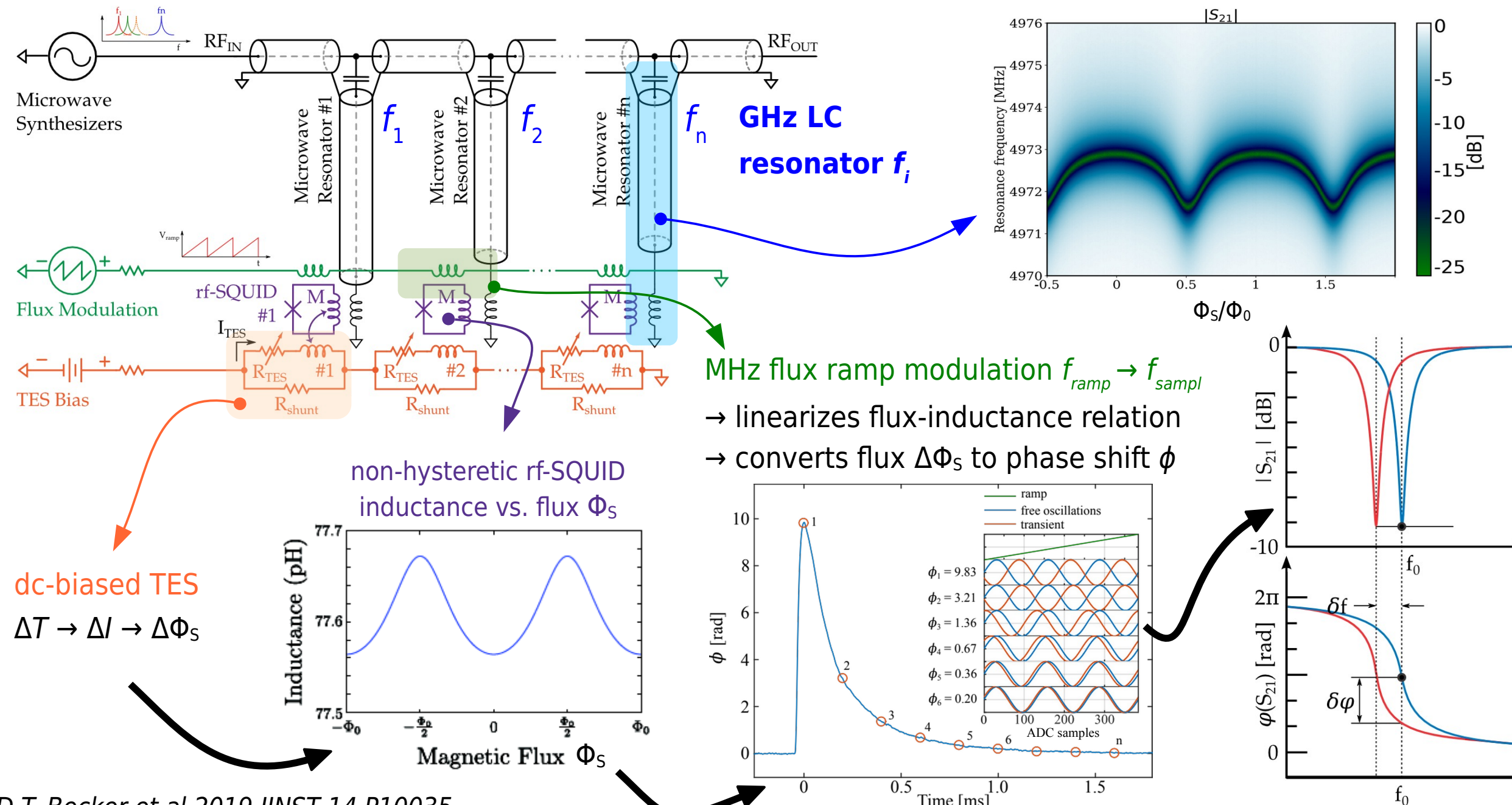
→ **720** wires from low to room temperature

→ not viable for ≥ 1000 channels ...

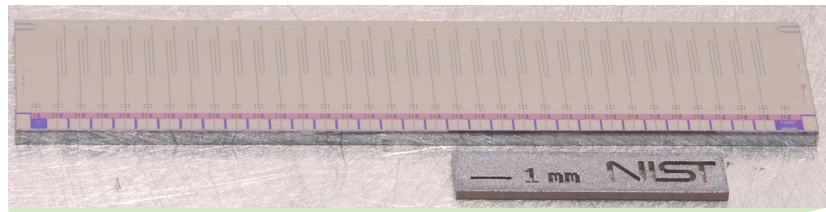
F. Mantegazzini et al. JINST16 (2021) P08003

Microwave multiplexing for array read-out

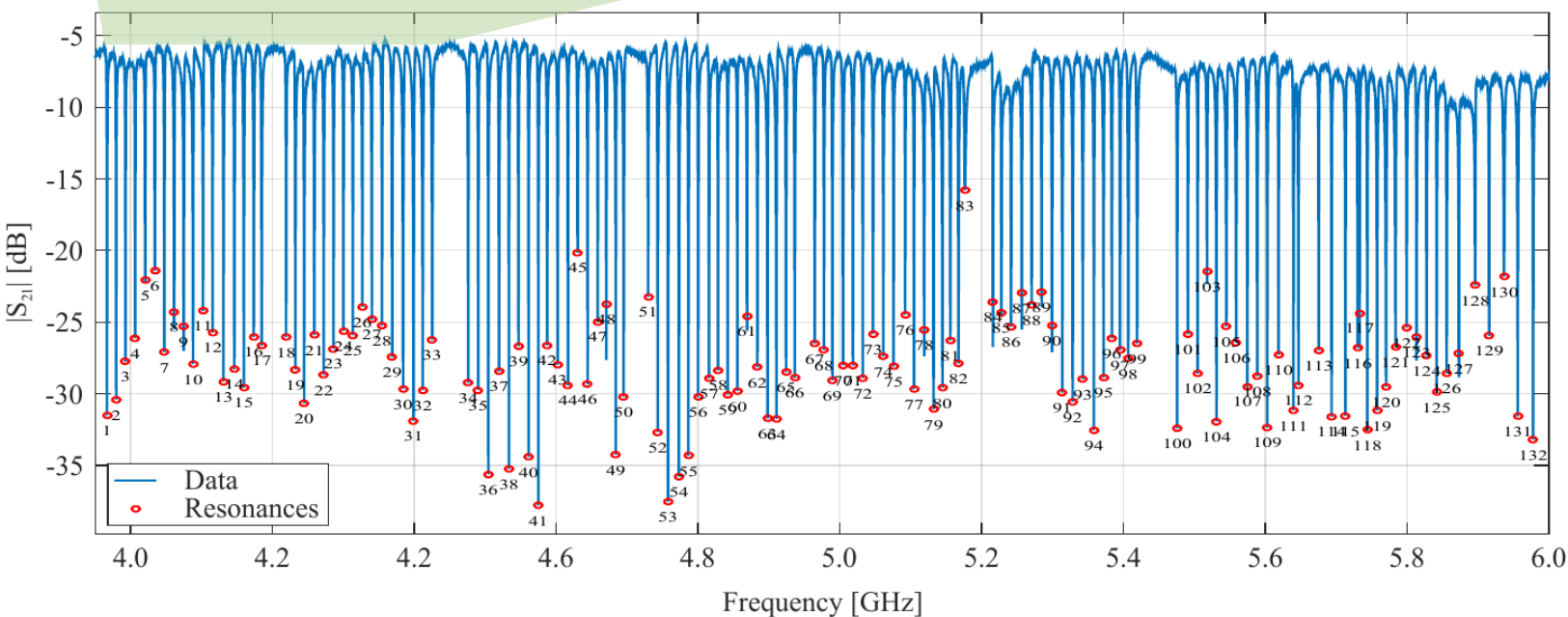
microwave multiplexing to read-out many detectors with one single RF line and HEMT amplifier



Microwave mux results: HOLMES



4 μmux chips in series
→ 132 resonances in 2 GHz

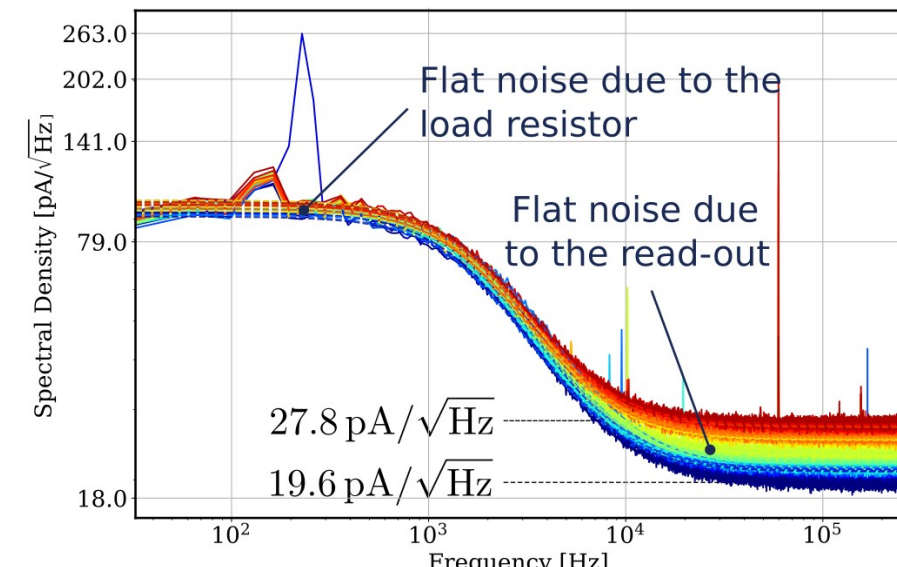
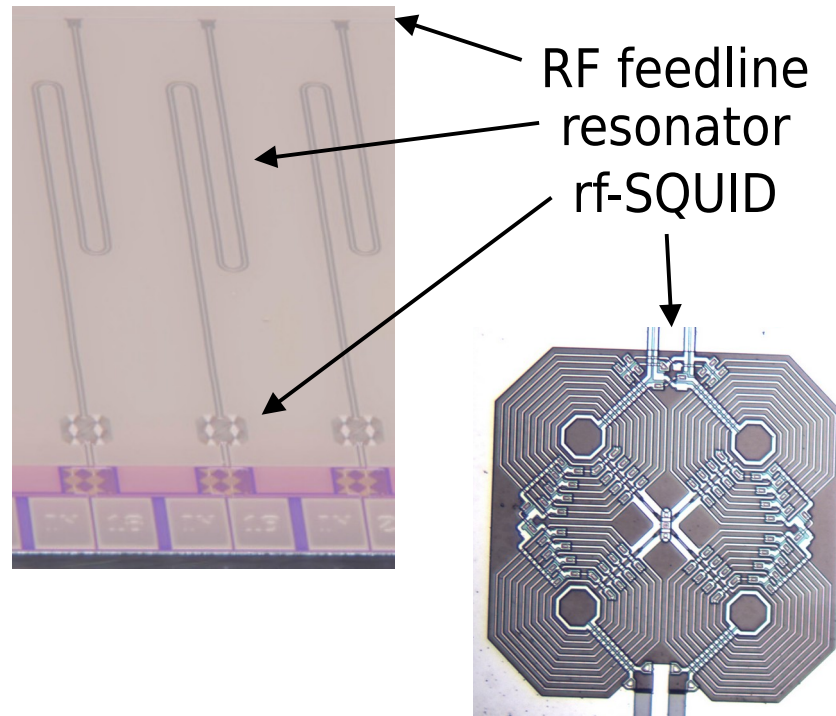


		required	measured
Resonator bandwidth	Δf_{BW} [MHz]	2	2 ± 1
Resonator spacing	Δf [MHz]	14	14 ± 1
Resonator depth	ΔS [dB]	>10	29 ± 6

$$\frac{n_{TES}}{f_{ADC}} \approx \frac{\tau_{rise}[\mu s]}{140} \frac{1}{MS/s}$$

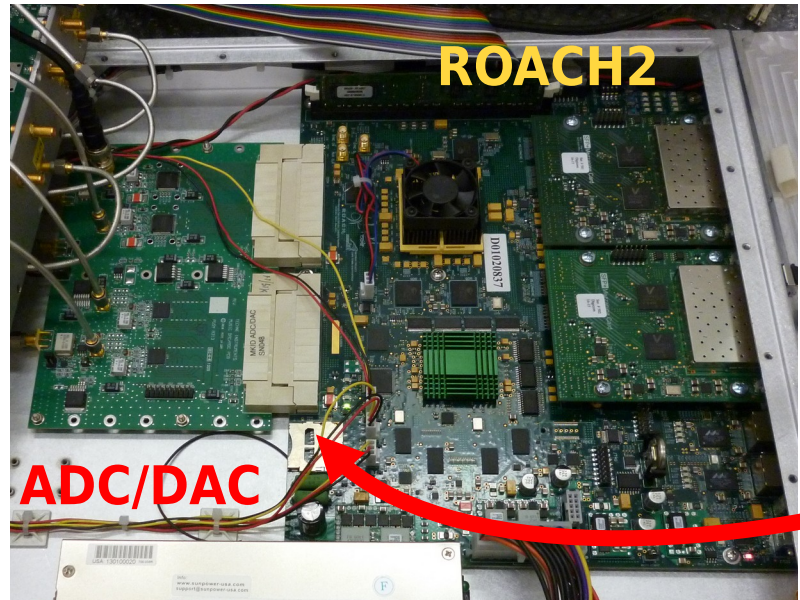
multiplexing factor n_{TES}
for $f_{ADC}=512$ MS/s and $\tau_{rise} \approx 10 \mu s$
→ $n_{TES} \approx 32$

D.T. Becker et al 2019 JINST 14 P10035

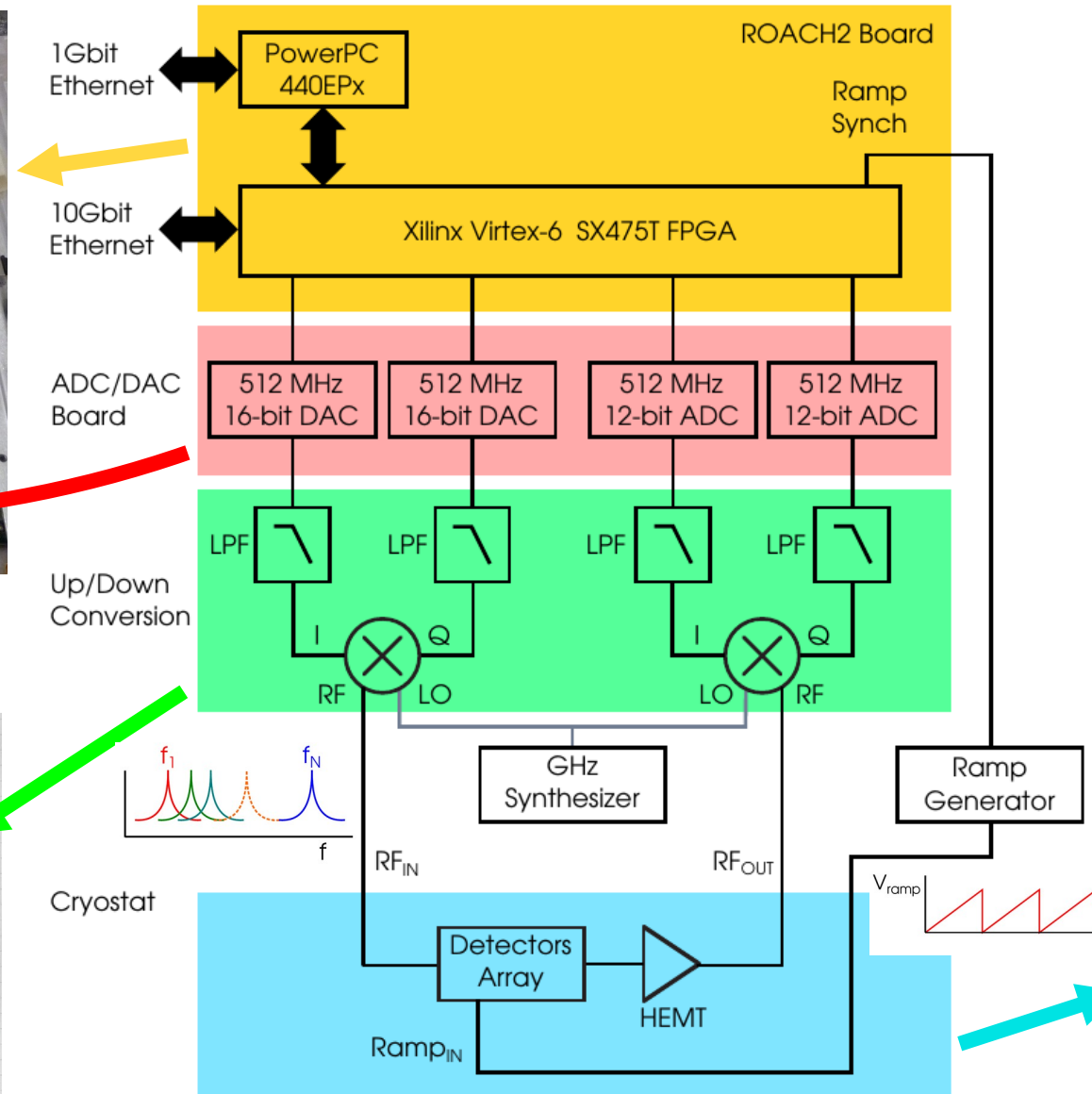


HOLMES heterodyne readout

Software Defined Radio generates RF tones and demodulates output RF signals

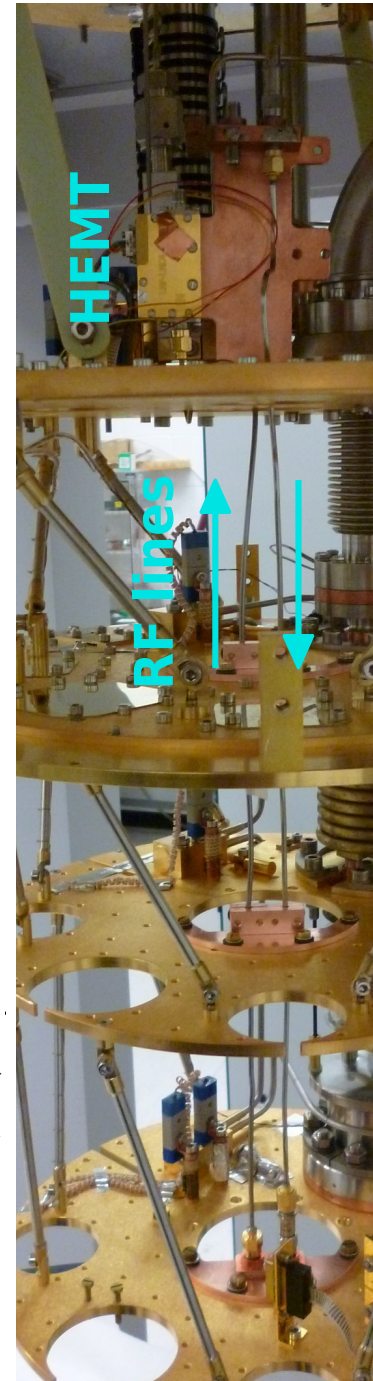


1 ROACH2 ($f_{ADC}=512$ MS/s)
for 32 detectors



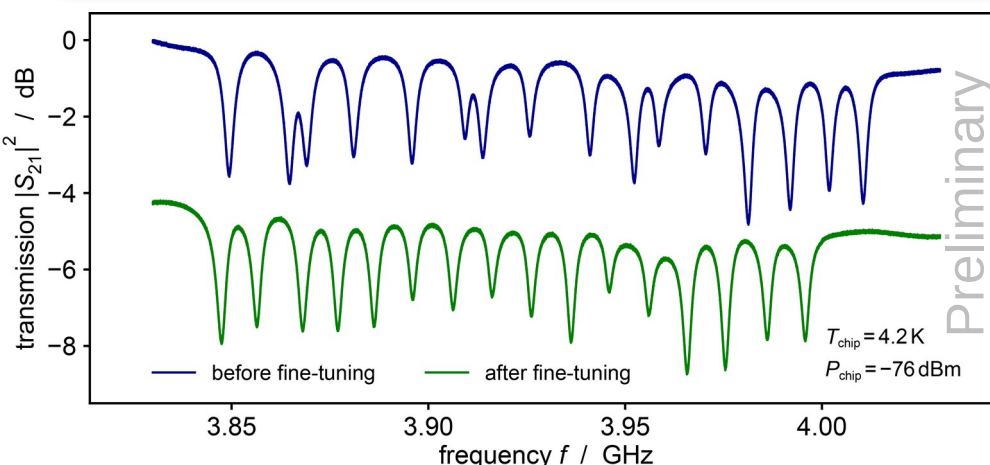
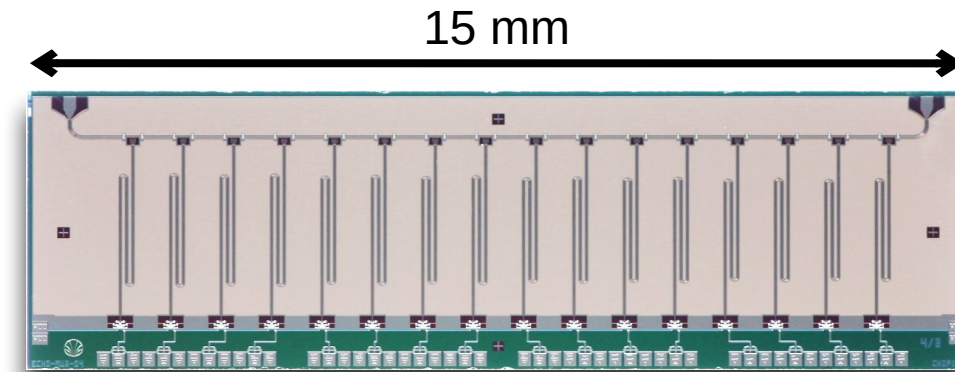
1 IF-board for 32 detectors

1 HEMT (BW 4-8 GHz)
for 256 detectors

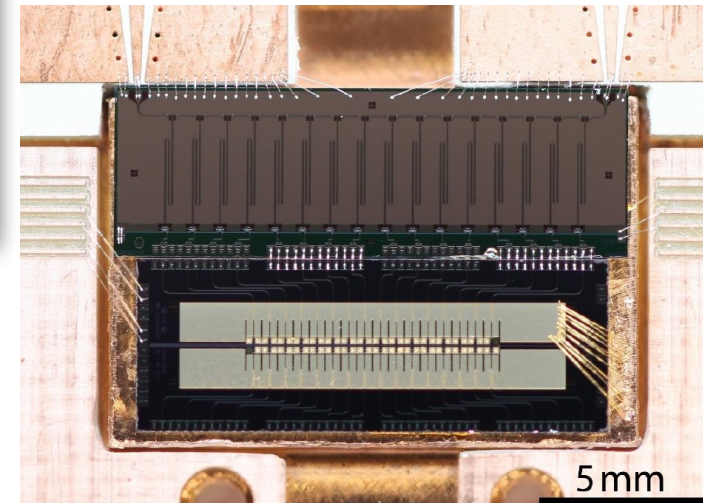


ECHO-100k

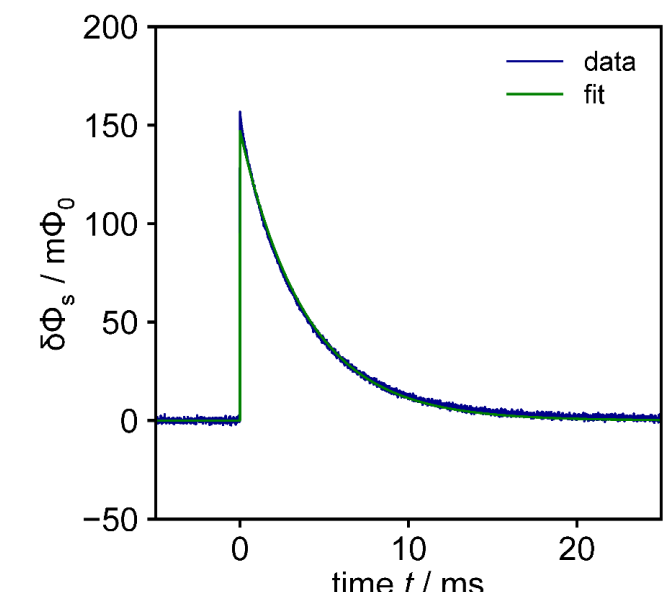
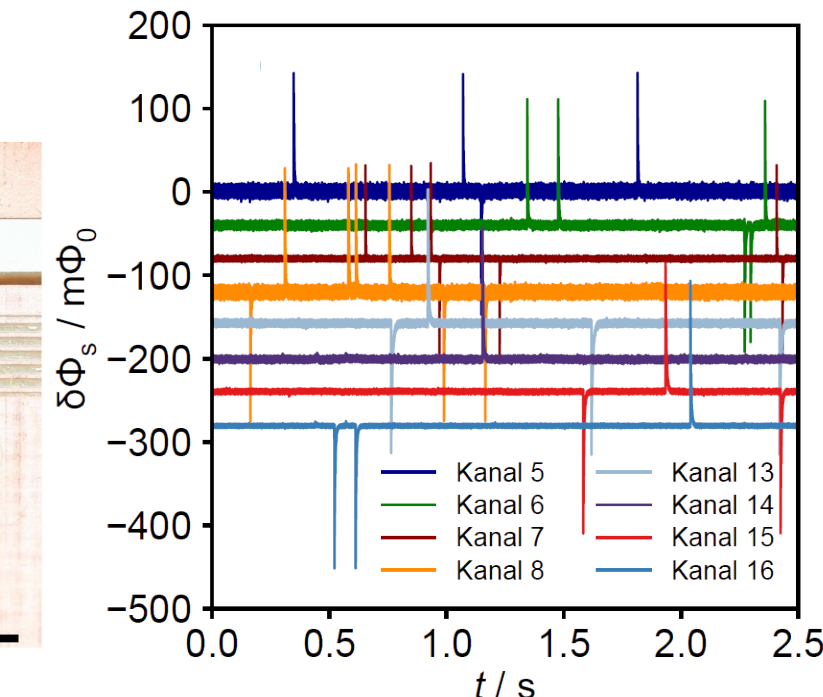
ECHO-100k will implement microwave multiplexing to readout 12000 MMCs



16 channel μ mux chip

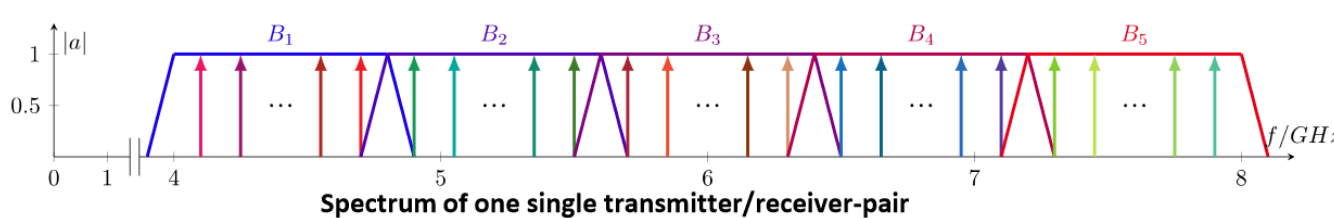
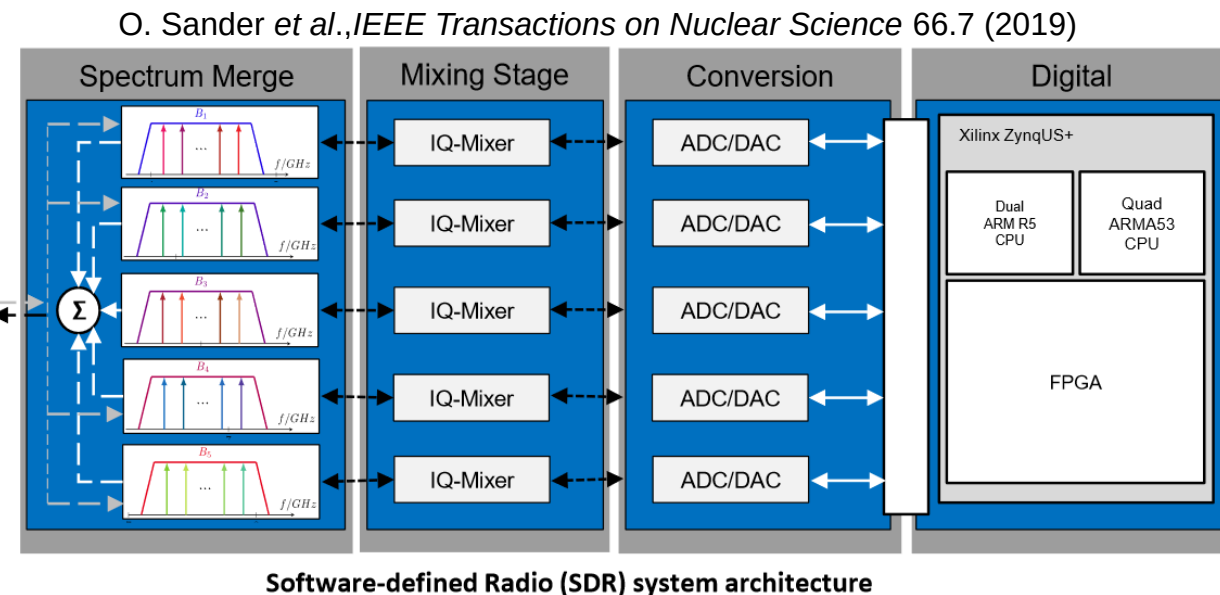
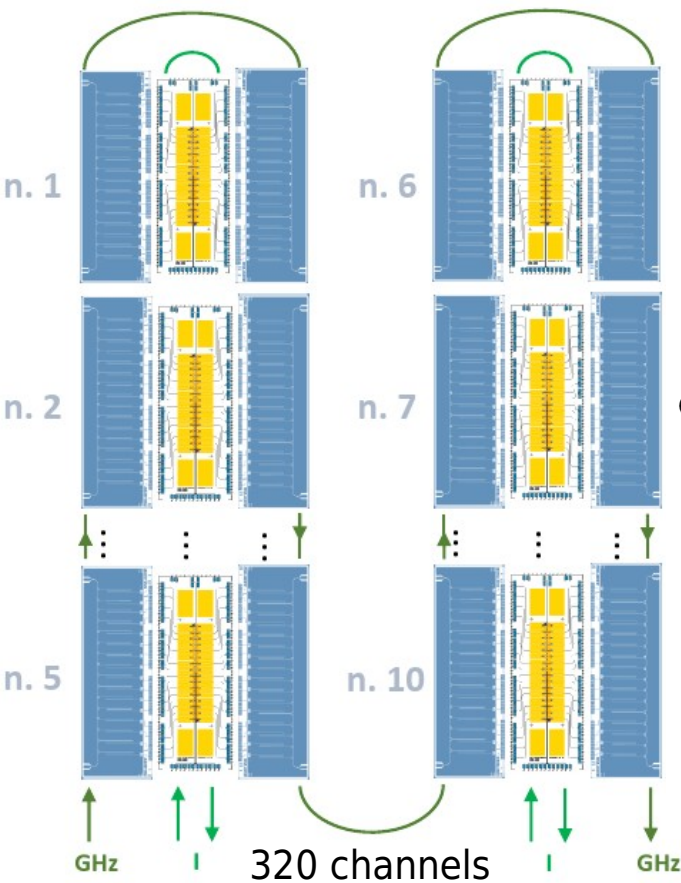


ECHO-100k
16+16 channels array
(32+32 pixels)



- successful read-out of 8 channels (16 pixels)
- noise limited by low available RF power
 - $\Delta E_{\text{FWHM}} \approx 10\text{-}30 \text{ eV}$ (low power) depending on Q_i
- with high power read-out of 2 channels
 - $\Delta E_{\text{FWHM}} \approx 9 \text{ eV}$

ECHO-100k: SDR for heterodyne readout development



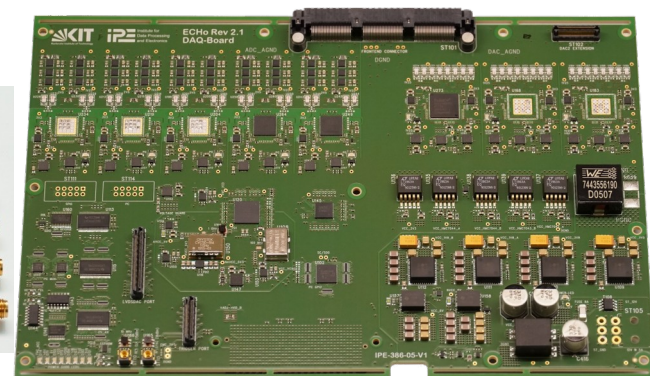
ECHO-100k

12000 MMC pixels =
400 MMC channels ×
15 SDR systems / HEMT

Mixing stage



1GS/s ADC / 500MS/s DAC Board



FPGA-Board



HEMT 4-8 GHz band covered by 5×800 MHz bands → 80 channel/band → 400 total channels



300K
4K
HEMTs
0.01K

Data analysis

First level data reduction



Evaluation of pulse information



Energy estimation

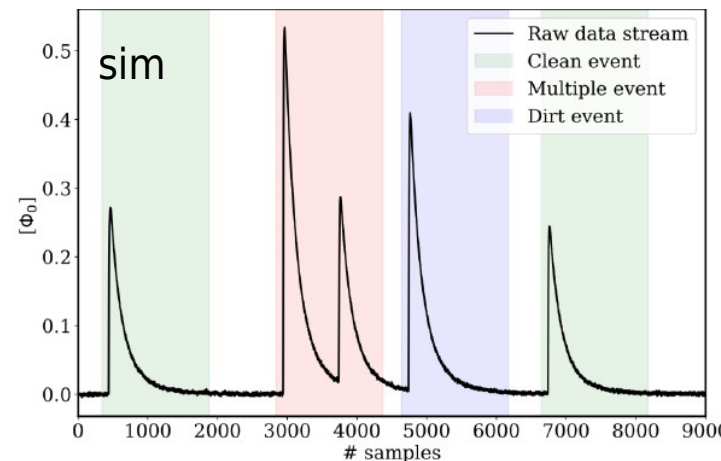
Optimum filter

Arrival time correction

Gain drift correction

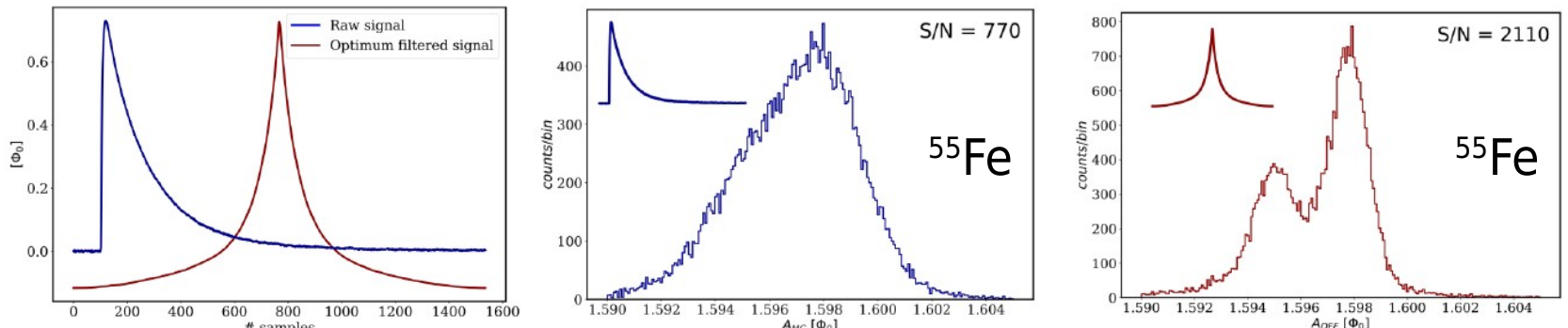
Energy calibration

Second level data reduction

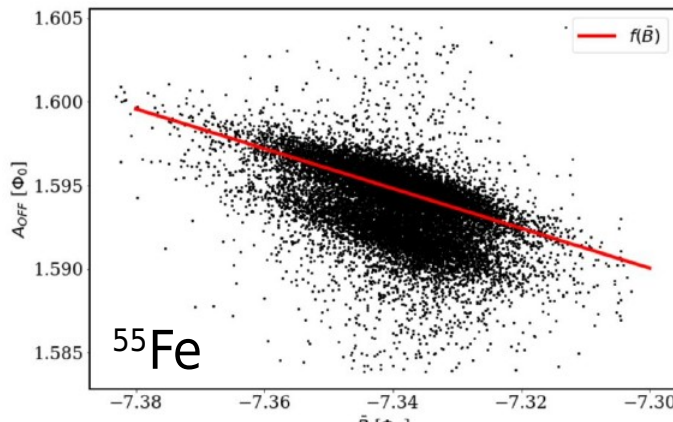


- classify events
- discard bad ones
- estimate time constants, arrival time, pretrigger level (baseline), and other parameters

energy estimator based on optimal filter in various implementations

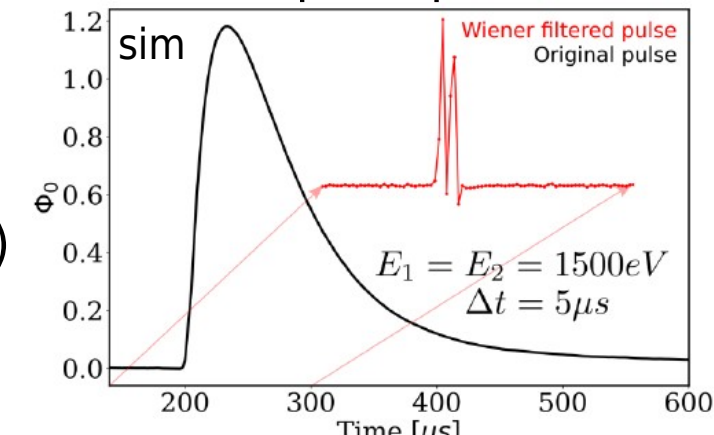


gain drift correction



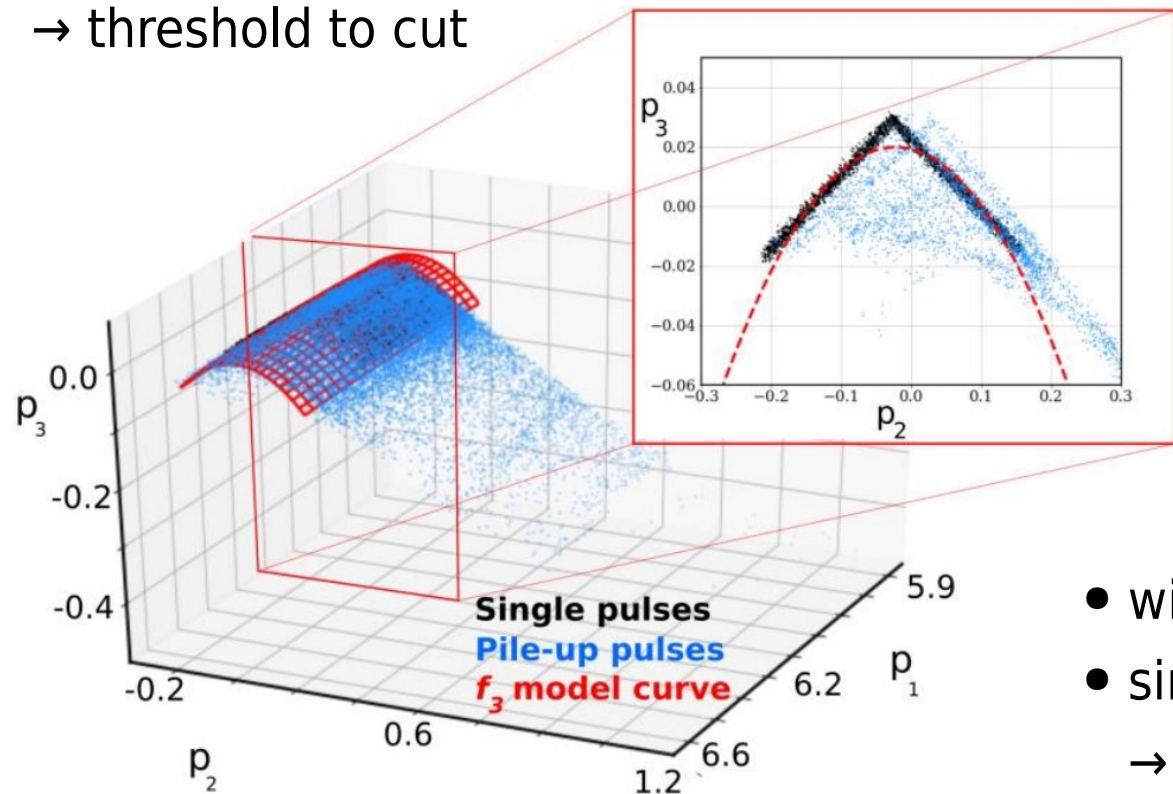
amplitude
vs.
baseline ($\propto T_{op}$)
correlation

rise time pile-up detection



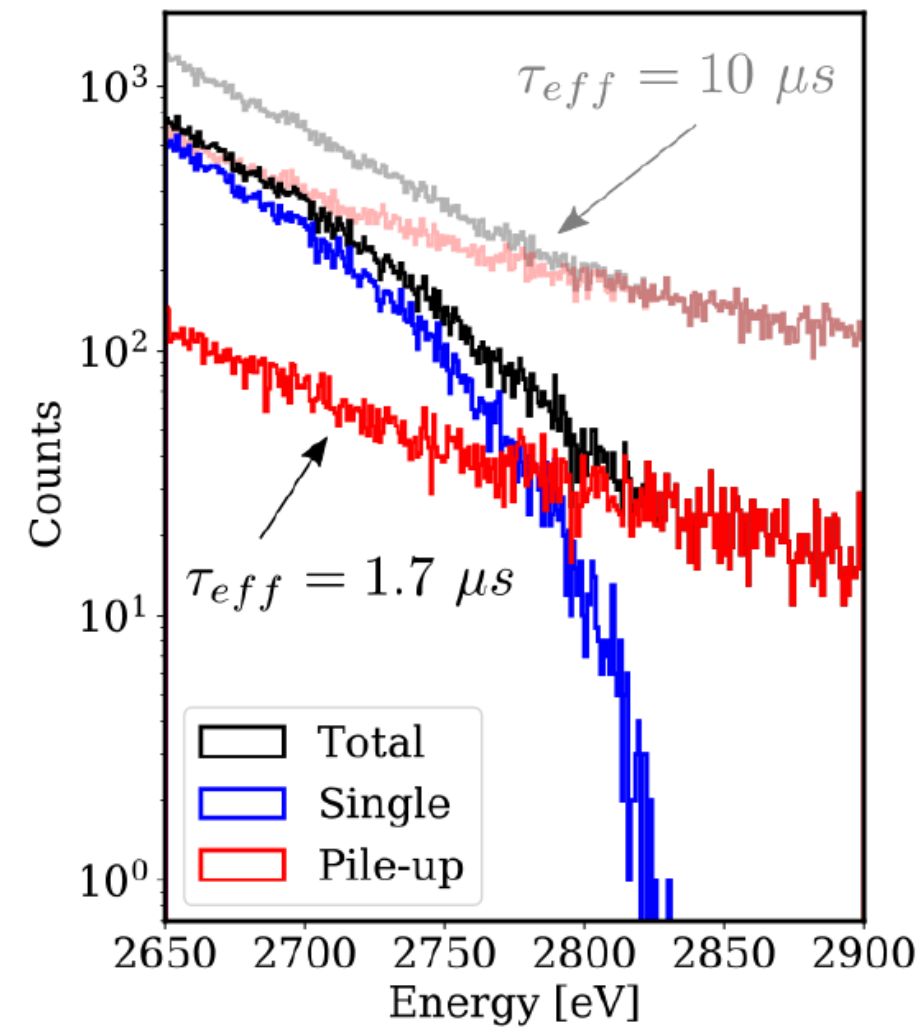
Pile-up discrimination

- advanced discrimination technique to identify pile-up events
 - Discrimination through Singular Vector Projections (DSVP)
 - “unsupervised learning” technique, based on singular value decomposition, PCA and multiple linear regression
- SVP decomposition
- raw dataset cleaning (PCA)
- model point distribution in singular vector projection space
- threshold to cut



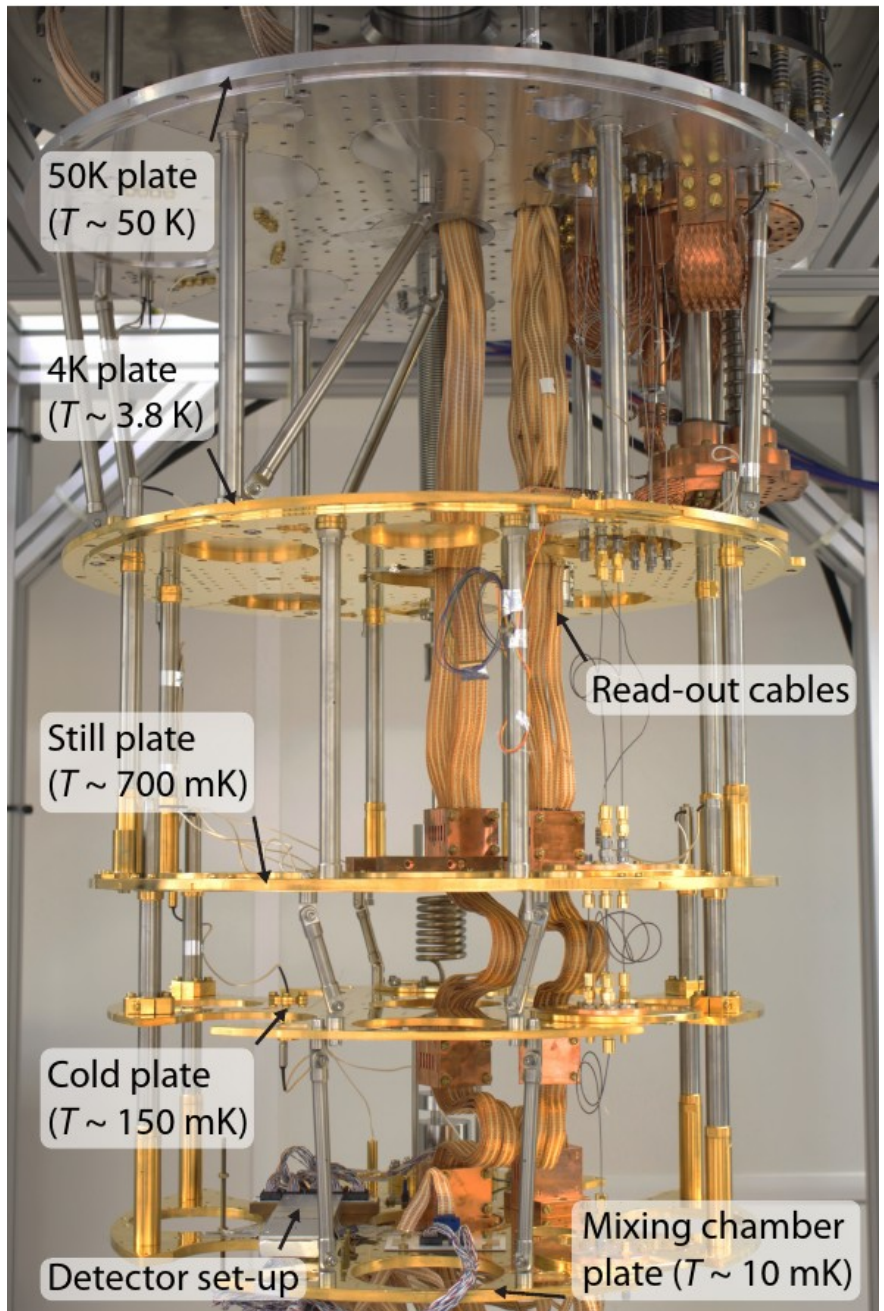
- with DSVP τ_R is limited by the pulse sampling time $1/f_{\text{ramp}}$
- simulations for HOLMES pulses
 - $\tau_R \approx 1-2 \mu\text{s}$ for $\tau_{\text{rise}} \approx 10-20 \mu\text{s}$ and $f_{\text{ramp}} = 500 \text{ kHz}$

ROI energy spectrum

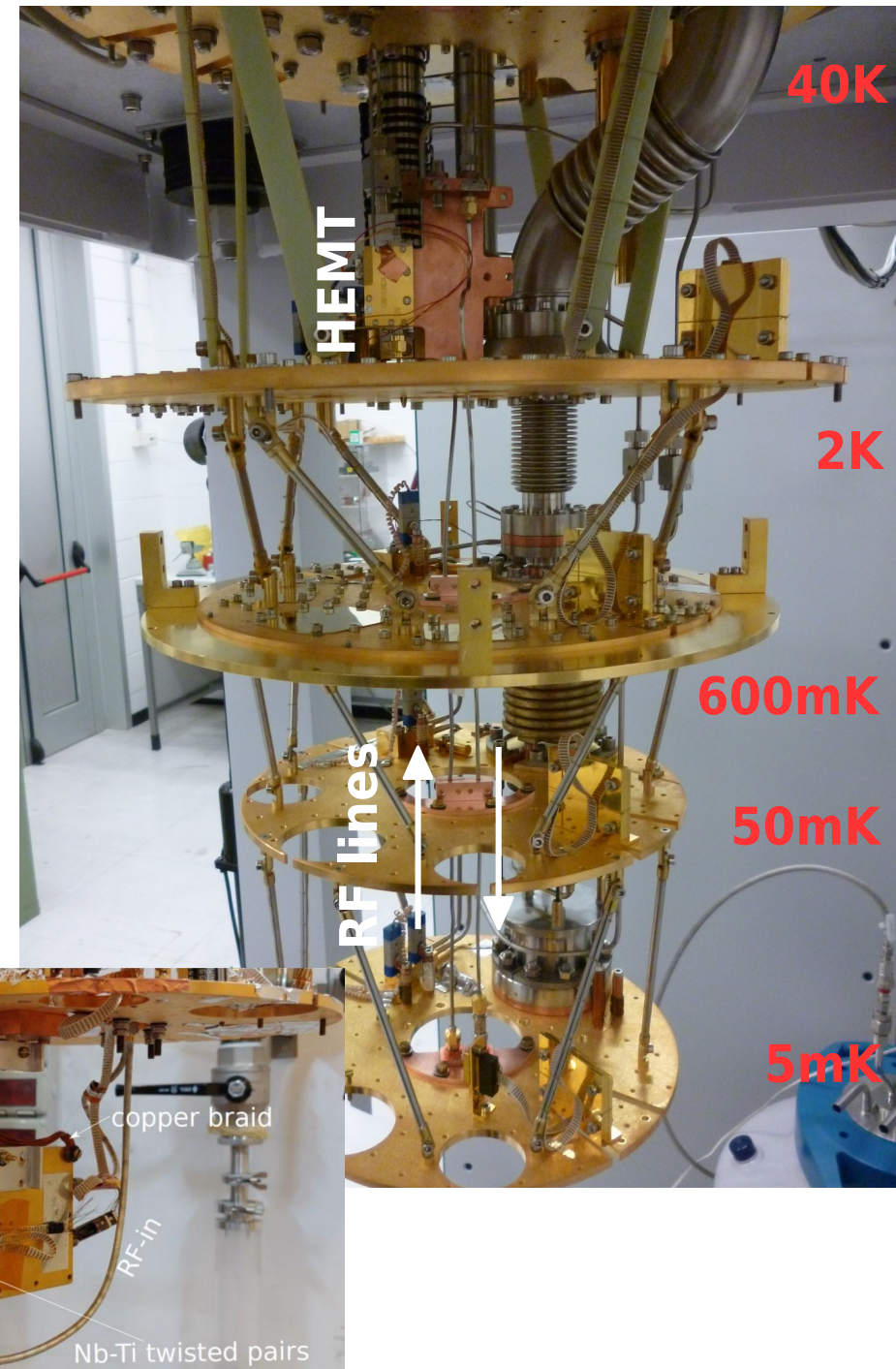


Cryogenic set-ups

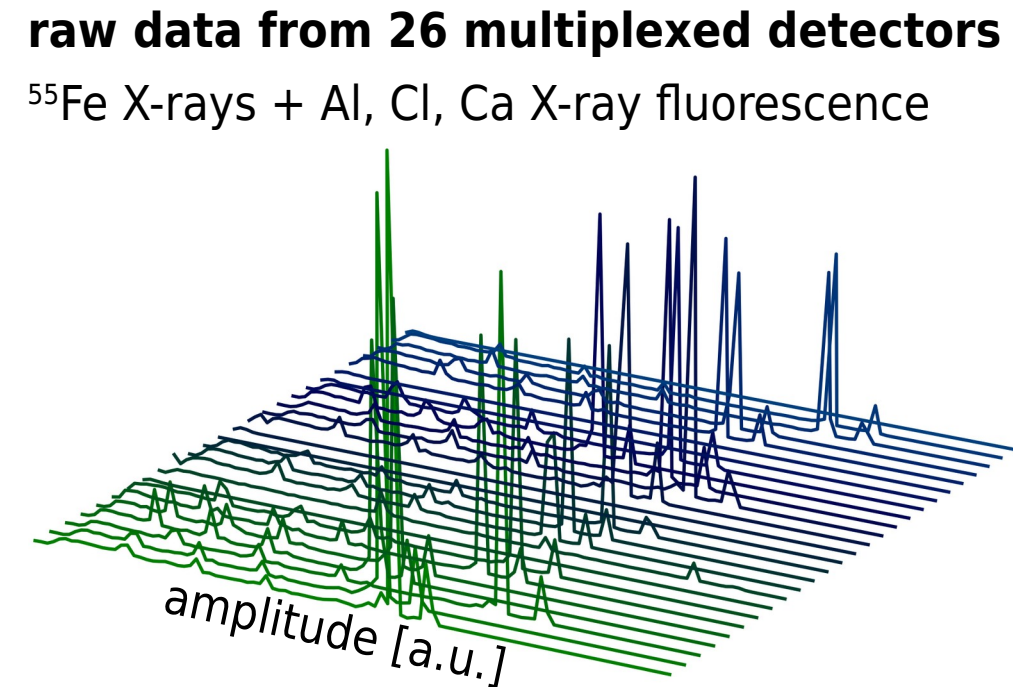
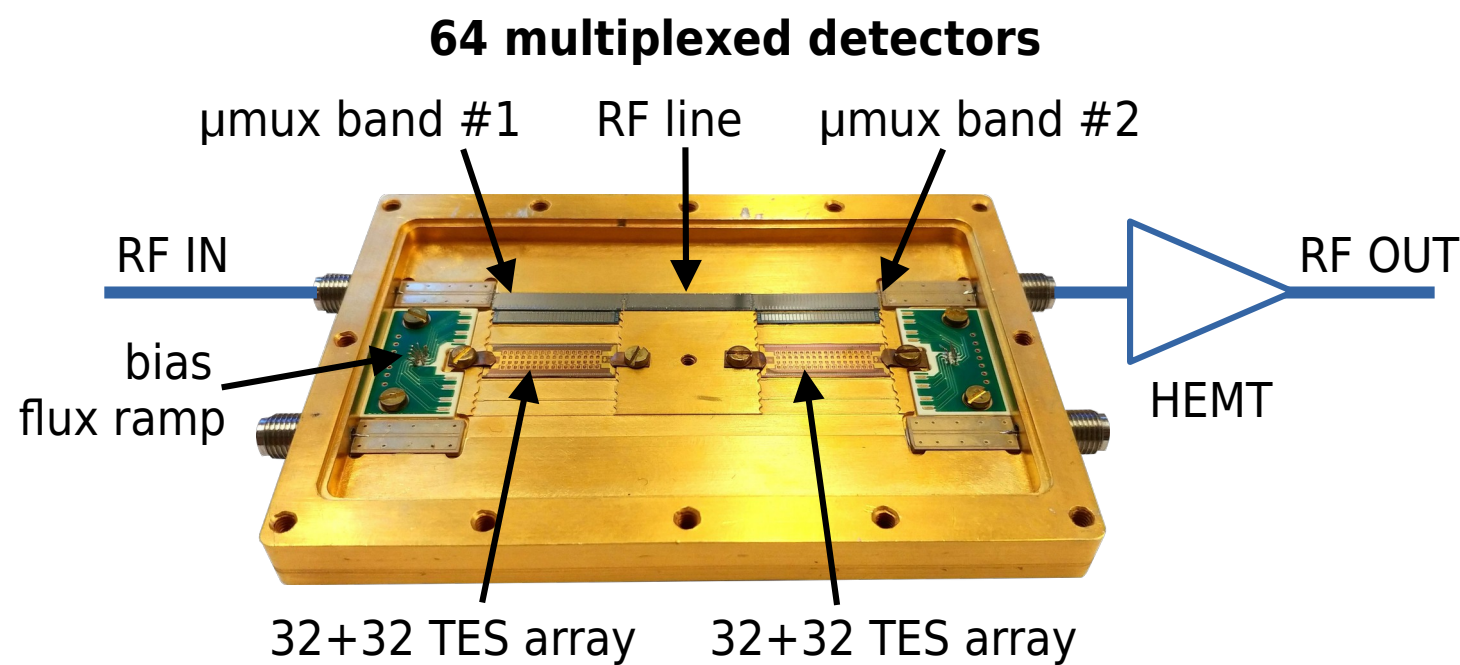
ECHo-1k



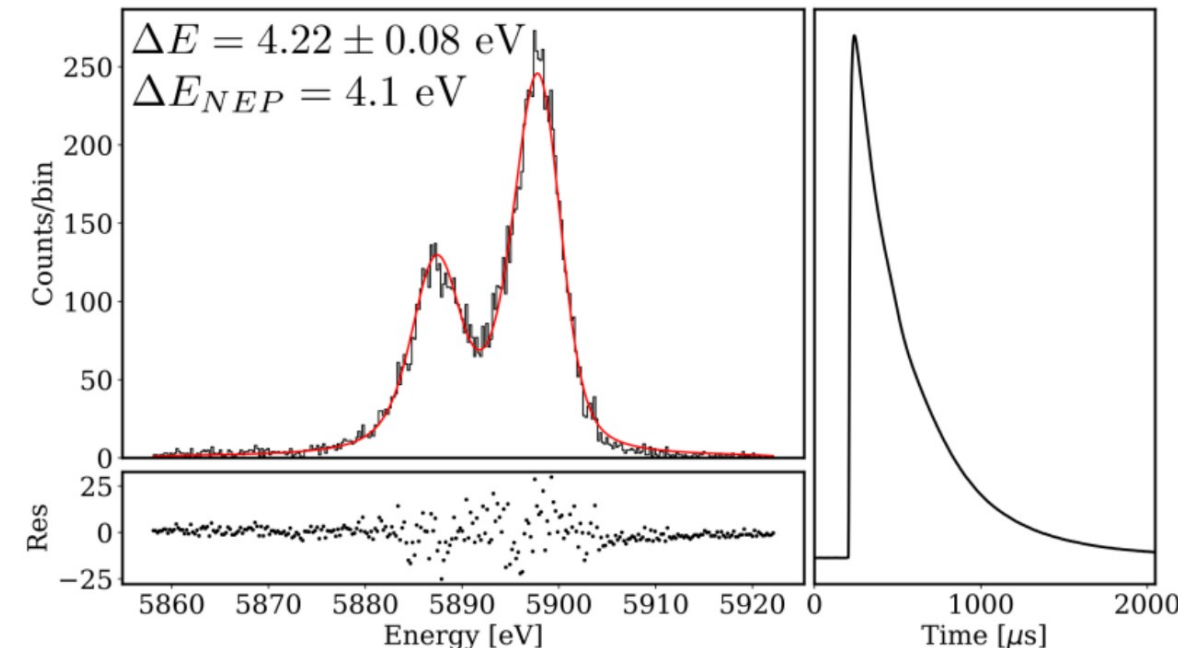
HOLMES (for 256 pixels)



HOLMES status: detectors, readout, analysis



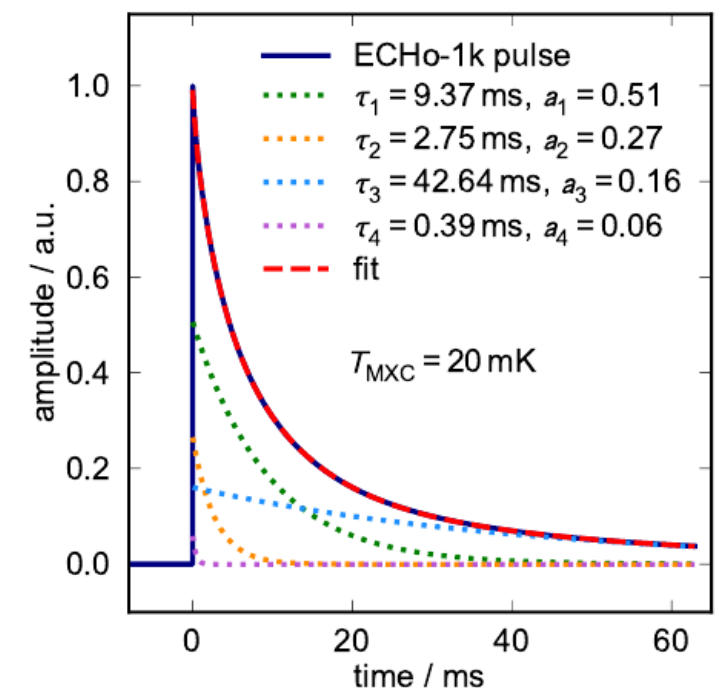
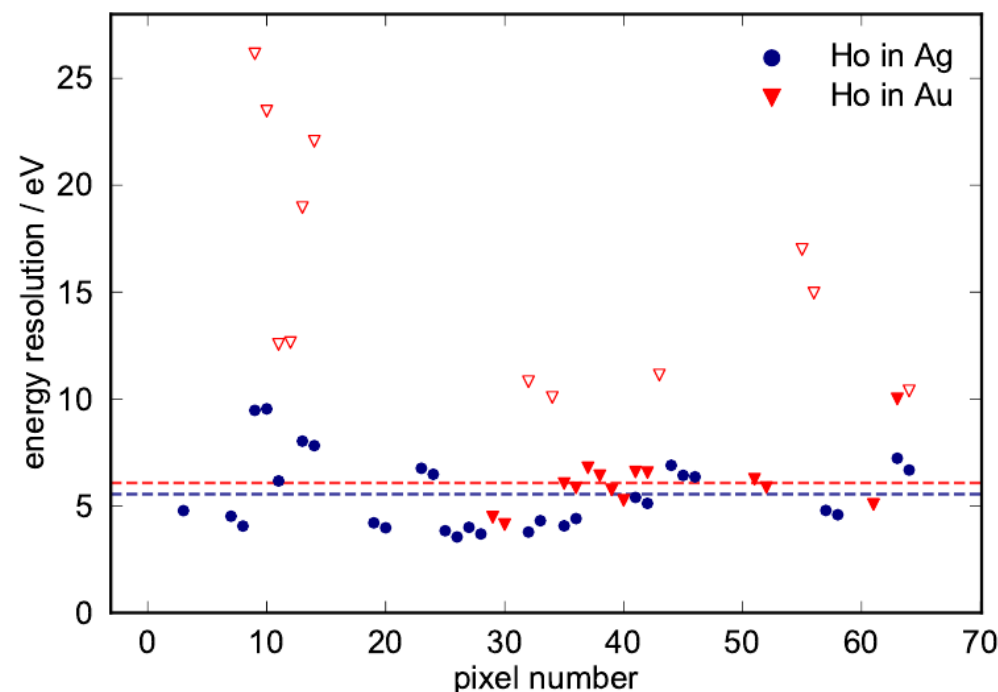
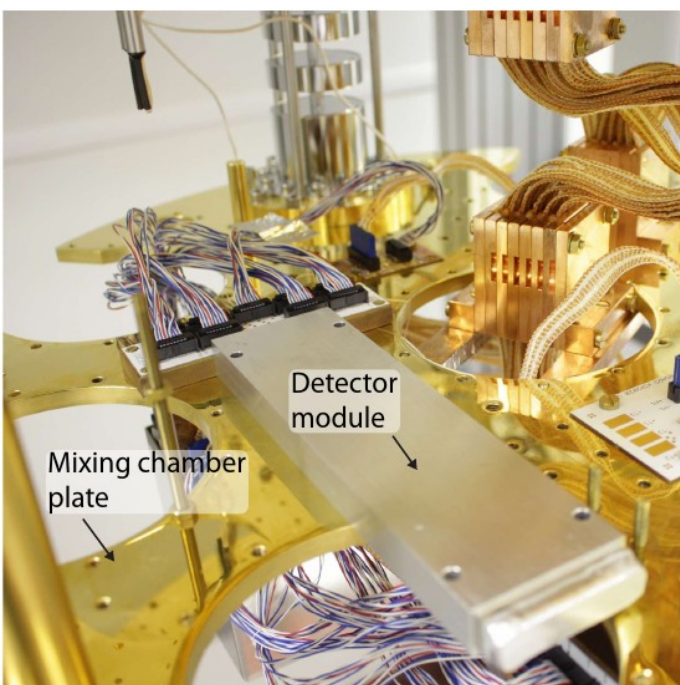
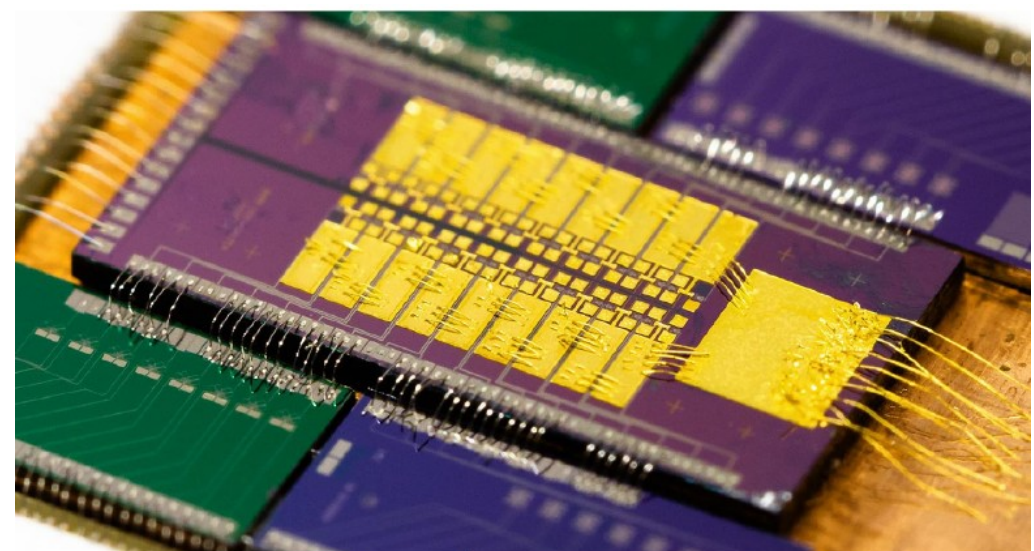
- fully processed TES arrays without ^{163}Ho implant
- set-up for 126 multiplexed pixels
- 2 μmux chips but only 32 bonded pixels
- 16 channel firmware version (stable) for ROACH2
- at 5.9 keV:
 - $\Delta E_{\text{FWHM}} \approx 4\text{-}6 \text{ eV}$
 - $\tau_{\text{rise}} \approx 15 \mu\text{s}$ (R/L limited to match DAQ) → $\tau_{\text{R}} \approx 1.5 \mu\text{s}$
 - $\tau_{\text{decay}} \approx 300 \mu\text{s}$



ECHO-1k status: detectors

2 detector modules with ^{163}Ho in Au and Ag host material
parallel dc-SQUID readout

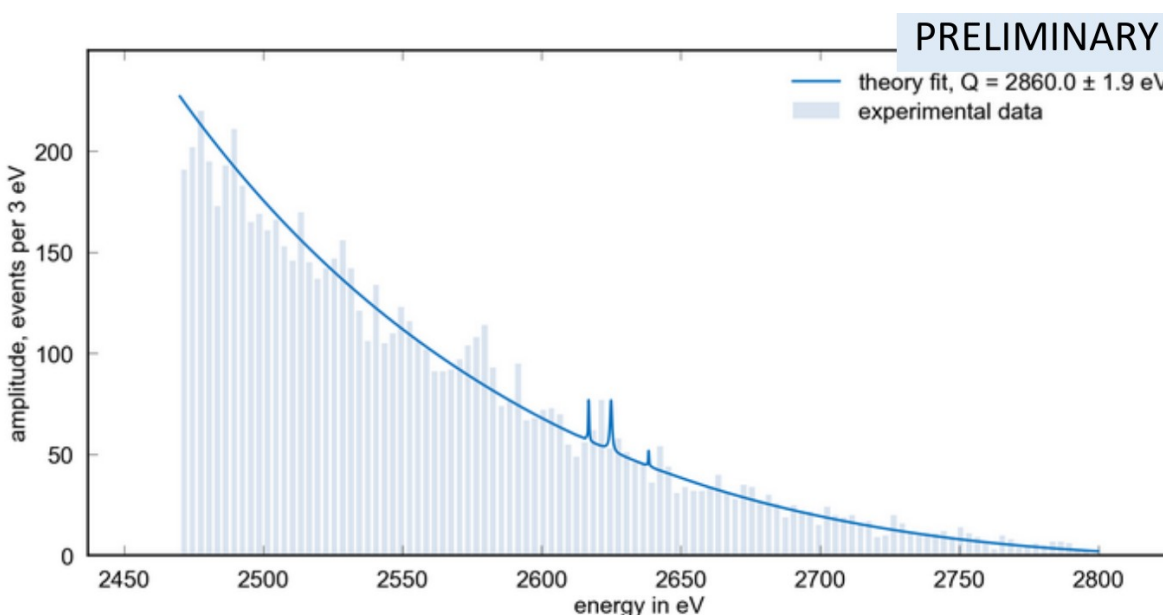
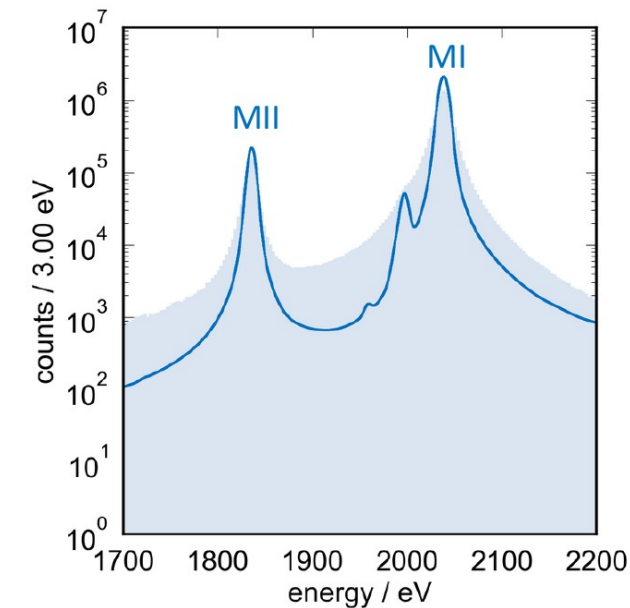
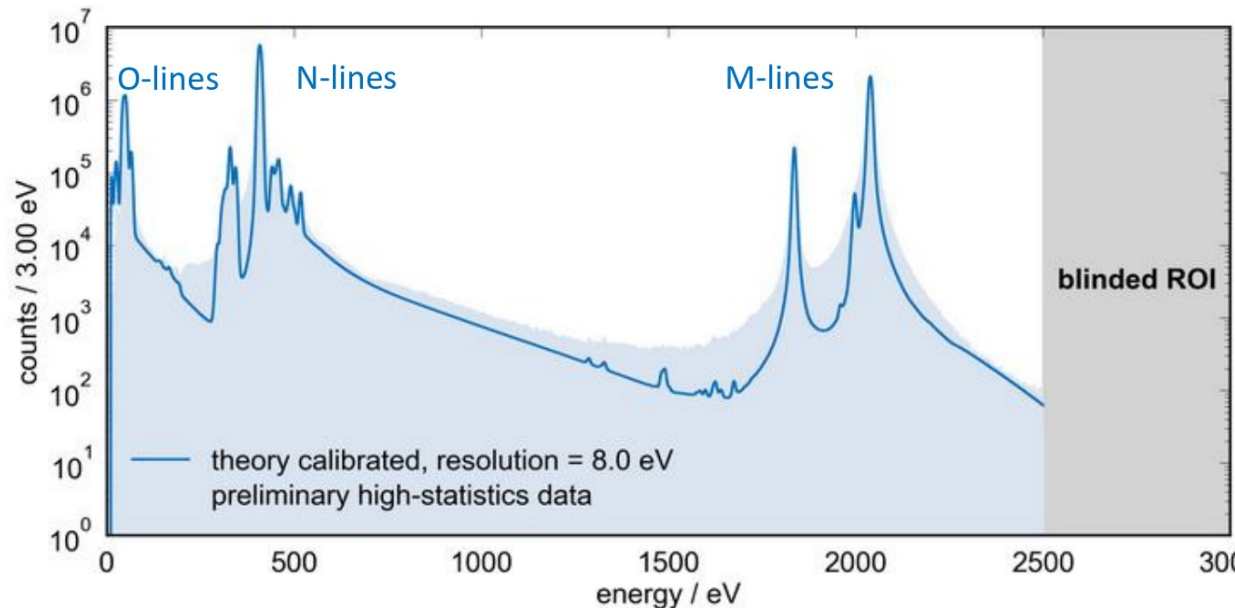
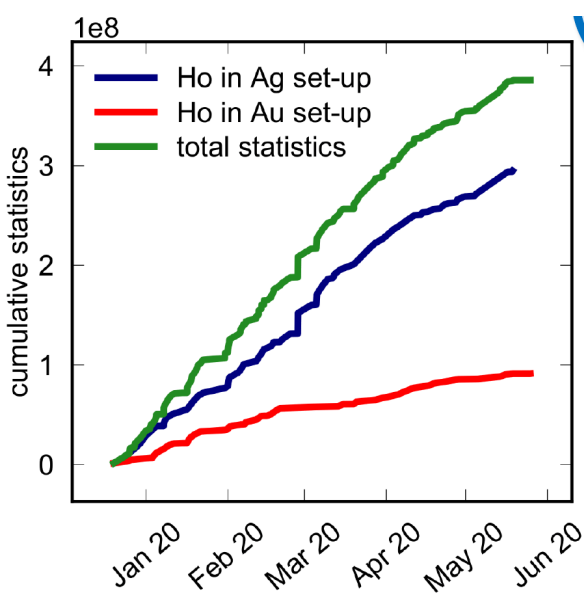
host	^{163}Ho pixels	bkg pixels	$\langle A \rangle [\text{Bq}]$	$A_{\text{tot}} [\text{Bq}]$
Au	23	3	0.94	28.1
Ag	34	6	0.71	25.9



- $\tau_{\text{rise}} \approx 1 \mu\text{s}$ limited by SQUID bandwidth
- complex decays time: mostly $\tau_1 \approx 10 \text{ ms}$

ECHO-1k status: 10^7 events spectrum

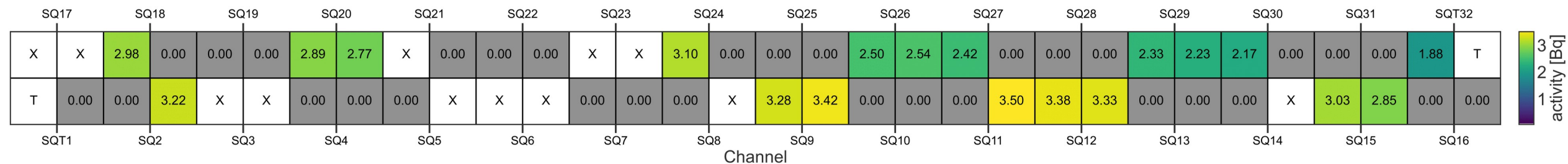
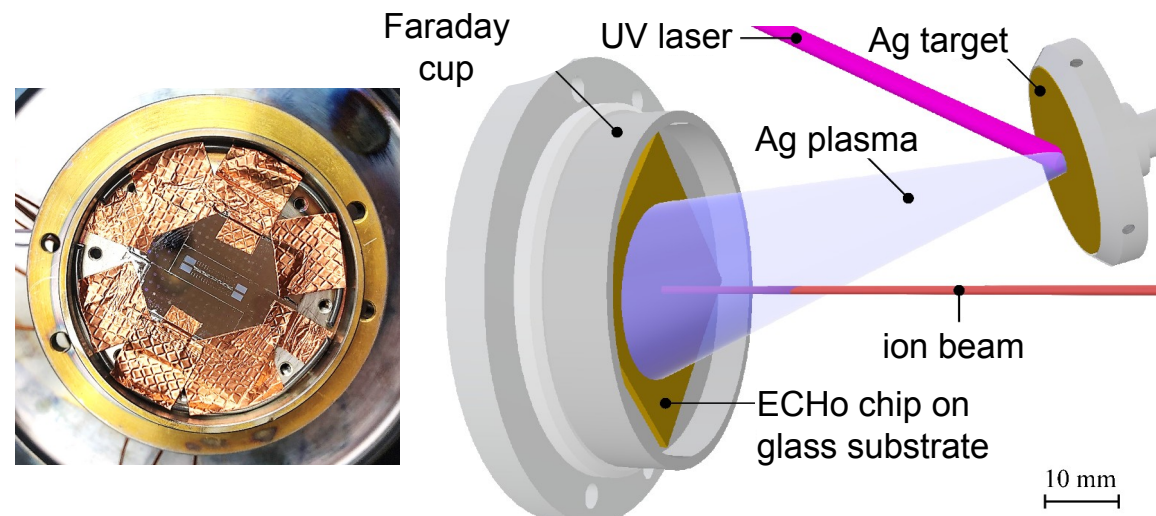
6×10^7 events acquired with detectors having ^{163}Ho in Ag host material



- end-point analysis in progress
- from preliminary end-point analysis
 - EC Brass & Haverkort theory
 - Flat background
- $Q_{\text{EC}} = (2860 \pm 2\text{stat} \pm 5\text{syst}) \text{ eV}$

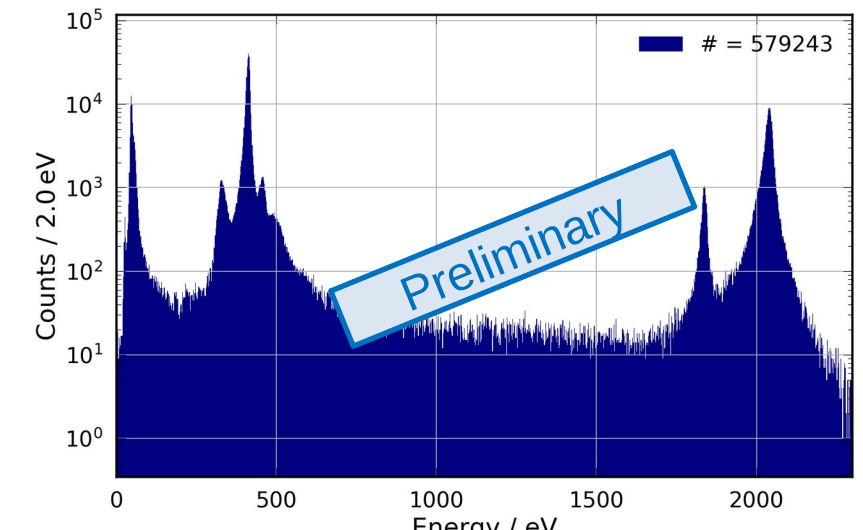
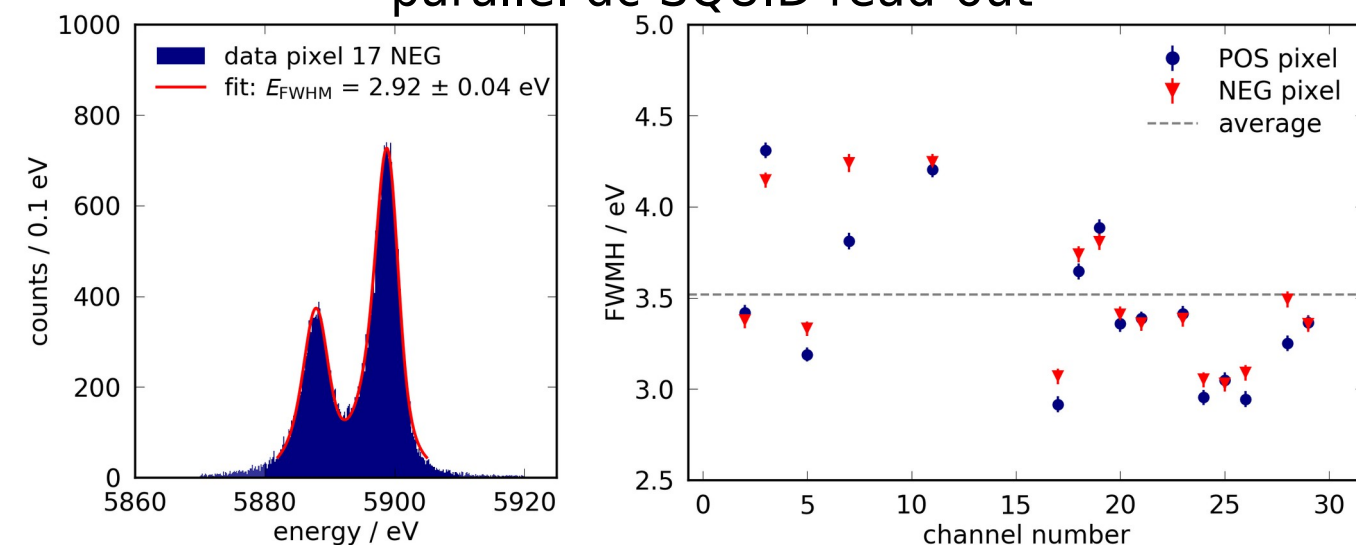
ECHO-100k progresses

- 30 MBq of pure ^{163}Ho available
- implant system improvements for 10 Bq
 - beam positioning on ECHO-100k wafer
 - co-deposition through PLD in progress
- pixel design optimization to minimize C
- μmux read-out system development in progress



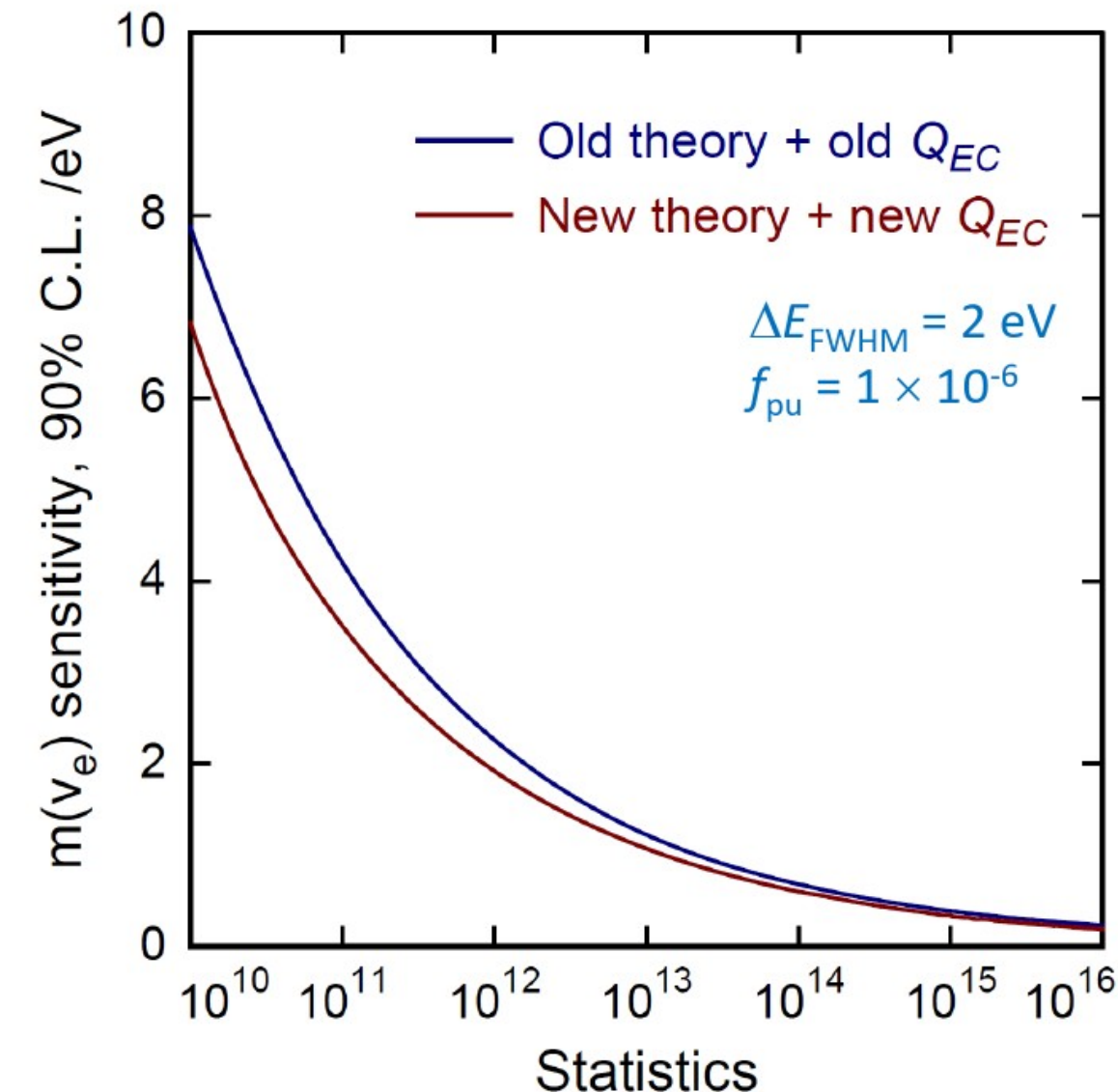
pixel characterization before ion implant
parallel dc-SQUID read-out

after ion implant without second Au layer
dc-SQUID read-out $\rightarrow \Delta E \approx 3.4 \text{ eV}$ at N1 line

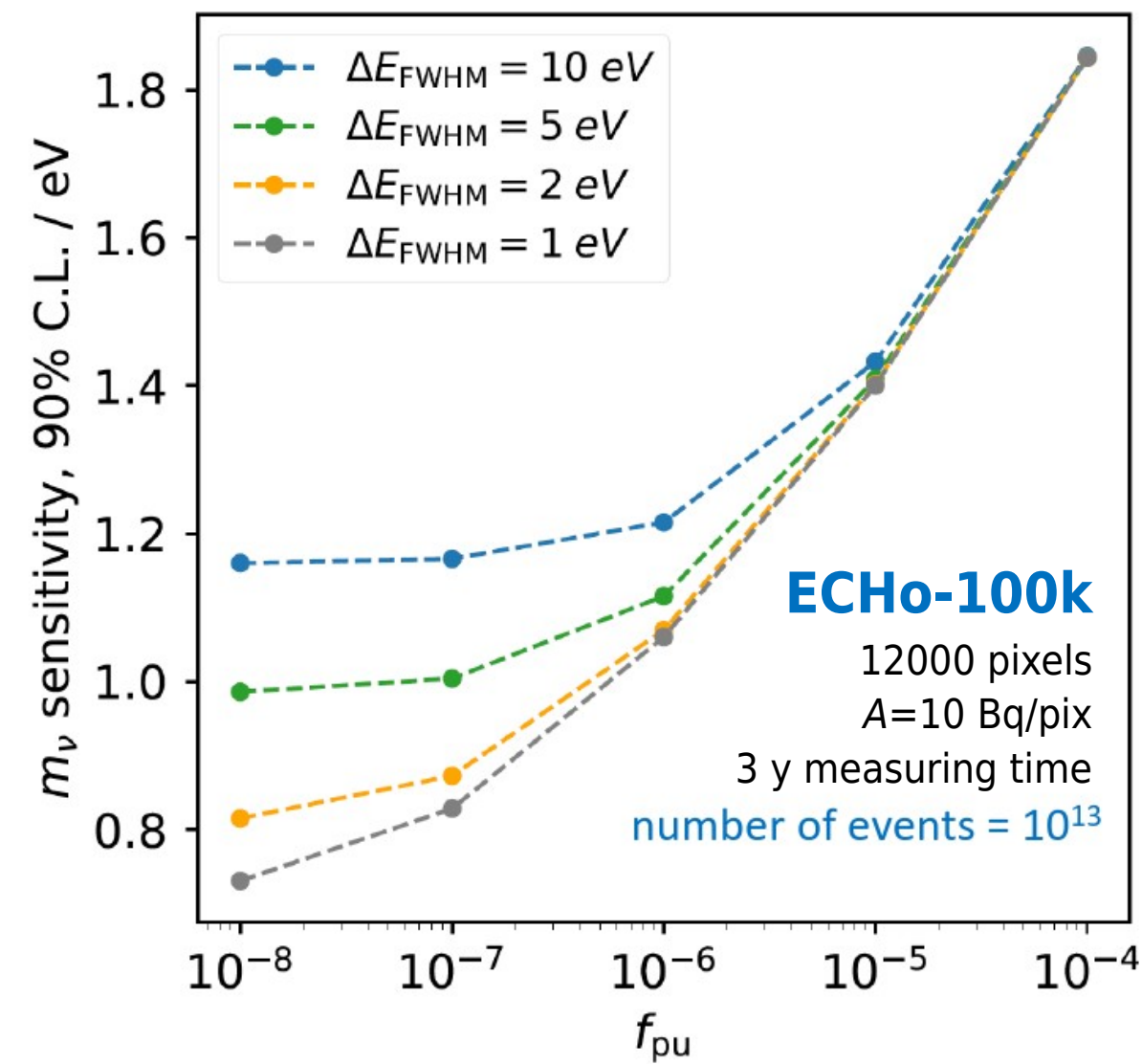


ECHO-100k updated expected sensitivity

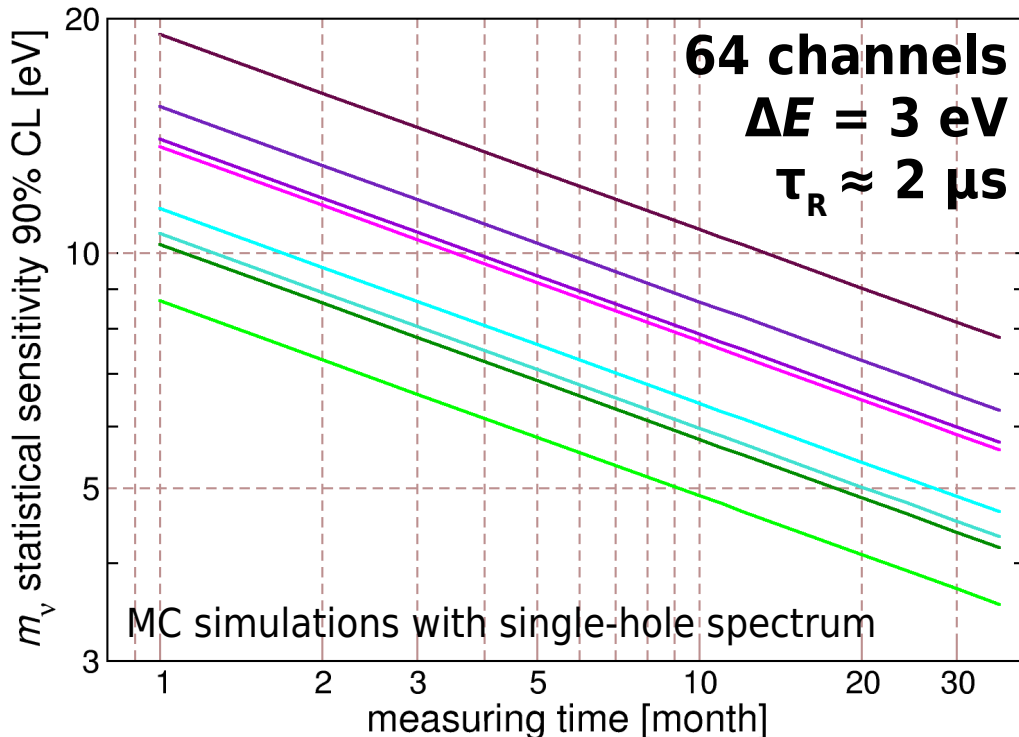
Brass & Haverkort theoretical model + new Q_{EC} -value



Sensitivity for the coming phase of ECHO



HOLMES sensitivity evolution vs. pixel activity



A = 1 Hz/det

A = 3 Hz/det

A = 5 Hz/det

A = 10 Hz/det

A = 30 Hz/det

A = 50 Hz/det

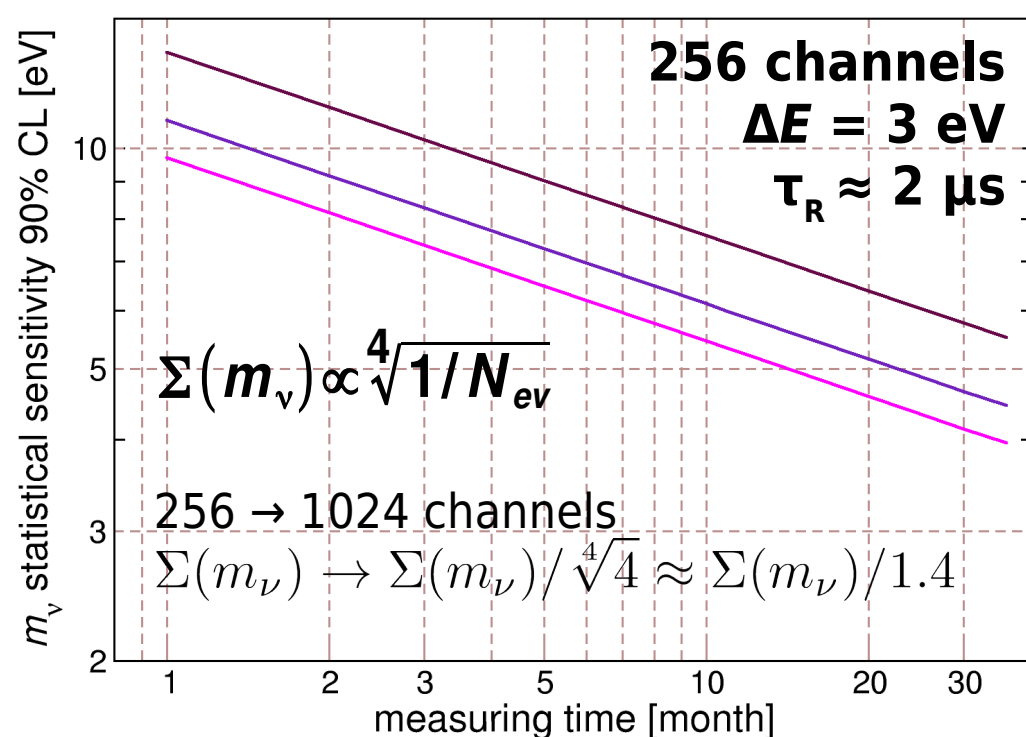
A = 100 Hz/det

A = 300 Hz/det

low dose

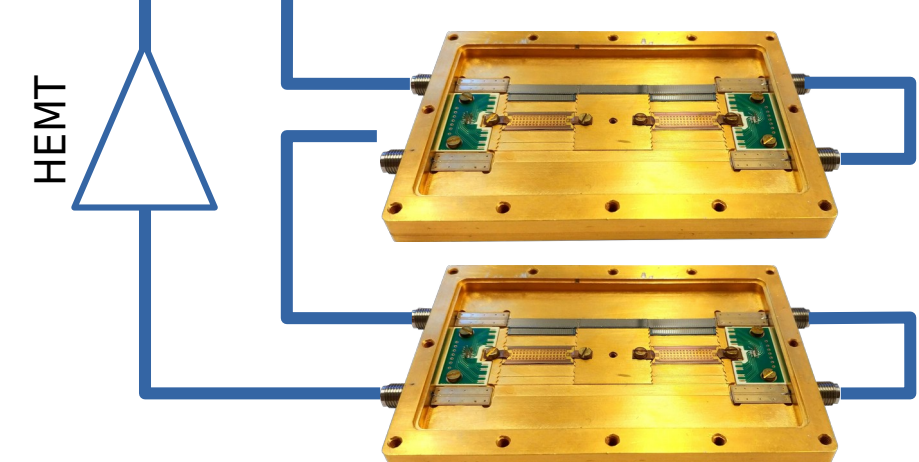
with
focusing

?



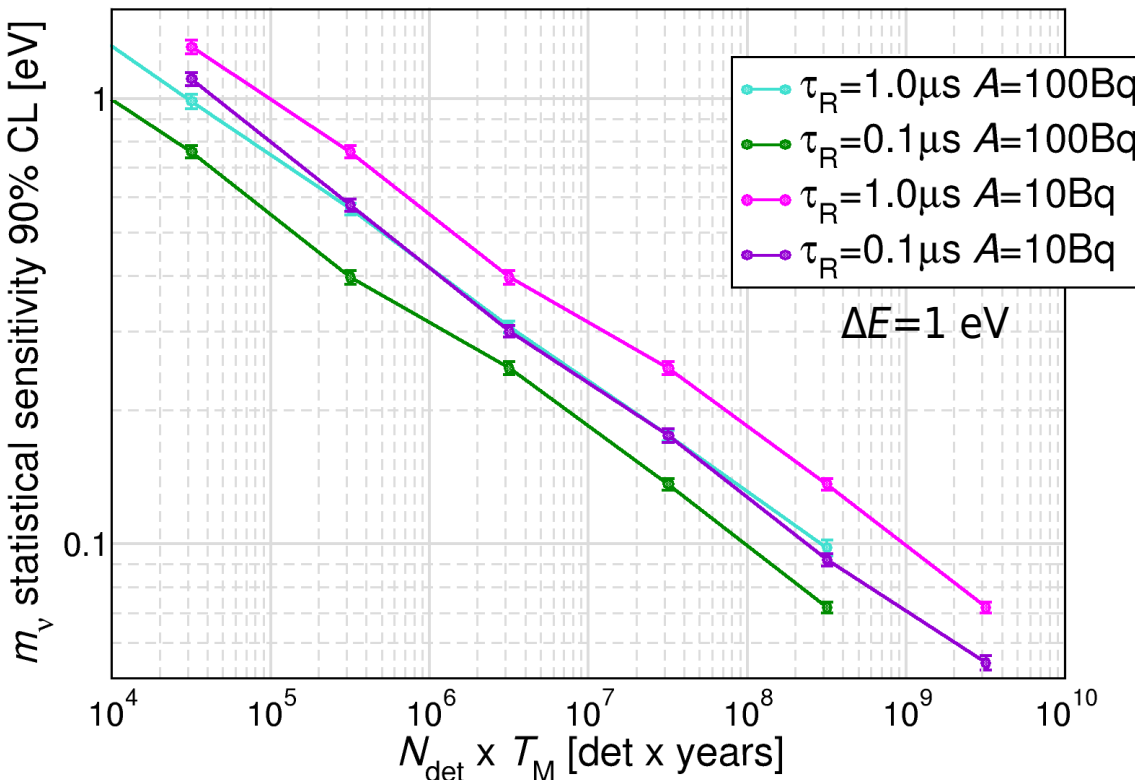
8 × ROACH2+IF boards

RF OUT RF IN



Beyond ECHO and HOLMES: a 0.1eV experiment

single hole spectrum with $Q_{EC}=2833$ eV



10 years measuring time

$A/\text{det} [\text{Bq}]$	10	10	100	100	1000	1000
$\tau_R [\mu\text{s}]$	0.1	1	0.1	1	0.1	1
f_{pp}	1.0E-06	1.0E-05	1.0E-05	1.0E-04	1.0E-04	1.0E-03
N_{det}	3.0E+07	9.8E+07	9.8E+06	3.0E+07	3.0E+06	1.3E+07
$A_{\text{total}} [\text{Bq}]$	3.0E+08	9.8E+08	9.8E+08	3.0E+09	3.0E+09	1.3E+10
$^{162}\text{Er} [\text{mg}] ^*$	2274	7429	7429	22742	22742	98548

* $^{162}\text{Er}/A(^{163}\text{Ho}) = 3790 \text{ mg/GBq} + 50\% \text{ usage efficiency}$

- pixel activity $\geq 100 \text{Bq/det} \leftrightarrow ^{163}\text{Ho}$ heat capacity
- time resolution below $0.1 \mu\text{s} \leftrightarrow$ multiplexing and DAQ bandwidth
- about 10M pixels \leftrightarrow multiplexing and DAQ bandwidth

Conclusions

- **ECHo and HOLMES are reaching a statistical sensitivity of order of 1 eV in few years**
 - many technical challenges faced successfully (also separately by ECHo and HOLMES)
 - production of large amounts of clean ^{163}Ho samples
 - efficient ion implantation
 - high resolution detectors with multiplexed read-out
 - sophisticated analysis tools
 - some activities are still required to fully assess the potential of holmium experiments
 - understanding the holmium decay spectrum
 - effect of high activities on detector performances
 - investigating systematic effects
- **longer term plans: next generation experiments for sub-eV sensitivities require**
 - larger international collaboration
 - increased single pixel activity
 - cost reduction (isotope production and efficient usage, readout electronics)

Collaborations



Università di Milano-Bicocca, Italy
INFN Milano-Bicocca, Italy
INFN Genova, Italy
INFN Roma, Italy
INFN LNGS, Italy
NIST, Boulder, USA
PSI, Villigen, Switzerland
ILL, Grenoble, France



Heidelberg University, Germany
Johannes Gutenberg University, Mainz, Germany
GSI, Darmstadt, Germany
Helmholtz Institute Mainz, Mainz, Germany
University of Tübingen, Tübingen, Germany
MPI für Kernphysik, Heidelberg, Germany
KIT, Karlsruhe, Germany
Petersburg Nuclear Physics Institute, Gatchina, Russia
Laboratoire Souterrain de Modane, Modane, France
CERN, Geneva, Switzerland
ILL, Grenoble, France

